



<https://theses.gla.ac.uk/>

Theses Digitisation:

<https://www.gla.ac.uk/myglasgow/research/enlighten/theses/digitisation/>

This is a digitised version of the original print thesis.

Copyright and moral rights for this work are retained by the author

A copy can be downloaded for personal non-commercial research or study,
without prior permission or charge

This work cannot be reproduced or quoted extensively from without first
obtaining permission in writing from the author

The content must not be changed in any way or sold commercially in any
format or medium without the formal permission of the author

When referring to this work, full bibliographic details including the author,
title, awarding institution and date of the thesis must be given

Enlighten: Theses

<https://theses.gla.ac.uk/>
research-enlighten@glasgow.ac.uk

STUDIES
IN
HEAT AND MASS TRANSFER

A thesis submitted to the University of Glasgow
in fulfilment of the requirements for the Degree
of Doctor of Philosophy

by
Daniel Cleland

Royal College of Science and Technology,
Glasgow.

January, 1961.

ProQuest Number: 10656254

All rights reserved

INFORMATION TO ALL USERS

The quality of this reproduction is dependent upon the quality of the copy submitted.

In the unlikely event that the author did not send a complete manuscript and there are missing pages, these will be noted. Also, if material had to be removed, a note will indicate the deletion.



ProQuest 10656254

Published by ProQuest LLC (2017). Copyright of the Dissertation is held by the Author.

All rights reserved.

This work is protected against unauthorized copying under Title 17, United States Code
Microform Edition © ProQuest LLC.

ProQuest LLC.
789 East Eisenhower Parkway
P.O. Box 1346
Ann Arbor, MI 48106 – 1346

Acknowledgements

The Author wishes to thank Professor P. D. Ritchie for permission to undertake this research within his department and to acknowledge the help and encouragement given by his supervisor, Dr. C. G. M. Slessor.

The Author is also indebted to the workshop staff for their assistance in the construction of the experimental equipment.

Index

Summary

1.	<u>Introduction</u>	1
1.2.	Boundary Layer Equations for Heat and Mass Transfer.	3
1.3.	Theoretical Equations for Heat and Mass Transfer.	8
1.4.	Review of Experimental Data.	10
1.4.1.	Heat Transfer.	10
1.4.1.1.	Flow through pipes.	10
1.4.1.2.	Flow at right angles to a cylinder.	13
1.4.2.	Mass Transfer.	13
1.4.2.1.	Wetted wall columns.	13
1.4.2.2.	Plane surfaces.	15
1.4.2.3.	Cylinders.	16
1.4.2.4.	Spheres.	17
1.4.3.	Conclusions from Review of Experimental and Theoretical Data.	18
2.	<u>Evaporation from Fibre Tows.</u>	20
2.2.	Continuous Fibre Drier.	20
2.3.	Drying.	21
2.3.2.	Movement of Liquid within a Material during the Falling Rate Period.	24
2.3.2.1.	Movement by diffusion.	24

2.3.2.2.	Capillary control.	27
2.3.3.	Through Circulation Drying.	28
2.3.4.	Drying of Textiles.	30
2.3.5.	Textile Driers.	32
2.4.	Artificial Fibres.	33
3.	<u>Apparatus and Procedure.</u>	34
3.1.	Apparatus.	34
3.1.2.	Drying Drum.	35
3.1.3.	Skew Roller.	35
3.1.4.	Drying Compartment.	36
3.1.5.	Heater System.	36
3.1.5.1.	Electric Heater.	37
3.1.5.2.	Steam Heater.	38
3.1.6.	U-tube.	38
3.1.7.	Transmission.	38
3.1.8.	Instrumentation.	39
3.1.8.1.	Air Temperature.	39
3.1.8.2.	Fibre Temperature.	40
3.1.8.3.	Humidity.	41
3.1.8.4.	Air flow.	43
3.2.	Procedure.	46
3.2.1.	Sampling.	47

3.2.2.	Moisture Contents of Samples.	47
3.3.	Initial Experiments.	48
4.	<u>Results - Part 1: The Constant Rate Period</u> of Drying.	51
4.1.	Introduction.	51
4.2.	Mass Transfer.	52
4.2.1.	Evaporation of Water.	52
4.2.1.1.	Procedure.	52
4.2.1.2.	Initial Tests.	53
4.2.1.3.	Repeatability.	54
4.2.1.4.	Air Velocity.	55
4.2.1.5.	Partial Pressure Difference.	57
4.2.1.6.	Comparison of Gradients.	58
4.2.1.7.	Tow Width.	60
4.2.2.	Evaporations of Alcohols.	62
4.2.2.1.	Procedure.	63
4.2.2.2.	Methanol.	64
4.2.2.2.1.	Air Velocity.	65
4.2.2.2.2.	Partial Pressure Difference.	66
4.2.2.3.	Ethanol.	67
4.2.2.3.1.	Air Velocity.	67
4.2.2.3.2.	Partial Pressure Difference.	68
4.2.2.4.	Propanol.	69

4.2.2.4.1.	Air Velocity.	69
4.2.2.4.2.	Partial Pressure Difference.	70
4.2.2.5.	N-butanol.	71
4.2.2.5.1.	Air Velocity.	71
4.2.2.5.2.	Partial Pressure Difference.	72
4.2.3.	Evaporation of Trichloroethylene.	73
4.2.3.1.	Procedure.	73
4.2.3.2.	Air Velocity.	74
4.2.3.3.	Partial Pressure Difference.	75
4.2.4.	Comparison of Results.	76
4.2.4.1.	Schmidt Group.	77
4.3.	Heat Transfer.	79
4.3.1.	Heat Transfer to a Continuous Tow.	79
4.3.2.	Evaporation of Water.	80
4.3.2.1.	Air Velocity.	80
4.3.2.2.	Tow Width.	80
4.3.3.	Evaporation of Other Liquids.	81
4.3.4.	Comparison of Results.	81
4.4.	Discussion.	84
4.4.1.	Introduction.	84
4.4.2.	Present System.	85
4.4.3.	Mass Transfer.	86
4.4.3.2.	Schmidt Group.	87

4.4.3.3.	Comparison with Correlations from Similar Systems.	88
4.4.4.	Heat Transfer.	89
4.4.5.	Heat and Mass Transfer.	90
4.4.6.	Application of j-Factors.	95
5.	<u>Results - Part 2: Falling Rate Period of Drying.</u>	96
5.1.	Introduction.	96
5.2.	Procedure.	96
5.3.	Results.	97
5.3.1.	Air Velocity.	99
5.3.2.	Air Temperature.	100
5.3.3.	Air Humidity.	100
5.4.	Discussion.	101
	<u>Nomenclature</u>	104
	<u>References</u>	106
	<u>Appendix I</u>	111
	<u>Appendix II</u>	117
	<u>Appendix III</u> - Tables I-X	119-146

Summary

The previous experimental and theoretical work on the relationships between the rates of heat and mass transfer was reviewed. Experimental work was conducted in order to accumulate sufficient data on the system of a gas flowing over an object of rectangular cross-section so that the rates of heat transfer, mass transfer, might be related to the flow characteristics of the system, expressed in terms of the Reynolds group.

The experimental work was carried out in a pilot plant continuous fibre drier. The fibre, moving through the drier, becomes compressed into the form of a continuous slab of rectangular section. In the drier, the air flows at right angles to one of the two larger surfaces of the fibre tow, giving the system desired. Water was evaporated from the fibre tow and the rates of heat and mass transfer measured during the constant rate period of drying over a wide range of air conditions. The following equations were used to correlate the results,

$$\frac{hd_l}{D} = f(Re, Sc)$$

$$Nu = f(Re, Pr)$$

In order to investigate the effect of the Schmidt group, liquids of varying physical properties, were evaporated from the fibre tow, the experiments being similar to those carried out with water. The results

were correlated by the following equations,

$$\text{Mass Transfer} \quad \frac{h_d l}{D} = 0.24 \text{ Re}^{0.76} \text{ Sc}^{0.33}$$

$$\text{Heat Transfer} \quad \text{Nu} = 0.32 \text{ Re}^{0.70} \text{ Pr}^{0.33}$$

The rates of heat and mass transfer were compared using j factors and j_d/j_h was found to be 1.05.

The drying characteristics of a continuous fibre drier were also investigated and the rate of drying during the constant rate period was found to be given by,

$$\frac{dw}{de} = 5.58 \times 10^{-6} (p_s - p_a) v^{0.74}$$

No method was found of predicting the critical moisture content under varying air conditions. The factors influencing the rate of drying during the falling rate period were also investigated and diffusion was found to be the controlling factor in the drying of fibre tows. Investigations into the falling rate period were carried out by comparing the drying curve to that for diffusion from a porous slab. The time taken for the fibre to dry from the critical moisture content W_o to some other value of moisture content (W) is given by the equation

$$\ln \frac{W - W_e}{W_o - W_e} = \frac{\pi^2 D_F}{4 a^2} e$$

The diffusion coefficient, D_F , was found to be influenced by

temperature, humidity, and air velocity. The effect of velocity was found to be related to the diffusion coefficient by the relationship,

$$D_F \propto v^{0.83}$$

However the effects of temperature and humidity could not be expressed in mathematical terms.

In order to obtain the relationship for the falling rate period, the equilibrium moisture contents over a wide range of ambient air conditions were measured.

Introduction

The processes of heat and mass transfer are basic to the many diverse operations of the chemical industry. In many of these operations, such as distillation, evaporation, drying, etc., heat and mass transfer occur simultaneously and are interrelated. The complete understanding of this relationship is desirable to enable the accurate designing of process equipment. The types of investigation into heat and mass transfer have varied widely, from the theoretical studies of workers such as Nusselt⁽¹⁾, to the empirical evaluations of specific pieces of process equipment.

The system which has attracted most investigation is that of a fluid flowing over a surface with heat flowing from the fluid to the surface and mass from the surface to the fluid. One of the main difficulties associated with this work has been the lack of knowledge of the region immediately adjacent to the surface. Several theories have been advanced, notably Prandtl's⁽²⁾ boundary layer theory. The experimental work relating to this system has been concentrated on the investigation of the relationship between skin friction, heat and mass transfer. In certain systems it has been shown that skin friction is related to the turbulence of the fluid⁽³⁾. Thus attempts have been made over the last forty years to relate turbulence to heat, and mass, transfer with a view to obtaining a relationship between heat and mass transfer. Interest in this

relationship is mainly due to the fact that in certain cases it is difficult to obtain, accurately, mass transfer data. Whereas the corresponding heat transfer data is relatively easy to obtain. Thus it follows that a relationship between heat and mass transfer would be extremely valuable in such cases. The systems investigated have been many and varied as there has always arisen some doubt as to the applicability of data obtained from one system to another system with entirely different flow characteristics. This factor is extremely important as in the basic units of the chemical industry the variations in flow characteristics are very wide. Thus it is desirable to apply the theoretical and semi-empirical relationships proposed to as many systems as possible.

BOUNDARY LAYER DIAGRAM

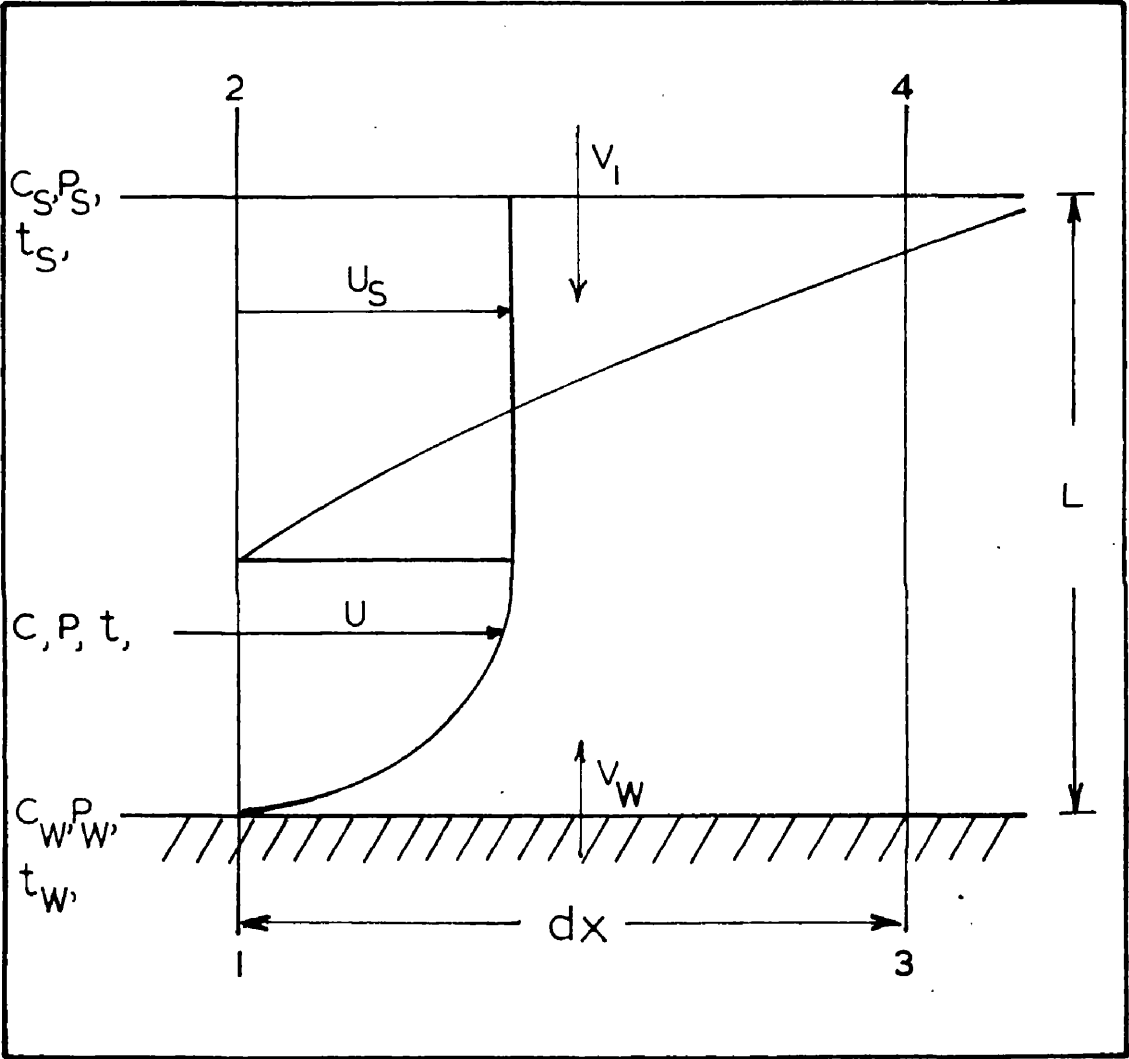


FIG. I. I.

1.2. Boundary Layer Equations for Heat and Mass Transfer.

When a gas flows over a liquid surface, any liquid vaporised is transported away largely by convection, the diffusion process being confined to a small region near the surface. The process is analogous to a heat transfer process where heat is transported away by conduction through the boundary layer and by convection outside it. The zone within which there is a measurable partial pressure gradient is called the mass transfer boundary layer. At the surface there is also a velocity boundary layer which may be of different thickness. Thus in a process such as drying where there is simultaneous heat and mass transfer we have three superimposed boundary layers.

Consider an elementary volume with dimensions dx and L near the surface from which there is mass transfer as in fig. 1.1. Let the normal to the plane be of unit length and the length L be greater than any of the boundary layer thicknesses. The velocity of the main gas stream outside the boundary layer is given by u_s , the temperature by t_s , and the partial pressure, of the vaporised liquid, by p_s , or the concentration by c_s . The surface velocity is zero, the temperature t_w , the vapour pressure p_w , and the vapour concentration c_w . At any distance y from the surface within the boundary layer, the respective values of velocity, temperature, partial pressure, and concentration are u , t , p , and c_v . The total pressure

P is assumed to be constant on any plane normal to the surface within the boundary layer since the boundary layer is small.

Mass transfer through the plane 1-2 is $\int_0^L \rho u \, dy$ and over the length dx changes by $\frac{d}{dx} \int_0^L \rho u \, dy \, dx$. In the steady state the same amount must enter through the planes 1-3 and 2-4. On the surface the velocity is v_w and the velocity through 2-4 is v_1 , therefore by continuity,

$$v_1 = \frac{d}{dx} \int_0^L \rho u \, dy - v_w \dots \dots \dots (1.1)$$

assuming the density ρ to be constant.

Since it is under steady state conditions the mass carried by the flow through the plane 1-2 and out of it through the plane 3-4 must enter the volume through the planes 1-3 and 2-4. Let the mass velocity of the vapour at the surface be w_{vw} .

Hence,

$$w_{vw} = \frac{d}{dx} \int_0^L c u \, dy - v_1 c_s \dots \dots \dots (1.2)$$

Substituting for v_1 and using partial pressures instead of concentrations,

$$\frac{d}{dx} \int_0^L (p_s - p) u \, dy - v_w p_s = -R_v T w_{vw} \dots \dots \dots (1.3)$$

Considering the process as the steady state diffusion of the vapour through the nondiffusing gas, it can be shown that,

$$w_v = - \frac{D}{R_v T} \cdot \frac{P}{P - p} \cdot \frac{dp}{dx} \dots \dots \dots (1.4)$$

Hence,

$$\frac{d}{dx} \int_0^L (p_s - p)u \, dy = D \left(\frac{dp}{dy} \right)_w + v_w (p_s - p_w) \dots \dots (1.5)$$

The heat flow equation is found in a similar manner using a heat balance on the volume element.

$$\text{Heat flow per unit area } q_w = \frac{d}{dx} \int_0^L C_p t u \, dy - C_p t_s v_1 \dots (1.6)$$

Heat is transferred by conduction and convection with the evaporating liquid.

$$q_w = -k \left(\frac{dt}{dy} \right)_w + C_p t_w v_w \dots \dots \dots (1.7)$$

C_p is the specific heat at constant pressure per unit volume.

Using the continuity equation, equation (1.6) becomes

$$\frac{d}{dx} \int_0^L (t_s - t)u \, dy = \alpha \left(\frac{dt}{dy} \right)_w + (t_s - t_w)v_w \dots \dots (1.8)$$

If there is no mass transfer then the term v_w is zero and the equation for heat transfer is as follows,

$$\frac{d}{dx} \int_0^L (t_s - t)u \, dy = \alpha \left(\frac{dt}{dy} \right)_w \dots \dots \dots (1.9)$$

Considering equations (1.5) and (1.8), if the partial pressure differences are small compared with the total pressure, the term v_w is negligible and can be omitted. This results in the similarity equations of Nusselt⁽¹⁾ and Schmidt⁽⁴⁾.

Heat Transfer

$$\frac{d}{dx} \int_0^L (t_s - t)u \, dy = \alpha \left(\frac{dt}{dy} \right)_w \dots \dots \dots (1.9a)$$

Mass Transfer

$$\frac{d}{dx} \int_0^L (p_s - p)u \, dy = D \left(\frac{dp}{dy} \right)_w \dots \dots \dots (1.10)$$

Since the equations are similar in form and similar to equation (1.9) which is for heat transfer alone, the solutions for all three equations must be similar.

The above equations are insoluble since the relationships between the terms t , p , u and y are unknown. They have, however, been used by Eckert⁽⁵⁾ to indicate the dimensionless groups which are related.

$$\text{Let } v' = \frac{t_s - t}{t_s - t_w}, \quad u' = \frac{u}{u_s}, \quad y' = \frac{y}{x}, \quad dy' = \frac{dy}{x}, \\ dx = \frac{dx}{x}, \quad L' = \frac{L}{x}, \quad \text{all of which are dimensionless.}$$

From equation (1.9),

$$u_s \frac{d}{dx'} \int_0^{L'} (1 - v')u' \, dy' = \frac{\alpha}{x} \left(\frac{dv'}{dy'} \right)_w \dots \dots \dots (1.11)$$

Divide by u_s ,

$$\frac{d}{dx'} \int_0^L (1 - v') u' dy' = \frac{\alpha}{x \cdot u_s} \left(\frac{dv'}{dy'} \right)_w \dots \dots \dots (1.12)$$

The dimensionless group $\frac{u_s x}{\alpha}$ is called the Peclet number.

$$\frac{d}{dx'} \int_0^L (1 - v') u' dy' = \frac{1}{Pe} \left(\frac{dv'}{dy'} \right)_w \dots \dots \dots (1.13)$$

$$v' = f(u', y', Pe) \dots \dots \dots (1.14)$$

From the corresponding equation for momentum transfer using a similar method it can be shown that,

$$u' = f(y', Re)$$

Hence $v' = f(y', Re, Pe) \dots \dots \dots (1.15)$

$$\frac{Pe}{Re} = Pr$$

$$v' = f(y', Re, Pr) \dots \dots \dots (1.16)$$

$$q = -h(t_s - t) = -k \left(\frac{dv}{dy} \right)_w \dots \dots \dots (1.17)$$

In dimensionless form this becomes

$$\frac{hx}{k} = \left(\frac{dv'}{dy'} \right)_w \dots \dots \dots (1.18)$$

The left-hand side is the Nusselt number. From equation (1.16), v' is a function of the distance from the wall, y' , Reynolds number, and the Prandtl number. Hence the same must be true of the

derivative dv'/dy' and the value at the wall must be a function of Reynolds and Prandtl numbers. Therefore

$$Nu = f(Re, Pr) \dots \dots \dots (1.19)$$

Similarly it can be shown that for mass transfer

$$\frac{h_d L}{D} = f(Re, Sc) \dots \dots \dots (1.20)$$

1.3. Theoretical Equations for Heat and Mass Transfer.

The original work was that of Reynolds⁽⁶⁾ who in 1874 deduced the following relationship between heat transfer and friction,

$$\frac{h}{C_p G} = \frac{f}{2} \dots \dots \dots (1.21)$$

This was later extended first by Prandtl⁽²⁾, and then by Taylor⁽⁷⁾, to include a laminar layer near the wall giving the following equation,

$$\frac{h}{C_p G} = \frac{\frac{f}{2}}{1 - r + r(Pr)} \dots \dots \dots (1.22)$$

where r depended on the ratio of the velocity at the edge of the laminar layer and the average velocity of the fluid.

Von Karman⁽⁸⁾ extended the above equation to include allowance for the buffer region and based his velocity profile on the experimental work of Nikuradse⁽⁹⁾.

$$\frac{h}{C_p G} = \frac{\frac{f}{2}}{1 + 5\sqrt{\frac{f}{2}} \left[Pr - 1 + \log_e \left\{ 1 + \frac{5}{6}(Pr - 1) \right\} \right]} \dots \dots (1.23)$$

A similar type of equation was derived by Boelter et al⁽¹⁰⁾.

$$\frac{h}{C_p G} = \frac{\frac{f}{2} (\Delta t_{\max} / \Delta t_m)}{y_1 \left[\text{Pr}_1 + \log_e \left[1 + \text{Pr} \left(\frac{30}{y_1} - 1 \right) \right] + \frac{2.5}{y} \log_e \frac{\text{Re} \sqrt{f}}{60} \right]} \dots (1.24)$$

The above equations are in agreement with the general equation for heat transfer, equation (1.19).

Sherwood⁽¹¹⁾ transformed the heat transfer equation (1.23) into mass transfer form, subsequently equation (1.24) was also transformed. In both instances the procedure was to replace the Prandtl number by the Schmidt number as indicated by the general equations (1.19) and (1.20).

After considering equation (1.22) and the corresponding mass transfer equation,

$$\frac{k_c P_{bm}}{U_{av} P} = \frac{f/2}{1 - a_1 + a_1 \left(\frac{\mu}{\rho D} \right)} \dots (1.25)$$

Chilton and Colburn⁽¹²⁾ found that the correlation for heat transfer could be improved if the term $\text{Pr}^{2/3}$ was substituted for the denominator of the right hand side of equation (1.22) and by analogy suggested that the denominator of equation (1.25) be replaced by $\text{Sc}^{2/3}$. Hence the equations become,

$$j_h = \frac{h}{C_p G} \left(\frac{C_p \mu}{k} \right)^{2/3} = \frac{f}{2} \dots (1.26)$$

$$j_d = \frac{k_c p_{bm}}{U_{av} P} \left(\frac{\mu}{\rho D} \right)^{2/3} = \frac{f}{2} \dots \dots \dots (1.27)$$

The term $\frac{p_{bm}}{P}$ is included because in the transfer in one direction, the concentration of the component B may alter substantially and $\frac{k_c p_{bm}}{P}$ has been found to be more nearly constant than k_c . The terms j_h and j_d have been found to be approximately equal to the friction term $\frac{f}{2}$ for certain cases such as streamline shapes but in cases where the form drag becomes appreciable, e.g. flow past bluff objects, this is no longer true mainly because friction factors are usually calculated from the total drag whereas the above equations refer to skin friction only.

1.4. Review of Experimental Data.

In order to examine how far the theoretical similarities in the processes of heat and mass transfer are confirmed by experiment, the experimental work on several systems which had previously been carried out for both heat and mass transfer was considered.

1.4.1. Heat Transfer.

1.4.1.1. Flow through Pipes.

In this, as in most systems, the variables can be

grouped together in three main groups, mass velocity ($G=\rho V$), a shape factor, and the physical properties of the fluid.

The effect of mass velocity was one of the first to be investigated and was found to be given by the relationship

$$h \propto G^n \quad \dots \dots \dots (1.28)$$

where the power n was quoted by various workers to range between 0.78 and 0.82. It is now generally accepted that the power 0.8 gives the most satisfactory relationship for turbulent flow.

The effect of the shape factor has not been so well established. The shape factor, in this case the diameter of the pipe, is that dimension which determines the velocity profile of the fluid and hence the degree of turbulence in the stream. From theory the relationship predicted is

$$h \propto d^{1-n} \quad \dots \dots \dots (1.29)$$

McAdams quotes a range of values for $(1 - n)$ from -0.16 to -0.26.

However since the range of possible values of d is limited compared to the range of mass velocity the relationship generally accepted is

$$h \propto d^{-0.2} \quad \dots \dots \dots (1.30)$$

The effect of the physical properties of the fluid is expressed in terms of the Prandtl group, $C_p\mu/k$, and since the range of variation for a given fluid is small, the power to which the group

is raised is given by a range of values, 0.3 to 0.4. The value of the power used also depends to a certain extent on whether the viscosity is evaluated at the surface, film, or main fluid temperature.

If the combined effects of the variables are expressed in the following relationship,

$$Nu = k Re^{0.8} Pr^m \dots \dots \dots (1.31)$$

the values of k and m given by various workers are shown below in table 1.1.

Table 1.1.

Author	Ref.	k	m	μ
Hinton	13	0.0281	0.355	μ
Dittus & Boelter	14	0.0243	0.4	μ
Sherwood and Petrie	15	0.024	0.4	μ
Colburn	16	0.023	0.33	μ_f
Sieder & Tate	17	0.027 (μ/μ_s)	0.33	μ, μ_s

If the value of μ is taken at the film temperature, McAdams⁽¹⁸⁾ has shown that the correlation of Sherwood and Petrie⁽¹⁵⁾ which in its original form gave a value of 0.4 for the power of the Prandtl number, is altered such that value is reduced to 0.33. This agrees with the work of Colburn⁽¹⁶⁾ who found that

$$Nu = 0.023 Re^{0.8} Pr^{0.33} \dots \dots \dots (1.32)$$

1.4.1.2. Flow at Right-angles to a Cylinder.

The correlations for this system are in the same general form as those for the previous system.

$$Nu = k Re^m Pr^n \dots \dots \dots (1.33)$$

The powers of the Reynolds number and Prandtl number were obtained by the same general technique as in the previous system, dividing the variables into groups. King and Knaus⁽¹⁹⁾ have obtained the following equation for the case of turbulent flow at right angles to a single cylinder.

$$Nu = 0.38 Re^{0.56} Pr^{0.3} \dots \dots \dots (1.34)$$

In reviewing the work of several workers McAdams⁽²⁰⁾ has recommended that the correlations can only be satisfactory over limited ranges of Reynolds numbers

$$Re = 0.1-1000 \quad Nu = (0.35 + 0.47 Re^{0.52})(Pr^{0.3}) \dots (1.35)$$

$$Re = 1000-50000 \quad Nu = 0.26 Re^{0.6} Pr^{0.3} \dots \dots \dots (1.36)$$

The accuracy claimed for the above correlation is ⁺ - 20 per cent.

1.4.2. Mass Transfer.

1.4.2.1. Wetted Wall Columns.

Extensive work on evaporating pure liquids into an air stream using a wetted wall column was carried out by Gilliland⁽²¹⁾.

J_D VS REYNOLDS NUMBER

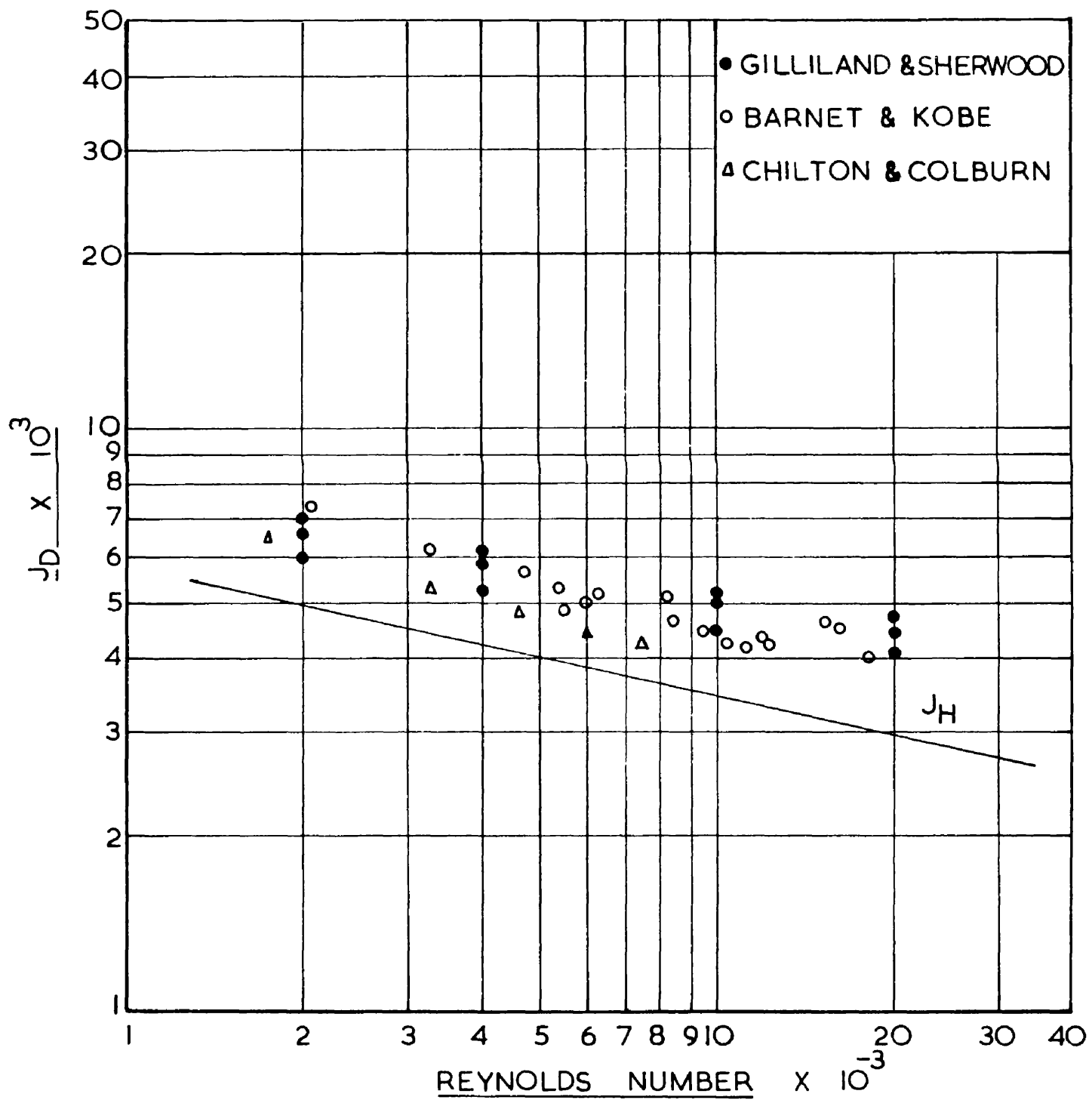


FIG. 1.2.

The liquids vaporised included water, toluene, aniline, chlorobenzene, ethyl acetate, etc. The apparatus consisted of a 1 inch diameter pipe down which the liquid flowed and a gas, air, is blown upwards. The tube was 18 inches long with calming sections at either end. The following empirical equation was derived for the experimental data obtained,

$$\frac{kcd}{D} \frac{P_{Bm}}{P} = 0.023 Re^{0.83} Sc^{0.44} \dots \dots \dots (1.37)$$

The above equation differs from the Chilton-Colburn equation in that the power of the Schmidt number is 0.44 as against 0.67 in equation (1.26). Since the range of Schmidt number investigated was from 0.6 to 2.4 this difference is of little significance.

Similar work has been carried out by other workers including Barnett and Kobe⁽²²⁾, Chilton and Colburn⁽¹²⁾, Uchida and Maeda⁽²³⁾, Kerbs⁽²⁴⁾, Greenwalt⁽²⁵⁾, and Cogan and Cogan⁽²⁶⁾. Typical values for j_d are shown opposite in fig. 1.2. Johnstone and Pigford⁽²⁷⁾ extended this type of work using the wetted wall column for the rectification of liquids. The mixtures used were ethanol-water, acetone - chloroform, benzene - toluene, etc. This gave a range of Schmidt numbers of 0.54 to 0.72. The results were correlated by the following equation,

$$j_d = 0.033 Re^{-0.23} \dots \dots \dots (1.38)$$

These results were confirmed by experimental work of Jackson and

Ceagelske⁽²⁸⁾ who studied 2-pentanol water system under total and partial reflux.

1.4.2.2. Plane Surfaces:

Evaporation for a liquid surface to an air stream is one of a number of standard systems which have been investigated extensively. Such investigations have ranged from those of meteorologists in reservoirs to those of experimenters working in wind tunnels to obtain data on the rates of evaporation of various liquids. It is the latter type of investigation which is of interest in the general study of heat and mass transfer. The earliest studies of evaporation were by Dalton in 1802 who found that the rate of evaporation was proportional to the difference between the vapour pressure of the liquid surface and the partial pressure of the liquid in the air stream. Hinchley and Himus⁽²⁹⁾ confirmed this using small rectangular heated pans in a wind tunnel. They recommended an empirical equation which related k_g as a linear function of the air velocity. Lurie and Michailoff⁽³⁰⁾ studied the rate of evaporation of water from pans flush with the floor of a wind tunnel. The air speed was varied up to 25 ft/sec. Powell and Griffiths⁽³¹⁾ used heated flat horizontal pan which was placed near the centre of a wind tunnel. The surface of the pan was linen which was wetted from the liquid below, the idea being that the linen presented a flat surface parallel to the air flow preventing the air impinging on it

at an angle giving exaggerated results. The rate of evaporation was found to be similar to that from a free liquid surface. This work was extended to organic liquids by Wade⁽³¹⁾ who studied the rates of evaporation of acetone, benzene, ethyl acetate, toluene, trichloroethylene etc. Similar work of this type was also carried out by Hine⁽³³⁾ and Pasquill⁽³⁴⁾. During their investigations Powell and Griffiths⁽³¹⁾ investigated the effect of blunt leading edges and obstructions likely to alter the flow pattern of the fluid. They found that by placing a ridge in front of the leading edge of the wet surface the rate of evaporation could be increased by up to 30 per cent when the height of the obstruction was 3 inches. This demonstrates the care required in comparing work of this type.

Some of the experimental data obtained by the above has been transformed by Coulson and Richardson⁽³⁵⁾ into j factor form and is shown in fig. 1.3. with the equation for heat transfer included for comparison.

1.4.2.3. Cylinders.

The system of a fluid flowing at right angles to the axis of a cylinder has been investigated by several workers. Powell⁽³⁶⁾ used eight cylinders of various diameters, 0.046 to 14.6 in., and varied the air speed up to a maximum of 32 ft/sec. He only considered the case where water was evaporating from the wet surface of a cylinder. Lohrisch⁽³⁷⁾ considered the system where water was being absorbed

MASS TRANSFER TO OR FROM A CYLINDER

J_D VS REYNOLDS NUMBER

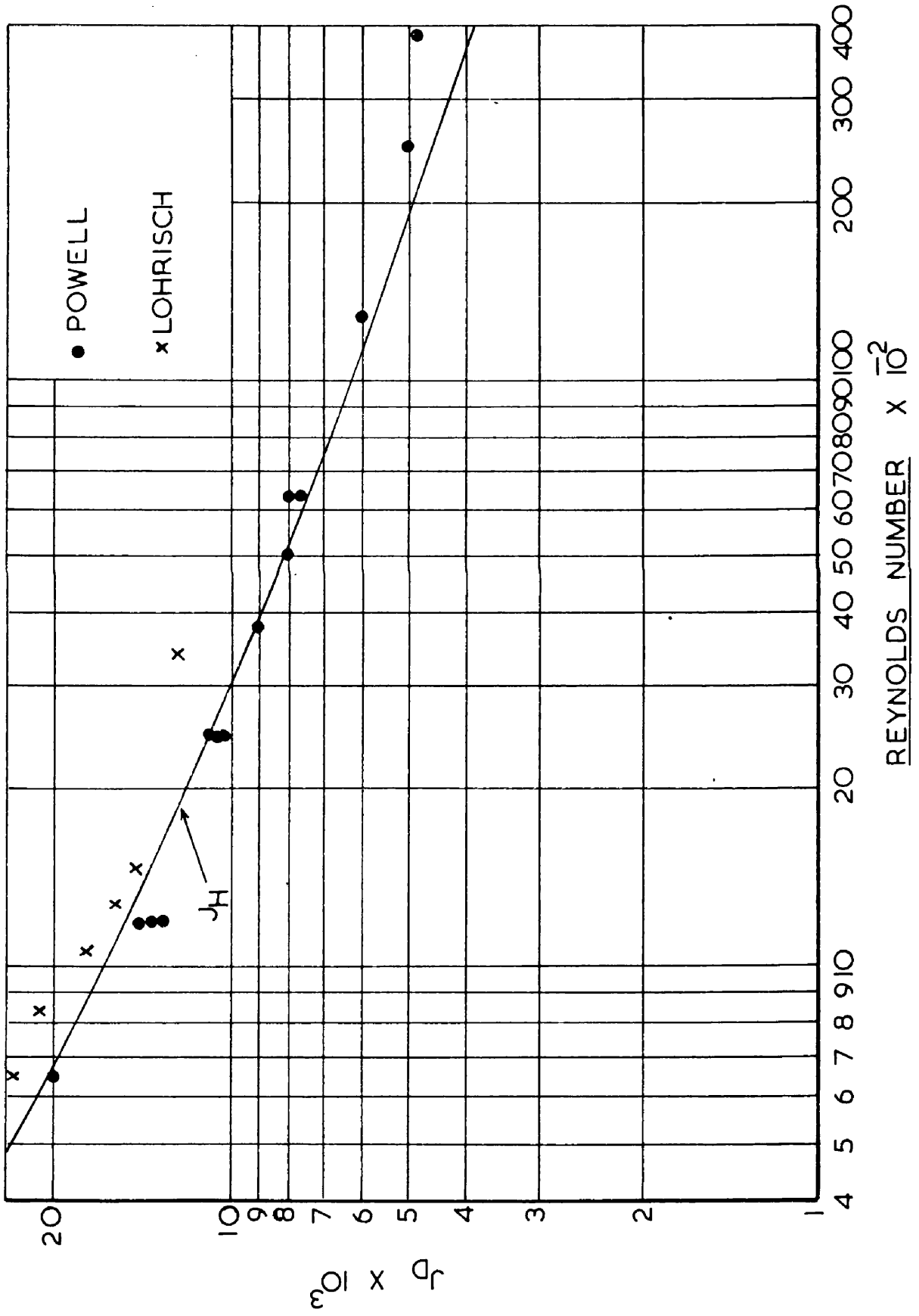


FIG. 1.4.

by solid cylinders of caustic and also the system where ammonia was absorbed by cylinders wetted with phosphoric acid. The results of Powell and Lorisich agree with the Chilton-Colburn equation and are shown in fig 1.4. Vint⁽³⁸⁾ extended the work of Powell to include other liquids, toluene, and n-butyl alcohol. Other systems investigated include the rate of solution of cylinders of benzoic acid into water. This work was carried out by Linton⁽³⁹⁾ who also studied the rates of solution of cinnamic acid. The effect of turbulence on the rates of heat and mass transfer from wet cylinders was studied by Comings, Clapp, and Taylor⁽⁴⁰⁾. By increasing the turbulence by the use of turbulence promoters, they were able to increase j_h by from 2 - 20 per cent by an increase of about 25 per cent in turbulence. Maisel⁽⁴¹⁾ found that the mass transfer coefficient could be increased by as much as 50 per cent by increasing the turbulence by from 3.5 to 24 per cent.

1.4.2.4. Spheres.

Mass transfer to spheres in a turbulent air stream has been investigated by several workers. In several instances they have correlated their data in a form other than the simple power form of equation (1.19) used in the previous systems. In order to compare most of the data the following general equation was used,

$$Sh = A + B Re.^m Sc.^n \quad (1.3)$$

The values obtained by several investigators are shown in table 1.2.

Table 1.2.

Author	Ref.	A	B	m	n	Range of Re
Frossling	42	2	0.55	0.50	0.33	2-2000
Powell	36	0	0.33	0.59	-	650-45000
Williams	43	0	0.43	0.56	0.33	400
Garner and Grafton	44	44	0.48	0.50	0.33	100-1000
Garner and Suckling	45	2	0.95	0.50	0.33	50-600

1.4.3. Conclusions from Review of Experimental and Theoretical Data.

From the review of data the similarities between the processes of heat and mass transfer, as indicated by equations (1.19) and (1.20) are partially substantiated. If one system, flow of a fluid through a pipe, is taken as representative, it can be seen that while for heat transfer the relationship is

$$Nu = 0.023 Re^{0.8} Pr^{0.33} \dots \dots \dots (1.32)$$

the corresponding system for mass transfer leads to the following expression

$$\frac{kcd}{D} \frac{P_{Bm}}{P} = 0.023 Re^{0.83} Sc^{0.44} \dots \dots \dots (1.37)$$

There are slight differences in the powers of the Reynolds groups in both equations as well as the differences between the powers of Prandtl and Schmidt groups. The significance of these differences is shown in

fig.1.2. where the data of Gilliland, on which equation (1.37) was based and several others is compared to the corresponding j_h values. It appears that in general when heat and mass transfer is expressed in terms of j_h and j_d the term j_d is slightly greater than j_h . This slight inequality has been confirmed by Gamson et al.⁽⁴⁶⁾ and several other workers^(47, 48). The actual extent to which the recorded variations in this inequality depend on the system being investigated is uncertain and requires further investigation.

EVAPORATION FROM FIBRE TOWS.

Evaporation from Fibre Tows

From the previous section it is evident that there are several features which are desirable in a system whose heat and mass transfer characteristics are to be investigated. Of primary importance is the geometry of the system which should be simple as it is difficult to assess the effects of the physical dimensions on the degree of turbulence in a complex system. In order to limit the number of complications the system should be a single film one, thus requiring the effects of diffusion through one film only to be considered. It is also desirable that steady state conditions should be maintained throughout the investigation. Hence the continuous fibre drier was chosen as fulfilling the above requirements.

2.2. Continuous Fibre Drier.

The continuous fibre drier is in essence a rectangular sectioned object of indefinite length over which an air stream passes at right angles to the surface. This system was studied by Powell⁽³⁶⁾ for the purpose of comparing the results with those obtained in the system where the air stream is parallel to the surface. Powell used a pan in a wind tunnel for the experimental work.

In investigating a system of this type one of the most important factors influencing the rate of evaporation is flow pattern of air stream surrounding the object. In this system there are two possibilities (a) as shown in fig. 2.1., where there is a region of

FLOW PATTERN PAST OBJECT

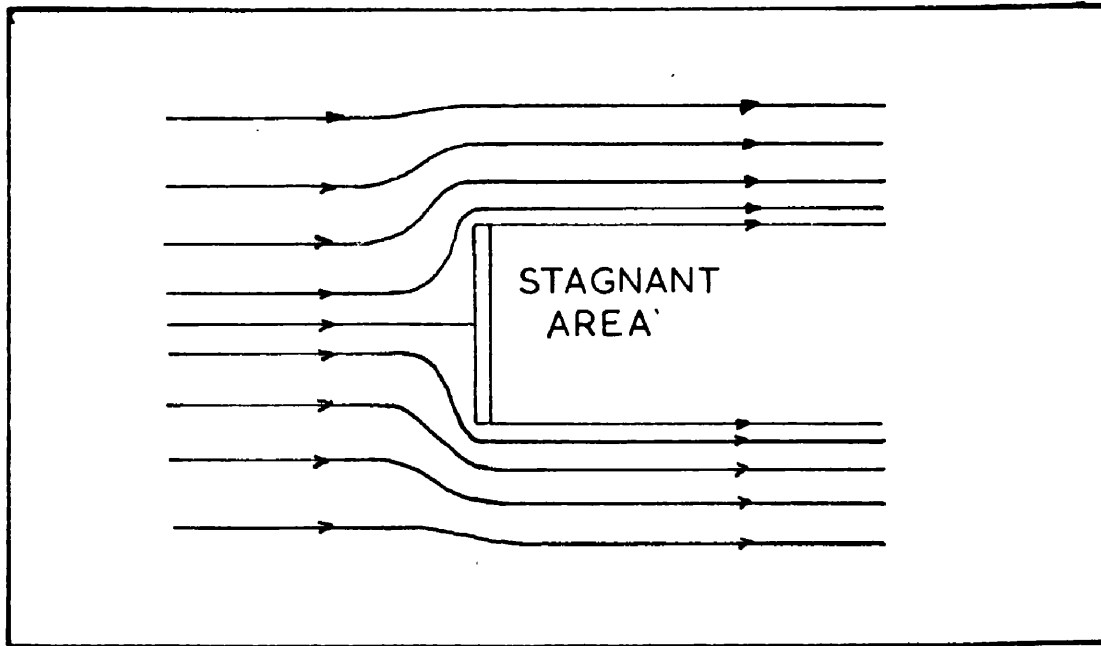


FIG. 2.1.

FLOW PATTERN PAST OBJECT

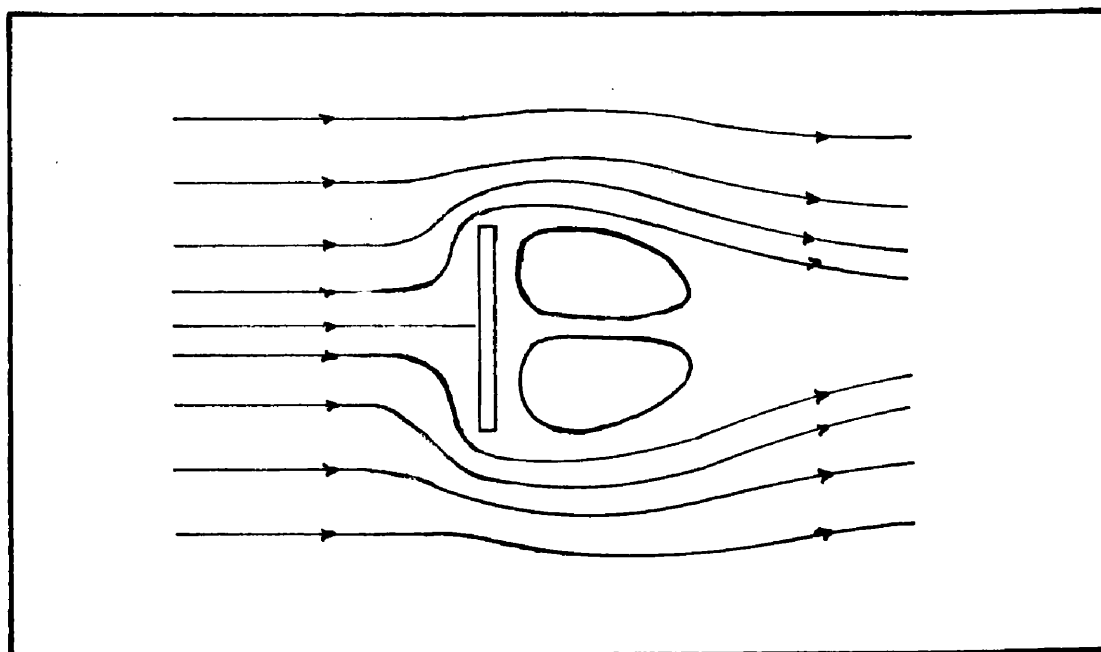


FIG. 2.2.

static air near the down stream surface of the object, (b) as shown in fig. 2.2. where the stream lines join forming a vortex street. The latter is more likely as in his investigations into rates of evaporation Powell measured the rates of evaporation from the down stream surface and found them to be not very much lower than those of the up stream surface. Other proof available is the fact that experimental drag coefficient is considerably greater than the theoretical value⁽⁴⁹⁾ calculated on the basis of a flow of the type in fig. 2.1.

Since it is impossible to measure the rates of evaporation from the individual surfaces in the present apparatus the total evaporation is used as the basis of calculation although the type of flow is different in both surfaces. This is similar to the basis used in the study of heat and mass transfer from cylinders and spheres.

2.3. Drying.

Drying is a term which is usually used when referring to the process of evaporating liquid from a solid by means of heat, usually accompanied by the removal of the vapour by a gas. It is a process which takes place in stages depending on the liquid content of the solid. In general there are four main stages, (a) this stage covers the period when the solid is heating up to the wet bulb temperature of the ambient gas, (b) during this period the

solid appears to act as a liquid surface and the rate of evaporation is controlled by the same laws, (c) there is now insufficient liquid at the surface to saturate the gas in contact with it and the rate of evaporation is controlled by the rate at which the liquid moves to the surface, (d) the surface is now dry and the plane of separation of the liquid and the gas has retreated within the solid. The period (a) is of little importance, period (b) is considered to be governed by the same laws as a free liquid surface. This has been demonstrated by Powell⁽³⁶⁾, and Gilliland⁽⁵⁰⁾ has shown that the rates of evaporation during this period are independent of the materials from which they are evaporated. The values for the rates of evaporation under constant conditions are given in table 2.1.

Table 2.1.

Material	Rate of Evaporation $\frac{\text{lb.}}{\text{ft}^2\text{hr.}}$
Water	0.55
Whiting pigment	0.427
Sand	0.407 - 0.488
Clays	0.468 - 0.55

The rate of drying under these conditions is calculated using the equation obtained for the diffusion of a vapour from a liquid into a gas.

$$\frac{dw}{de} = K_g a (p_s - p_a) \dots \dots \dots (2.1)$$

where $\frac{dw}{de}$ is the rate of evaporation lb/hr., K_g is the mass transfer coefficient.

p_s is the vapour pressure of the liquid at the surface temperature.

p_a is the partial pressure of the liquid vapour in the gas.

a is the surface area.

If h is the heat transfer coefficient from the air to the wet surface and Δt is the temperature difference between the air and the surface, it follows that,

$$\frac{dw}{de} = \frac{h a \Delta t}{\alpha} \quad \text{where } \alpha \text{ is the latent heat. . . (2.2)}$$

The rate of evaporation is also a function of the velocity of the gas stream and the direction of the gas flow. Powell and Griffiths⁽⁵¹⁾ found that it also depended on the shape of the surface, obtaining the following equation,

Velocity u , between 100 and 300 cm/sec.

$$\frac{dw}{de} = 2.12 \times 10^{-7} L^{0.77} B (p_s - p_a) (1 + 0.212 u^{0.85}) \dots (2.3)$$

where L and B are the length and breadth of the surface.

During the periods (b) and (c) the rate of evaporation tends to fall with the decrease in the moisture content of the solid. The controlling factors in the falling rate period are very complex. In several instances one particular factor is so

dominant that the effects of the others can be neglected. The two factors which have been found to be most important are diffusion and capillary action. The texture of the material and the manner in which the moisture is bound to the solid determines which is the most important.

2.3.2. Movement of Liquid within a Material during the Falling - Rate Period.

2.3.2.1. Movement by Diffusion.

When the surface layer of moisture on a material has been partially removed, the surface concentration is then lower than the concentration in the layers below the surface, thus setting up a concentration gradient. This gradient causes the moisture to migrate toward the surface. This migration has been compared to a state of unsteady state diffusion in one direction. The general equation for a process of this type is

$$\frac{dw}{de} = D \frac{d^2w}{dx^2} \dots \dots \dots (2.4)$$

where W is the moisture concentration

e is the time

D is the diffusivity

x is the distance from the centre of the material to the surface.

Sherwood⁽⁵²⁾ and later Newman⁽⁵³⁾ applied the above

equation to problems of diffusion from various differently shaped objects, a slab, a cylinder, and a sphere. The most useful one being the slab with sealed edges.

Consider a slab of thickness $2a$, W as the moisture content at any time e , W_0 is the moisture content at the beginning of the diffusion period, W_e is the equilibrium moisture content, the equation becomes

$$\frac{W - W_e}{W_0 - W_e} = \frac{8}{\pi^2} \left\{ e^{-De(\frac{\pi}{2a})^2} + \frac{1}{9} e^{-9De(\frac{\pi}{2a})^2} + \dots \right\} \dots (2.5)$$

It was also stated that a simplified version of the above equation gave a fairly good correlation for the falling rate period.

$$e = \frac{4a^2}{D\pi^2} \ln \frac{W - W_e}{W_0 - W_e} \dots \dots \dots (2.6)$$

This form of equation is applicable only when e is large. Newman also gave other simple expressions for the falling rate period.

The above expressions assume that D , the diffusivity, is constant and that W_e is also constant. The diffusivity has been found to be influenced by moisture content, humidity, and temperature. The variations in diffusivity due to these factors was noted by Bateman, Hoff, and Stamm⁽⁵⁴⁾, and also by Hougen, McCauley, and Marshall⁽⁵⁵⁾. The latter commented on the limitations of this type of approach and the types of materials to which it is applicable. Van Ardsel⁽⁵⁶⁾

considered integrations of equation allowing for variations in diffusivity, developing a graphical method allowing for the variations due to moisture content in the drying of hydrophobic solids at low moisture contents.

In diffusion studies, the resistance of the solid to moisture movement is referred to as the permeability when the driving force is vapour pressure, and diffusivity when the driving force is moisture concentration. The diffusivity is related to the permeability by the following expression,

$$D = \frac{P}{s} \frac{dp}{dT} \dots \dots \dots (2.7)$$

where $\frac{dp}{dT}$ is the moisture content - vapour pressure isotherm of the material. If the permeability varies the diffusion equation becomes,

$$\frac{dT}{de} = \frac{1}{s} \frac{d}{dx} \left(P \frac{dp}{dx} \right) \dots \dots \dots (2.8)$$

where s is the mass of dry solid per unit volume.

Using this equation Van Arsdol⁽⁵⁶⁾ evaluated approximate numerical solutions for an infinite slab, a sphere, and also a long cylinder. He also investigated the relationship between the change of permeability with moisture content and the drying rate curves. He found that the curves were comparable but there was no simple relationship between the shape of the permeability curve and the form of the drying rate curve.

2.3.2.2. Capillary Control.

When the moisture associated with the solid is bound to it in the pores of the material as a liquid it is subject to movement by gravity and capillarity if the pores are continuous. This is sometimes the case in textiles, paper and leather as well as granular solids.

Water may flow from regions of low concentration to those of high concentration if the pore size is suitable. It was for this and other reasons that Ceaglske and Hougen⁽⁵⁷⁾ suggested the Capillary theory. The importance of the pore spaces between the granular particles was first noted by Slichter⁽⁵⁸⁾ when studying the movement of moisture in soils. Later this work was enlarged by Haines⁽⁵⁹⁾ who showed that various configurations were possible in beds of spheres.

When water evaporates from a bed of spheres, the water recedes in the waists between the particles of the top layer and a suction potential is developed in the liquid. When the menisci of these cubical waists have receded to the narrowest section, the suction potential at the surface can be expressed as

$$h_s = \frac{4.28\sigma}{r\rho g} \dots \dots \dots (2.9)$$

σ = the surface tension

r = the radius of the sphere

ρ = density of the liquid.

Further evaporation results in h_s increasing so that the menisci on the surface cubical waists will collapse and the larger pores will open. As h_s steadily increases the entry suction of the progressively smaller surface waists will be reached so that the menisci collapse into the adjacent pores which are thereby opened.

Since most granular materials are of non-uniform particles, the suction potential cannot be calculated and must be found experimentally by methods used by Haines⁽⁶⁰⁾ and Newitt et al.⁽⁶¹⁾ or in the case of textiles the methods of Preston and Nimkar⁽⁶²⁾.

2.3.3. Through-Circulation Drying.

The through circulation drying of various materials, ranging from steel pellets to seaweed, has been investigated thoroughly resulting in the publication of a large amount of data. Marshall and Houghen⁽⁶³⁾ investigated the drying characteristics of various different materials. They found that the drying rate during the constant rate period could be given by the expression,

$$\frac{dw}{de} = k G^{0.81} (H_s - H_a) \dots \dots \dots (2.10)$$

where G = air velocity

H_s = saturation humidity

H_a = air humidity

k varied from 3 for clays to 220 for fibres. Similar type of investigation was carried out by Gamson et al.⁽⁴⁶⁾ who studied the

through circulation drying of catalyst pellets and correlated their results with the following equation,

$$\frac{dw}{de} = \frac{0.42 a G^{0.59} \Delta H_m}{\rho D_p^{0.41}}$$

where D_p = mean particle size (ft.)

ρ = bulk density (lb/ft³)

a = drying area (ft²/ft³)

ΔH = log. mean humidity difference (lb/lb).

G = mass velocity ($\frac{\text{lb. dry air}}{\text{hr. ft.}^2}$)

$$\frac{dw}{de} = \frac{\text{lb. water}}{\text{hr. lb. dry material}}$$

Wilke and Hougen⁽⁶⁴⁾ extended the work of Gamson et al.⁽⁴⁶⁾ to streamline flow and gave expressions for the constant rate period.

A large proportion of the work on through circulation drying has been done with particular reference to the drying of fruits and vegetables. Marshall⁽⁶⁵⁾ gave details of experiments using fruits and vegetables at different loadings, also varying the air temperature and velocity. He suggested that correlations for the constant rate period could be more reliably correlated using heat transfer coefficients. He suggested the following correlation,

$$\frac{dw}{de} = h A (t_a - t_s) \dots \dots \dots (2.12)$$

Brown, Kilpatrick and Van Arsdel⁽⁶⁶⁾ presented their experimental data on the drying of potatoes in the form of a nomograph. Special attention was paid to the problem of obtaining an even air flow distribution. This was achieved using a perforated sheet giving a high pressure drop across it. Ede and Hales⁽⁶⁷⁾ investigating the dehydration of fruit and vegetables found that through circulation drying was more suitable for fruit than vegetables which tend to shrink and matt giving uneven air flow conditions. Other products which have been dried in this manner include grain, grass, sugar beet, meat, and seaweed. Of the latter group of materials, Gardner and Mitchell⁽⁶⁸⁾, and later Potts and Mitchell⁽⁶⁹⁾, employed wet bulb depression methods to establish a prediction method for certain varieties of seaweed. This investigation was extended to include a general study of vegetable materials by Potts and Mitchell⁽⁶⁹⁾, and Hughes and Mitchell⁽⁷⁰⁾, who applied single layer techniques to deeper beds.

2.3.4. Drying of Textiles.

The drying of textiles is usually performed with the yarn in skein form. The drying of rayon skeins was investigated by Simons, Koffolt, and Withrow⁽⁷¹⁾ who dried yarn which had been previously centrifuged. They used a through circulation drier. placing the skeins on trays. The air conditions were varied widely, temperature, humidity and mass throughput. Since the material had been centrifuged before

drying the results cover the falling rate period only. They were found to satisfy the following equation,

$$\frac{dw}{de} = 1.24 G^{1.47} \Delta H. W. \dots \dots \dots (2.13)$$

where dw/de = rate of drying lb/hr. per lb. dry stock

G = mass throughput lb/min per sq.ft. area

ΔH = humidity difference

W = free moisture content of stock.

The through circulation drying of rayon staple was studied by Coles⁽⁷²⁾.

The drying of thick porous bodies was investigated by Nissan, Kaye, and Bell⁽⁷³⁾. They studied the falling rate period of the drying of terylene which had been woven and wound on to a bobbin with an aerodynamically shaped end. The bobbin was placed in a wind tunnel such that the terylene surface was parallel to the air stream. The experiments were repeated using wool in place of terylene. From the results of their studies of the rates of heat transfer and the temperature distribution at various depths, they proposed a pseudo wet-bulb temperature for the falling rate period. Much of the work on the drying of textiles has been conducted with a view to studying the rates of drying of various materials when manufactured into different types of garments. An example of this type of work is that of Coplan⁽⁷⁴⁾ who dried socks of various synthetic fibres.

2.3.5. Textile Driers.

The type of drier most widely used in the textile industry is the tunnel drier. This consists of a continuously moving belt on which are hooked skeins of yarn. Air is blown past the yarn as it moves through the drier. This type of drier has the disadvantage of discontinuity at the entrance and exit of the drier. The yarn has to be in skein form before it can be dried thus the drier cannot be used where a continuous fibre tow is desired.

There are two types of driers which are used to dry continuous fibre tows, the through circulation conveyor type and the continuous tension type. In the former the fibre is fed continuously on to a chain type conveyor belt, the feed scanning the width of the belt to spread the fibre evenly in a single layer over the entire area of the belt. The air is blown through the fibre and recirculated. This type of drier tends to have interruptions in continuity due to entanglement at the off take end of the conveyor. This can be overcome to a certain extent by withdrawing the fibre vertically downwards from a secondary split conveyor belt. The alternative is to use the continuous tension type of drier.

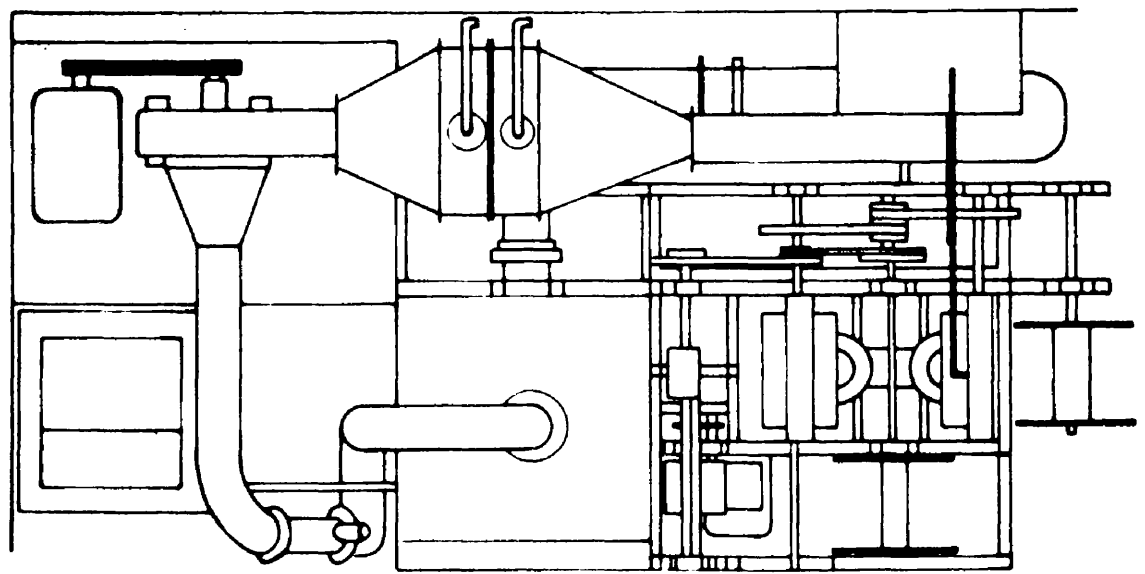
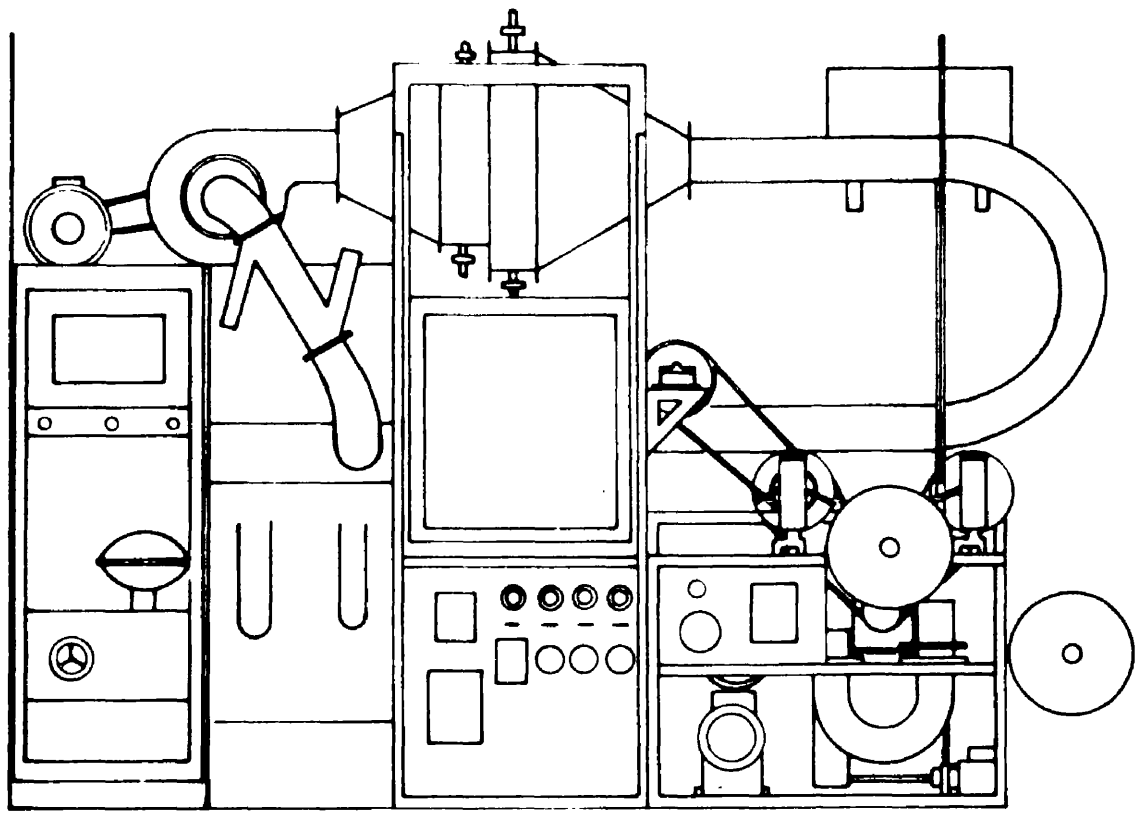
In the continuous tension drier the fibre is wound on to a drum under tension. Air is blown out from the central shaft of the cage through the fibre. The fibre which is wound round the cage many times is moved along the cage either by using a skew roller or a tapered

cage. The tension at the off-take end of the cage is maintained by a pair of adjustable rollers.

2.4. Artificial Fibres.

The main fibre used in the experimental work was Ardil, a protein fibre, and for comparison several experiments were carried out using Terylene, a polyester fibre. These two fibres are representative of the two main groups into which artificial fibres can be subdivided. The two groups are generally referred to under the following headings, Regenerated Protein and synthetic. These two groups have very distinct differences in their properties, in general protein fibres are hydrophylic whereas synthetic fibres are hydrophobic. This example of the difference in properties is very important in the drying of the fibres.

APPARATUS AND PROCEDURE.



Continuous Fibre Drier.

Fig. 3. 1.

3.1. Apparatus.

The apparatus used was the continuous fibre drier shown in fig.3.1. The drier consists of a high pressure centrifugal blower which discharges air into a heater. The hot air from the heater passes through lagged flexible ducting to the drying drum, entering the drum through the hollow shaft and flowing out radially through the holes in the shaft wall. The air from the diffuser passes over the fibre which is wound round the perimeter of the drum. The drum is totally enclosed in a lagged compartment. The air extracted from the compartment, or drying box, and the amount recirculated is controlled by a system of butterfly valves.

The fibre is drawn off the storage drum by a pair of adjustable rollers, then passing through a U-tube in which water flows co-current with the fibre tow. On leaving the U-tube the fibre is pressed between a second pair of rollers which remove a large proportion of the associated moisture. The fibre is then put under tension by passing it over a tensioning roller. The tension is increased as the fibre passes from the tension roller to the main drying drum. On leaving the tension roller the fibre passes through the inlet in the side of the drying box before being wound, between eight and eighteen times, round the drum and the skew roller. The fibre, leaving the drum, passes through the outlet in the box wall on to the off-take rollers, again under additional tension. From the

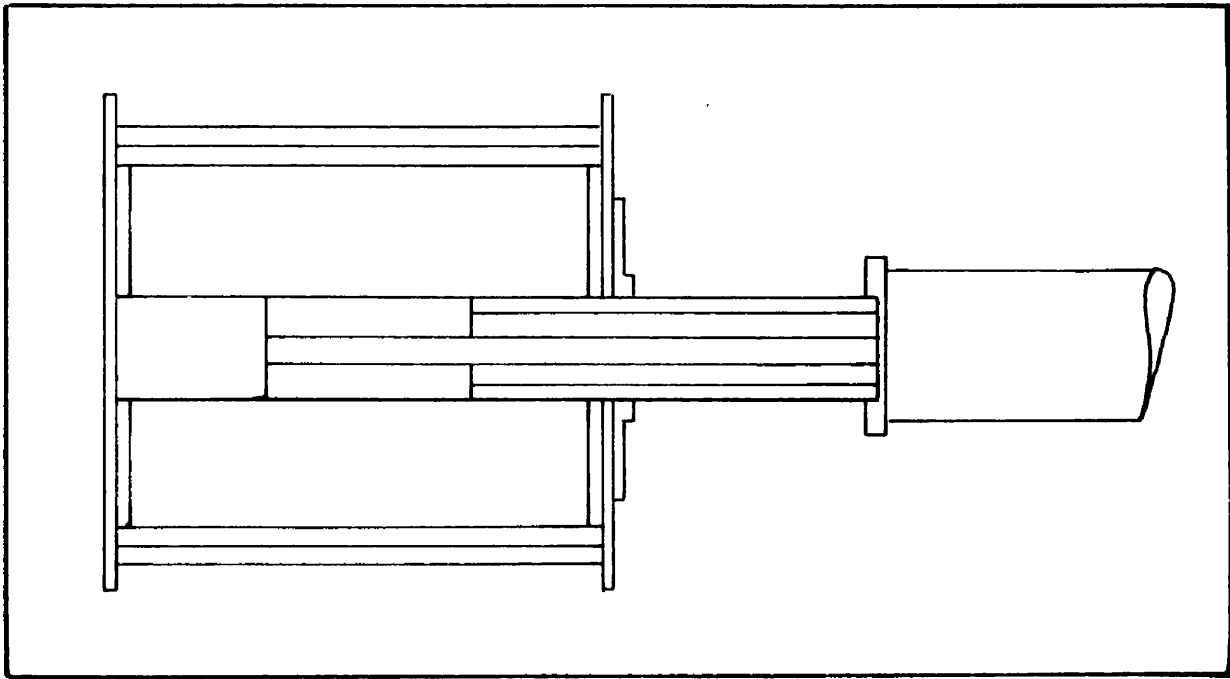


FIG.3.2. SECTIONAL VIEW OF DRYING DRUM

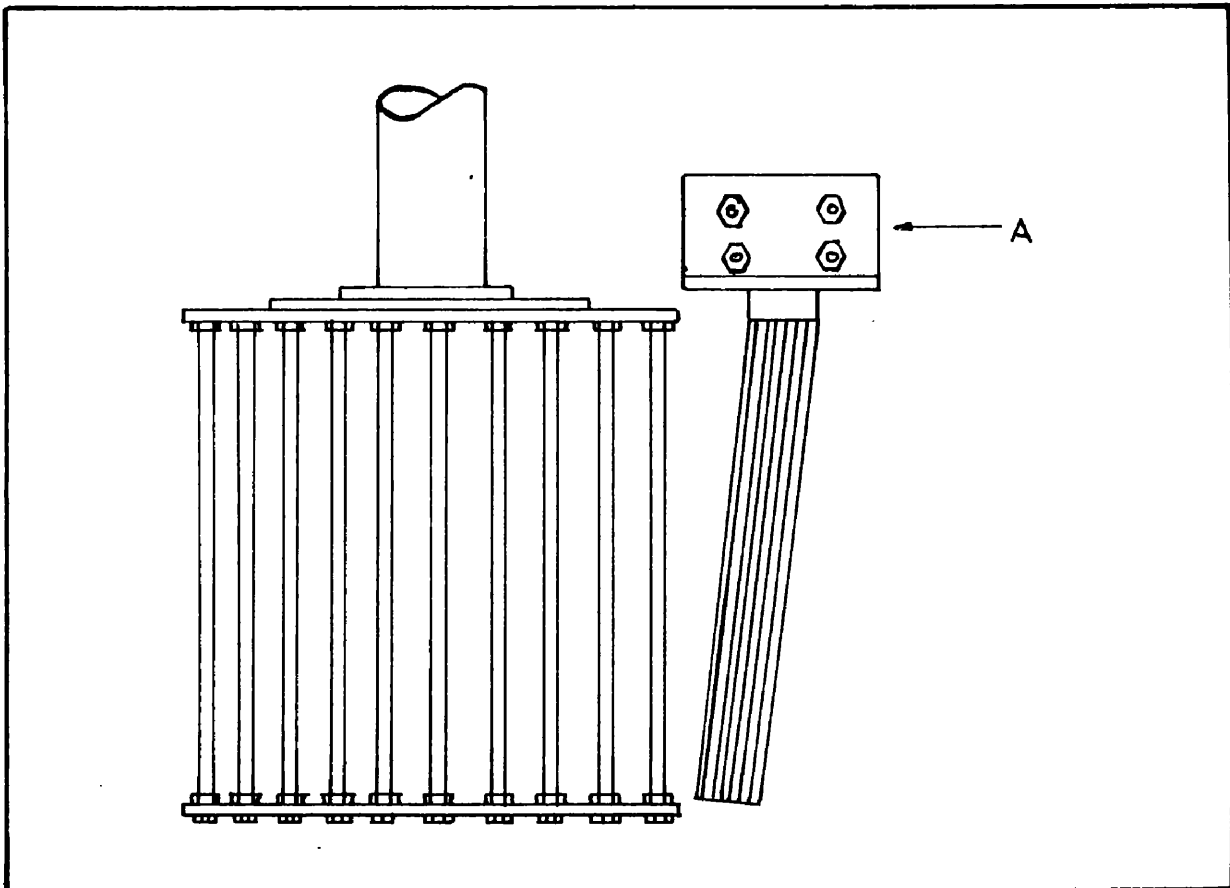


FIG.3.3. DRYING DRUM & SKEW ROLLER

off-take rollers the fibre is wound on to a storage drum.

3.1.2. Drying Drum.

The drying drum, shown in fig. 3.2 consists of a $4 \frac{3}{8}$ " dia. hollow shaft on to which are bolted two stainless steel, $16 \frac{1}{4}$ " dia., plates. The drum shape is completed by 16, $1 \frac{1}{2}$ " dia., stainless steel rods which are bolted to each of the end plates. The shaft is supported on two 1" white metal bearings and driven by a 9" dia. The shaft has $\frac{3}{4}$ " dia. holes at 1" centres drilled in the wall between the two end plates. Each of the holes has a piece of angled blading press fitted into it to varying depths depending on the position along the shaft and in addition there are deflector plates along the shaft at regular intervals. The blading and the deflector plates are made of aluminium. Wire mesh is wound round wooden formers which are 14" dia. The drum also carries two seal rings which prevent air leakage from the drying compartment where the shaft passes through the wall and from the flexible ducting where it joins the shaft.

3.1.3. Skew Roller.

The skew roller is a 2" dia. stainless steel shaft with a bearing at one end. The bearing is carried in an end plate. This end plate is bolted to a fixed plate (A in fig. 3.3) in such a manner that the axis of the roller can be altered relative to the plate A. This is achieved by six screws, three of which are screwed

through the plate A and press on the end plate of the roller. These screws fix the position of the roller. The other three screws pass through the clearing holes in plate A and are screwed into the roller end plate. The latter screws fix the roller to the plate A and lock it in the angle fixed by the other three screws.

3.1.4. Drying Compartment.

The drying compartment is a box constructed of 1/4" thick asbestos sheet and lagged with 1" thick fibreglass insulation. There is a window on one side which allows access to the drying drum which is inside the compartment. The window is of double glass with a 1/8" space between the sheets. It is opened by lifting vertically and can be locked in the upper position. One of the walls has two 4" squares cut out of it to allow the fibre in and out of the compartment. The inlet and outlet have perspex sliding windows to cut down leakage to a minimum. Extraction ducts are connected to the top and bottom of the compartment.

3.1.5. Heater System.

During the initial period of operation of the plant an electric heater was used, however latterly, when solvents other than water were used it was necessary to install a steam heated exchanger.

3.1.5.1. Electric Heater.

The electric heater was constructed of 1/4" thick asbestos sheet. It was 12" square in cross-section and 36" long, including the end pieces to connect the heater to the fan outlet at one end and to the circular ducting at the other. The end pieces were of sheet metal and the whole heater was lagged with 1" thick fibreglass insulation. The interior of the heater was subdivided by baffles which were supported on rods fixed to the base of the heater. Holes were bored in the baffles, nichrome coils were woven through them and the ends of the coils were connected to a panel on the outside of the heater. Four coils were used in the heater, one with a maximum output of 4 kw. on a 250 volt supply, the other three each have an output of 2 kw. Each of the heating coils could be switched on individually. One of the 2 kw. heaters was connected to a Variac voltage regulator. This arrangement allowed the total input of the heater to be varied over a range 0-10 kw. with a fine degree of control. The Variac was linked to an air actuated motor, the input to which was controlled by a Honeywell-Brown three term controller. The input signal to the controller was the voltage from a thermocouple placed in the duct leading to the drying drum. The controller maintained the air temperature to within + or - 1/2 a degree centigrade.

3.1.5.2. Steam Heater.

The steam heater was fabricated with sheet steel. It consists of two separate banks of heaters bolted together and to the end pieces which join them to the fan and the ducting as in the electric heater. Each bank of tubes consists of two rows of finned tubes. Each bank of tubes can be controlled individually. The steam heater also has provision for injecting live steam into the air duct.

3.1.6. U - Tube.

The U-tube is made of glass and has an overflow which connects it to an overflow tank. The overflow tank is connected to a centrifugal pump which pumps the solvent to an overhead tank which is fitted with a thermostatically controlled heater. The feed from the tank to the U-tube is by gravity. A proportion of the feed is used to spray the fibre as it passes through the first set of rollers.

3.1.7. Transmission.

The power to drive the drying drum and the ancillary rollers is taken from a Kopp Variator motor. The motor is connected to the first lay-shaft by a chain drive with no speed reduction. The first lay-shaft drives the second with a 2:1 reduction in speed. The second lay-shaft transmits power to the drying drum through a clutch without any further reduction in speed. The output side of the clutch

is connected to a third lay-shaft, the speed being increased by 3.04 : 1. There is a further increase in speed in the drive connecting the third lay-shaft to the off-take rollers. The off-take rollers consist of three rollers, two rubber rollers which are driven and a third roller which is of aluminium and is free running. The aluminium roller can be adjusted to give variations in the pressure between it and the other two rollers.

The first lay-shaft drives the tension roller with a 2:1 increase in speed. A drive from the tension roller connects it to the second pair of rollers with another increase in speed of 1.81 : 1. The two pairs of rollers are connected to a Croft speed variator which allows the speed of the first pair to be altered relative to the second pair. There is also a drive from the second pair of rollers to the shaft which carries the exit storage drum. There is a friction clutch on the shaft which is adjusted so that it slips when any tension occurs as the fibre is wound on to the drum.

3.1.8. Instrumentation.

3.1.8.1. Air Temperature.

The air temperature is controlled and continuously recorded by a three term automatic controller. This gives the temperature of the air stream at a position in the duct before it enters the drier. The corresponding temperature of the air as it

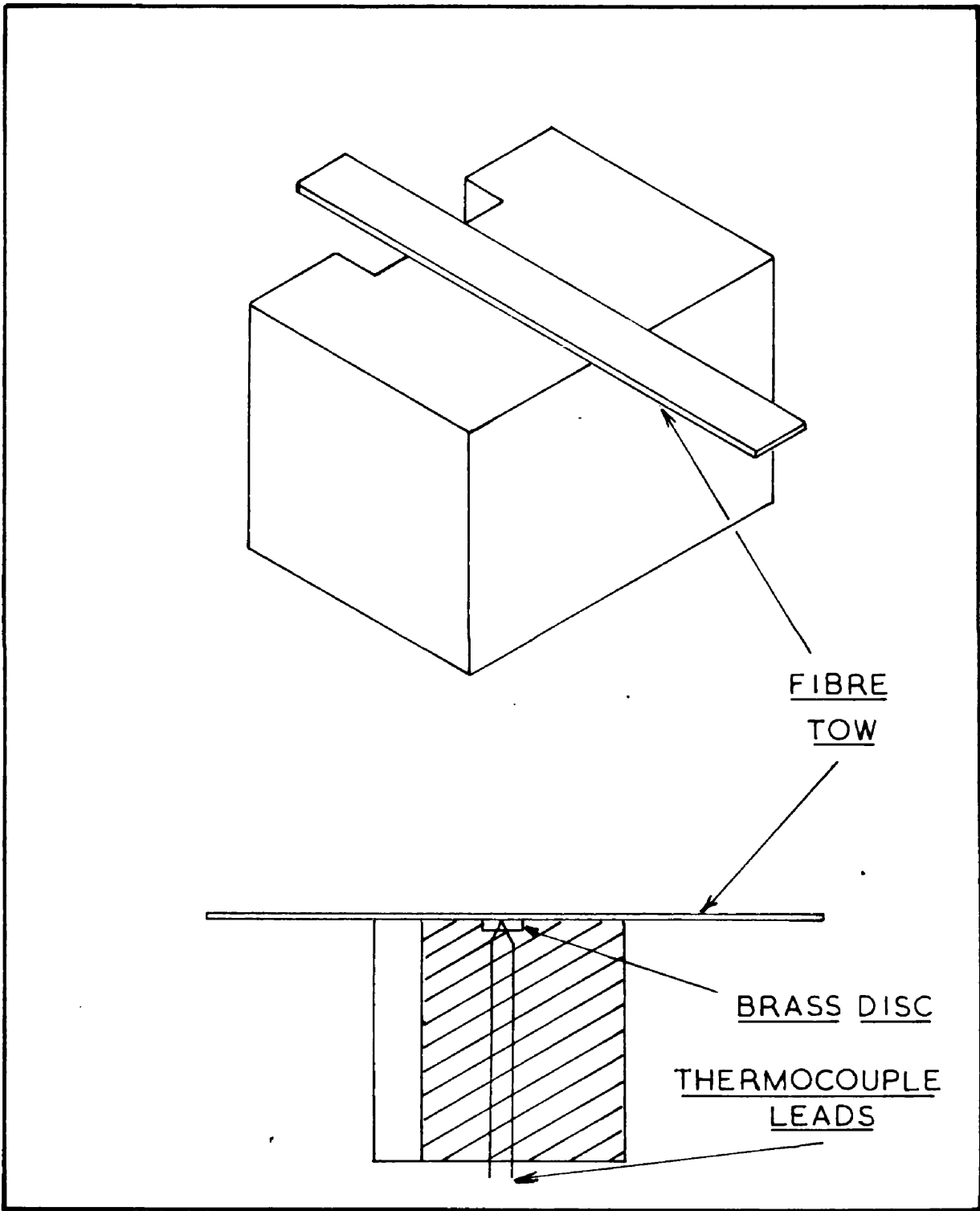


FIG.3.4. SURFACE TEMPERATURE MEASUREMENT BLOCKS

passes over the fibre is obtained by calibrating the drier with the drum at rest. Thus a series of calibration graphs are obtained for each temperature and air throughout.

3.1.8.2. Fibre Temperature.

The surface temperature of the fibre is measured indirectly since the ambient temperature in the drying compartment is greater than that of the surface. A thermocouple is used to measure the temperature difference between the air stream and the surface, using the surface as the cold junction. Hence the temperature of the surface could be calculated as the temperature of the air is known. The cold junction is embedded in a plastic block, as shown in fig.3.4 to prevent it becoming entangled with the fibre and also to enable the ambient air to be excluded from the area around the junction. The latter condition is achieved by arranging the block so that it is pressing against the fibre tow. This arrangement has the disadvantage of tending to interfere with the moisture distribution, so this method was only used in those experiments where the falling rate period was being investigated, as the effect at such low values of moisture content appeared to be negligible. During the constant rate period it was found that reliable results could be obtained by measuring the temperature, using a block as shown in fig. 3.4 at the outlet from the drying compartment. The effect of friction heating the block appeared to be negligible.

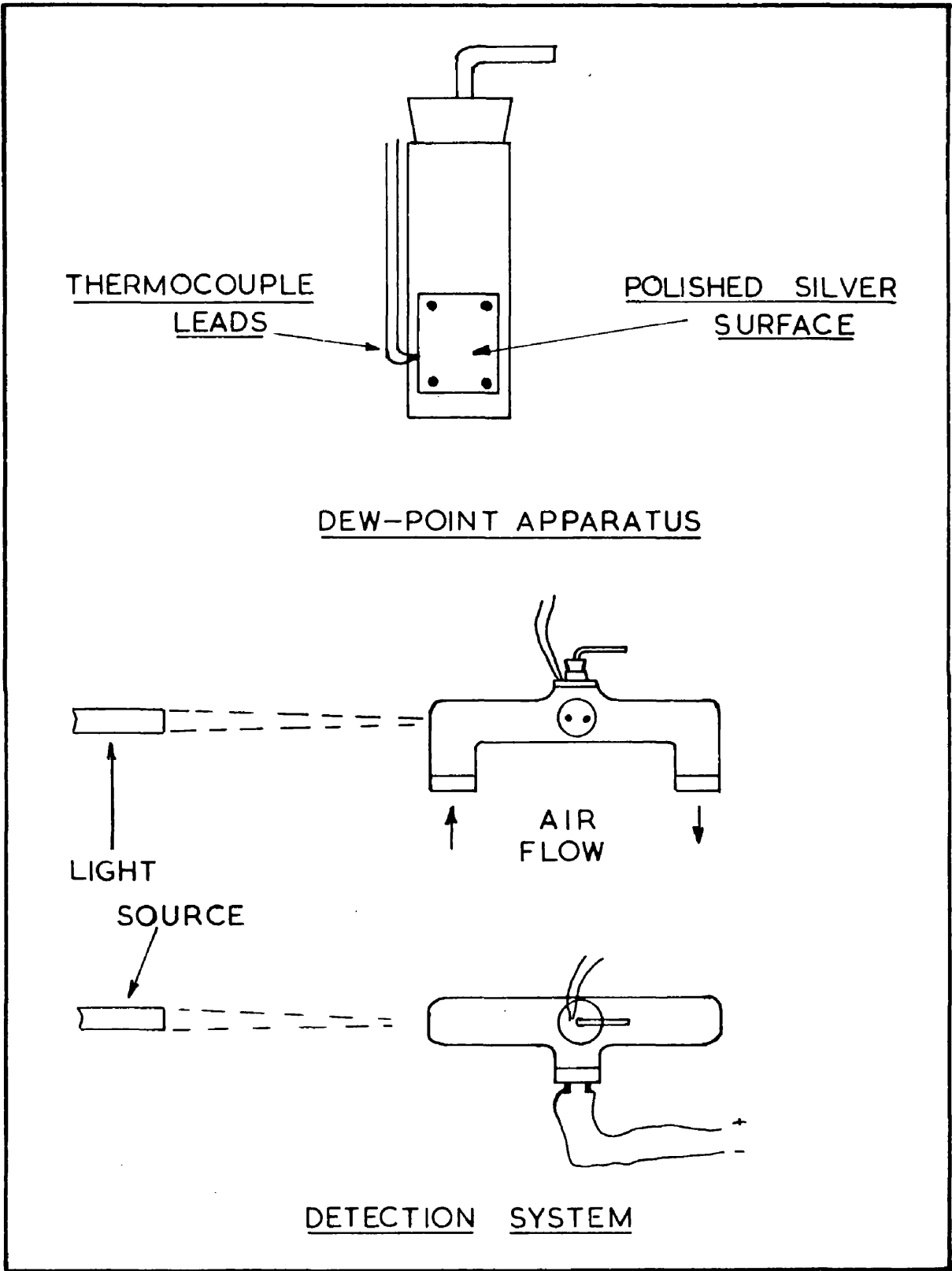


FIG. 3.5.

3.1.8.3. Humidity.

The humidity in the circulating air is measured in two ways, (a) wet and dry thermometers, (b) dew-point apparatus.

The principle of the dew-point apparatus is that, when the temperature of a highly polished metal surface is lowered, at a certain temperature the surface becomes clouded. This cloudiness is due to the vapour in the air stream condensing on the cold surface. The temperature at which this cloudiness first appears is called the Dew-point and the vapour pressure corresponding to this temperature gives the vapour pressure of the liquid present in the air stream.

The apparatus, shown in fig. 3.5 consists of a copper tube with 1/2" x 1/4" piece of 24 S.W.G. silver inserted in the lower half. Another piece of silver of similar shape is screwed on to the first with a thermocouple inserted in a groove between them. The surface of the top sheet of silver is highly polished and cleaned carefully to remove any trace of grease. The surface is cooled by a refrigerant which flows through a tube down the centre of the cylinder and out through a hole at the top. As the free volume is small and the throughput of refrigerant large, the instrument is responsive to changes in the temperature of the coolant. The refrigerant used is air which passes through a cold trap to remove most of the associated moisture, then through a calcium chloride drying tube to remove the remaining moisture, and finally through a cooling coil which is

immersed in a mixture of acetone and carbon dioxide. The temperature of the polished surface is regulated by the amount of refrigerant which is passed through the cylinder.

The detection system is shown in fig. 3.5. A beam of light is focused on the highly polished silver surface and the reflected light from it is measured by a photo-cell. The current from the photo-cell is measured by a ballistic galvanometer. As the surface becomes cloudy, the light reflected by the surface is scattered and hence the amount detected by the photo-cell decreased. In order to eliminate light reflected from the other surfaces two masks were placed in front of the photo-cell and all other surfaces were painted with flat black paint.

The apparatus is used in the following way. The temperature of the surface is lowered slowly and as the surface starts to cloud, the galvanometer reading falls slowly at first and then more rapidly as the size and number of the droplets increases. The throughput of the coolant is decreased until the surface temperature has risen sufficiently to make the galvanometer reading return to its original value. The procedure is then repeated and the temperature at which the galvanometer reading just begins to fall is noted as the dew-point.

In order to study the characteristics of the instrument the output from the photo-cell was for a time connected

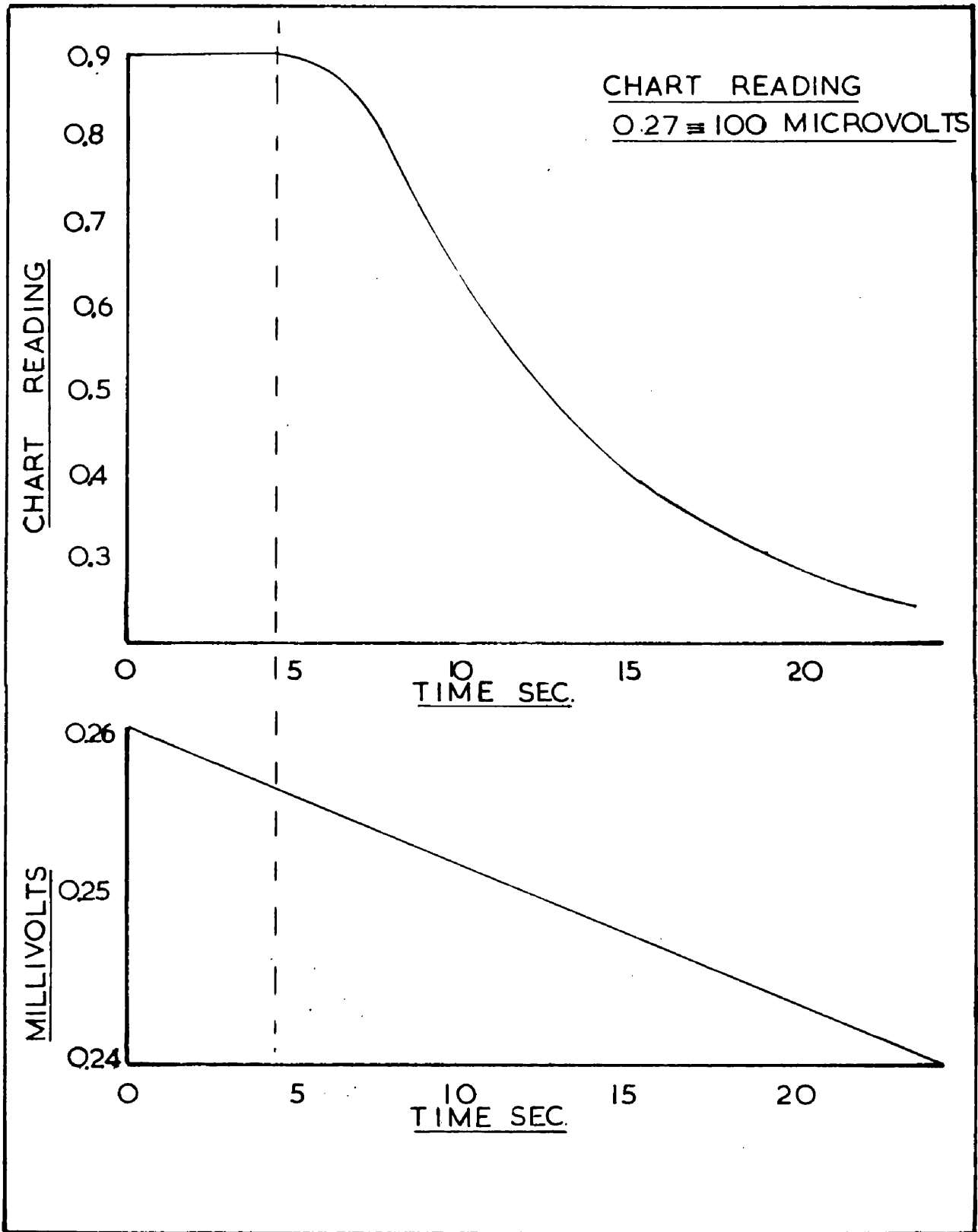


FIG.3.6 CHARACTERISTICS OF DETECTION
SYSTEM

via an amplifier to a recorder. Thus a continuous record of the photo-cell output was obtained. At the same time the rate of change of temperature with time was noted, allowing the prediction of the dew point to be made much more accurately. The characteristics of the instrument are shown in fig. 3.6. The ideal for an instrument of this type would be two synchronised recorders enabling very accurate measurements to be made. Using the ballistic galvanometer the accuracy was found to be within $1/2$ a degree centrigade.

3.1.8.4. Air Flow.

The amount of air circulating in the system is measured by a calibrated orifice plate. The pressure drop across the orifice plate is measured by a manometer. Using this value and the free area for flow at the drum perimeter, the average velocity of the air as it passed the fibre can be calculated. In order that the distribution along the drum could be measured, an instrument had to be developed to measure very low air velocities. The type of instrument which was reputed to have the desired characteristics was the heated thermocouple anemometer.

The instrument developed was based on the anemometer
(75)
of Lowe and Hawes who developed their instrument from the original heated thermocouple anemometer of W.V. Hukill of the U.S. Dept. of Agriculture. The sensing element of the instrument is shown in fig. 3.7 and consists of two thermocouples in opposition, one of the junctions

HEATED THERMOCOUPLE ANEMOMETER

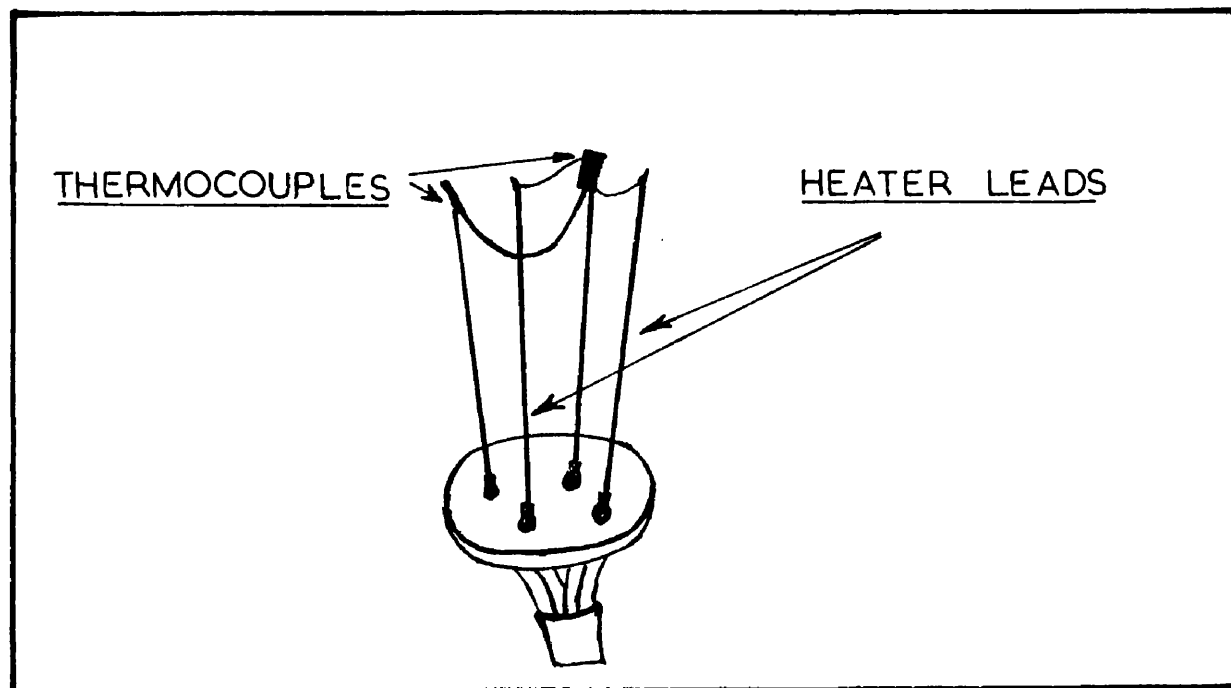


FIG. 3.7.

CIRCUIT DIAGRAM

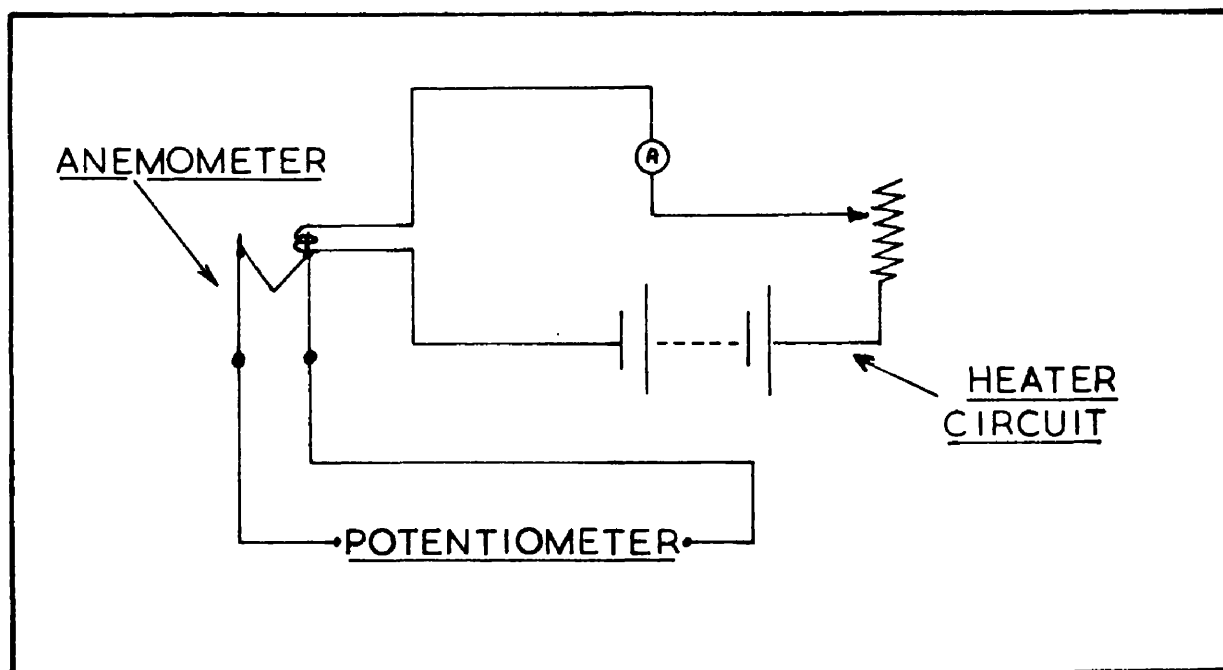


FIG. 3.8.

ANEMOMETER CALIBRATION CHART

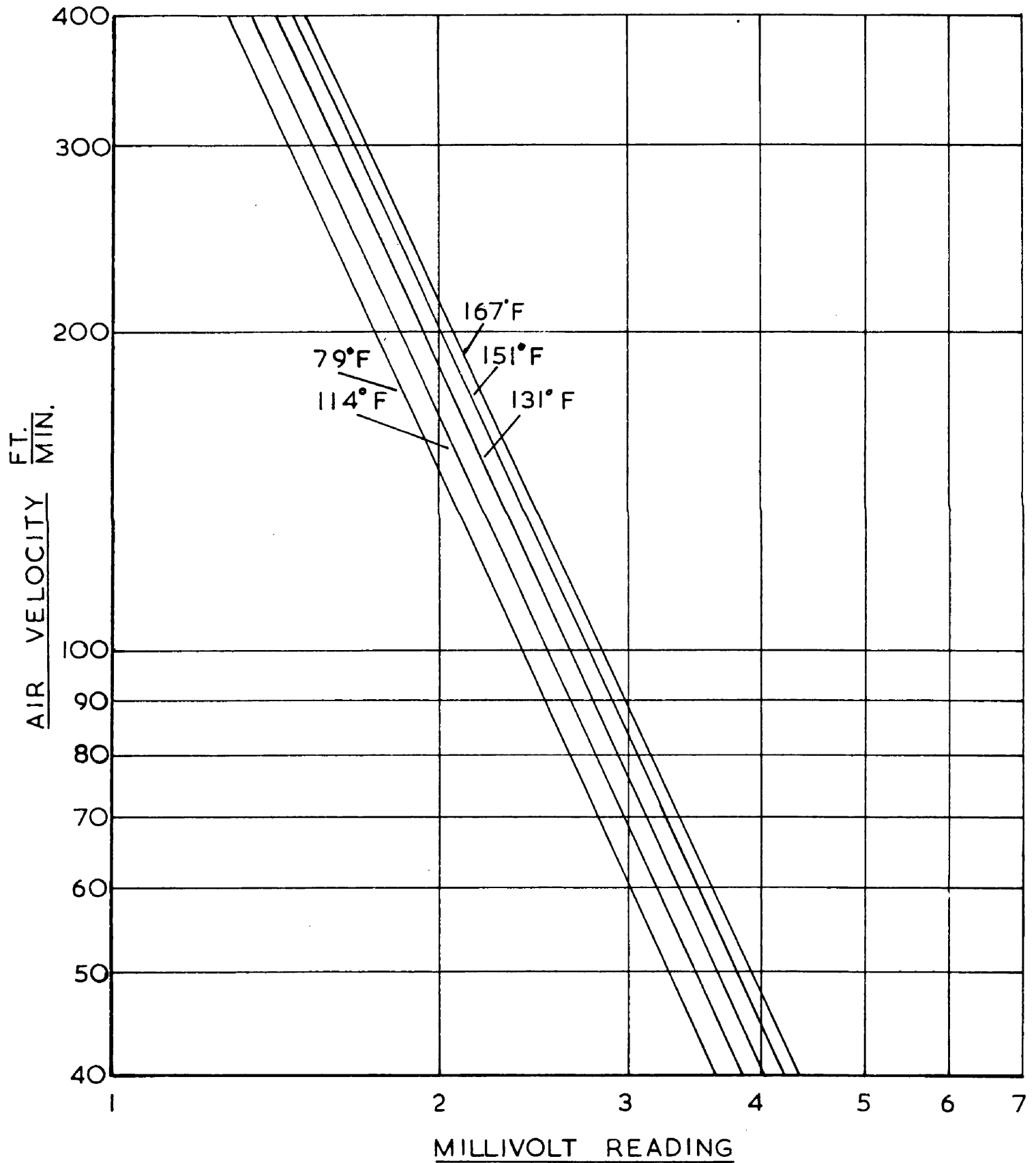


FIG. 3.9.

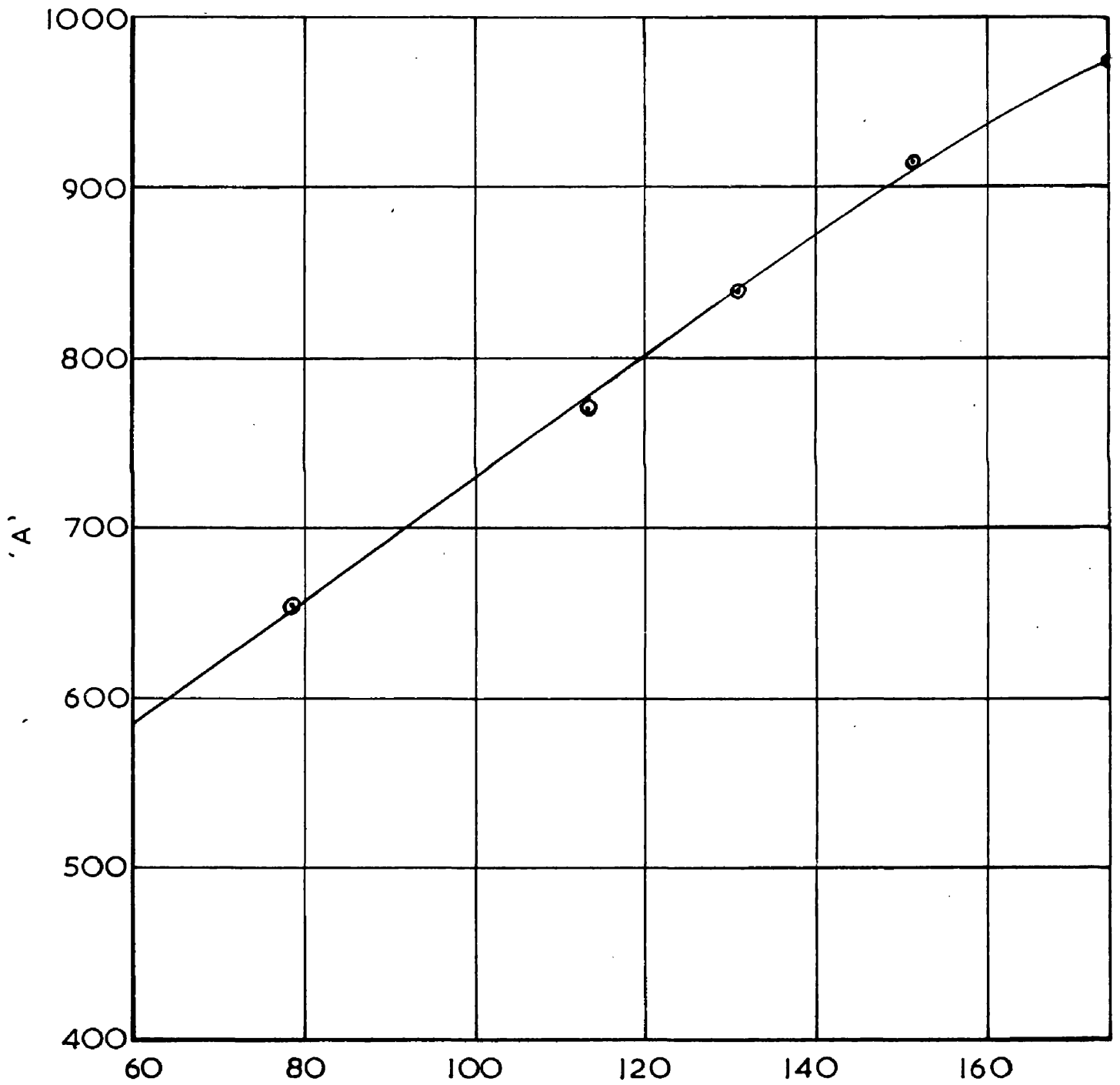
being heated externally by a coil of heating wire wound round the junction. The temperature difference between the two junctions is a function of the rate of cooling of the heated thermocouple as affected by the velocity of the air moving past the junction. The difference in temperature causes an e.m.f. to be developed between the thermocouples. This e.m.f. is measured by a potentiometer circuit. By increasing the current in the heating circuit it is possible to measure air velocities over a wide range.

The sensing element is shown in fig.3.7 The thermocouple junctions are made from 18 S.W.G. enamelled copper and 22 S.W.G. constantan wire twisted and soldered together. The heated junction is covered by a sleeve of fibreglass insulation. Constantan, 40 S.W.G., is wound round the insulation and the ends of the coil connected to copper leads which together with the free ends of the thermocouples are mounted on a Bakelite holder for rigidity and ease with which the extension wires could be connected. The circuit diagram for the complete instrument is shown in fig. 3.8 The heating current for the hot junction is supplied by the battery B, the actual current flowing through the heating circuit can be adjusted by the variable resistance R, and is indicated on the ammeter A.

A calibration graph for air at various temperatures is shown in fig. 3.9 The e.m.f. - velocity relationship can be expressed by the following relationship,

$$y = A x^{-2.19}$$

VARIATION OF 'A' WITH TEMPERATURE



TEMPERATURE °F.

FIG. 3.10.

POSITION OF ANEMOMETER

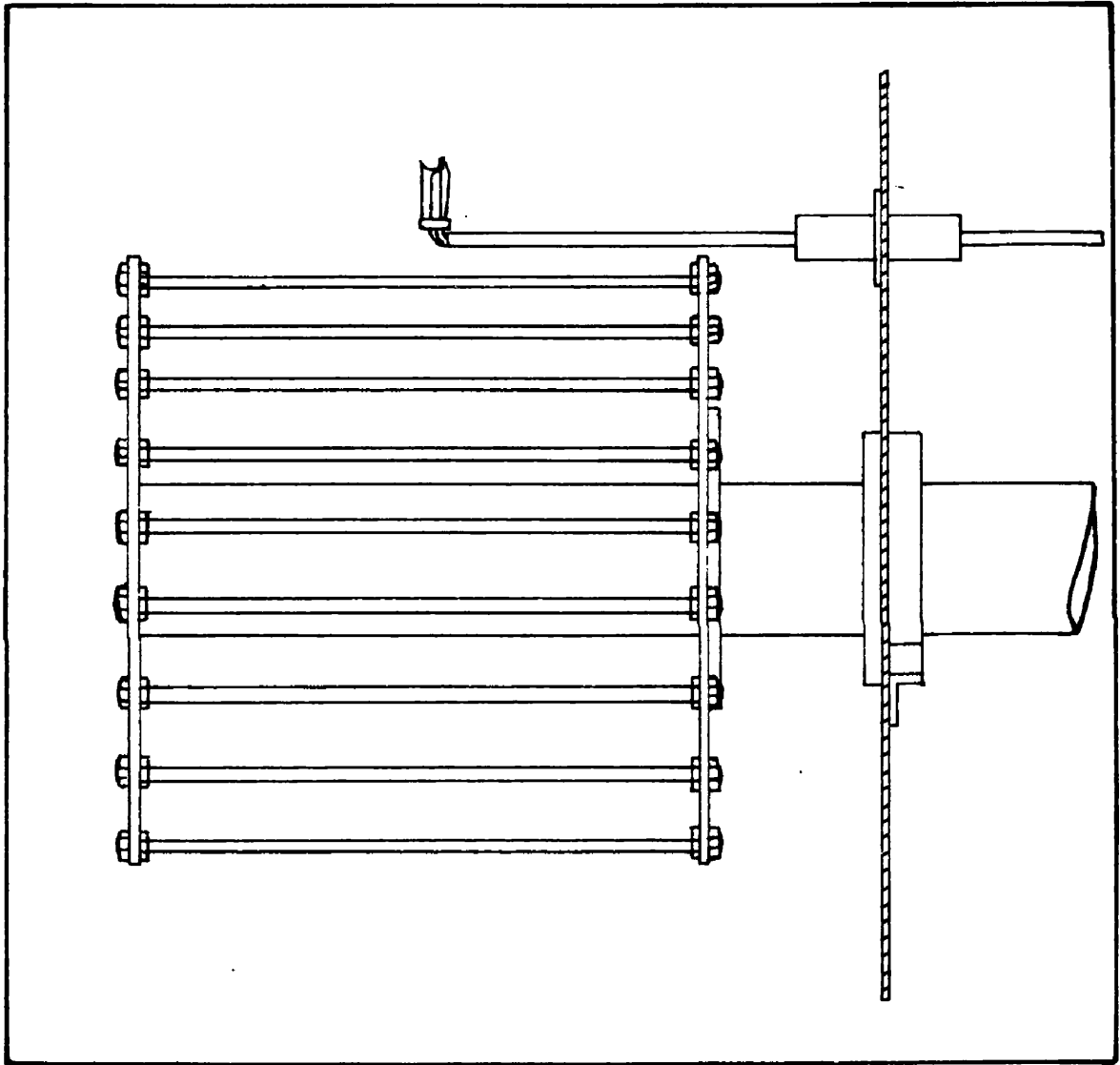


FIG. 3.II.

where y is the air velocity in ft./min. and x the millivolt reading. The constant A has various values which depend on temperature, the relationship is shown in fig. 3.10.

The position of the anemometer in the drier is shown in fig.3.11. The long arm which extends over the top of the drier is used to adjust the position of the anemometer over the length of the drum and when rotated through ninety degrees the anemometer scans the area between the rods of the cage. The minimum reading gives the maximum velocity of the air stream. In order to use this procedure the rotation of the drum must be stopped to prevent the anemometer fouling the rods of the drum.

3.2. Procedure.

The plant is started up by switching on the fan and subsequently a sufficient number of heaters to give approximately the correct temperature. The automatic controller is then set to the required air temperature and the throughput of the air system adjusted to give the desired value. The plant is then allowed to heat up for about 30 minutes. In the interval the recirculation pump of the U-tube is switched on and adjustments made to prevent overflowing. The fibre supply drum is then put on to the machine and the fibre from it passed through the first pair of rollers into the U-tube where it is allowed to accumulate so that there is always a two minute time lag between the fibre entering and leaving the tube. The fibre is now passed through the second pair of rollers and over the tension roller. The main motor is then switched on and the fibre wound round the cage and the skew roller the required number of times. The fibre leaving the cage is then fed through the off-take rollers, round the guide and on to the final storage drum.

The temperature and humidity of the air stream is checked, and in the case of the air water system, the humidity can be adjusted by injecting live steam into the duct to give the desired value of humidity. The plant is then run under constant conditions for about thirty minutes to ensure that equilibrium conditions are established. During this period readings of the various instruments

are checked at regular intervals. After the final set of readings are taken the window of the drying compartment is opened and samples of the fibre taken at regular intervals along the drum.

3.2.1. Sampling.

The samples to be taken are marked by clips to ensure that they are taken at regular intervals. This is necessary as after the first sample is taken, the tow which is under tension tends to move round the drum when this tension is released. The samples are quickly cut and placed in air tight containers.

3.2.2. Moisture Content of Samples.

Various methods of determining the moisture content of the samples were reviewed such as Karl Fischer⁽⁷⁶⁾, etc. The method of vacuum drying was found to be the most reliable. The samples were heated at 60°C in a vacuum drier for a period of not less than 12 hours. The loss in weight of the samples is attributed to loss of moisture. The moisture content of the initial sample is expressed as a percentage of the dry fibre weight.

3.3. Initial Experiments.

The first series of experiments were concerned with the satisfactory flow of the fibre through the machine. These experiments revealed the necessity for some type of drum off-take as initially the fibre from the off-take rollers was allowed to fall freely into a box. The fibre tended to wrap itself round the off-take rollers and stop the machine. This was overcome by arranging that the fibre was always under tension from the off-take rollers to the storage drum which had replaced the storage box. This drum was fixed by a grub screw to a driven shaft which is itself driven through a friction clutch. The clutch was adjusted such that it was continually slipping under the slight tension on the fibre tow being wound on to the drum. The fibre was wound evenly on to the drum by passing the fibre round a guide which could be moved back and forwards along the length of the drum. Guides were also inserted before the first pair of rollers and before the tension roller to prevent the fibre moving along the rollers and in the case of the guide before the tension roller to control the position at which the tow winds on to the drying drum.

When the plant was first erected, the drying cage consisted of the drum as described on page 35. without the complicated system of air distribution within the central shaft. The initial runs with the air circulating were designed to measure the variation in air

AIR VELOCITY DISTRIBUTION (1)

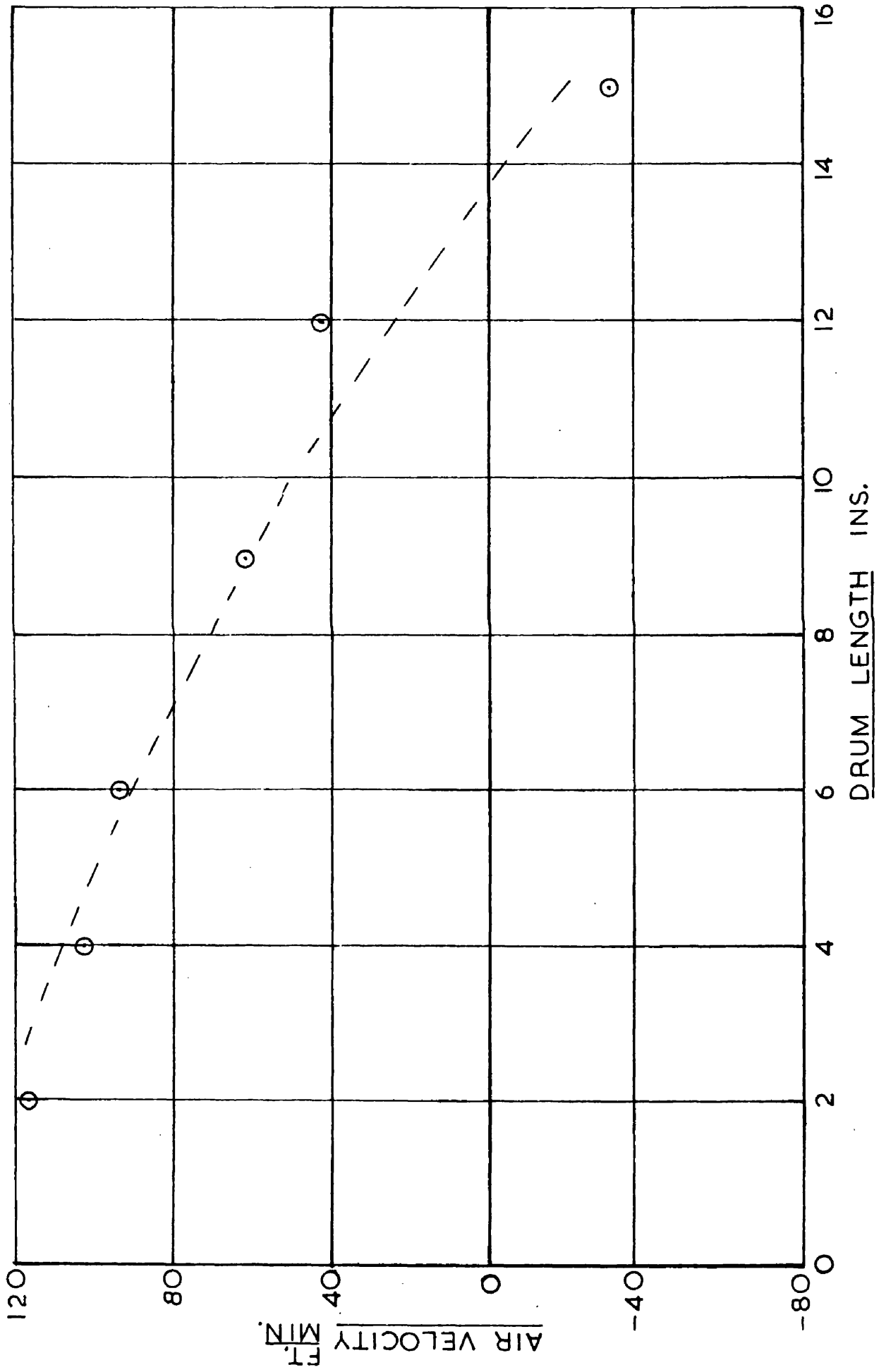
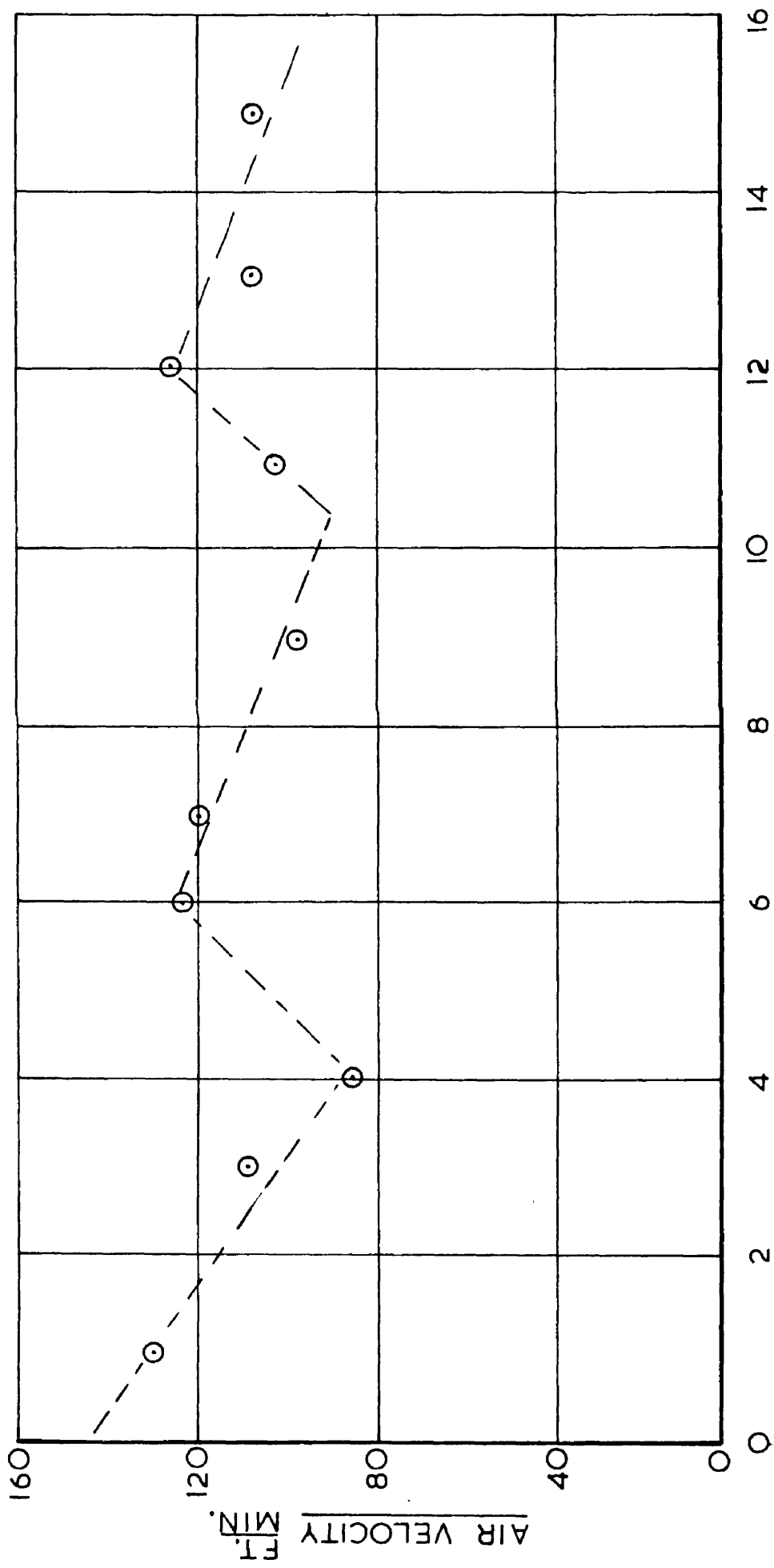


FIG. 3.12.

AIR VELOCITY DISTRIBUTION (II)



DRUM LENGTH INS.

FIG. 3.13.

velocity along the length of the drum. In these experiments the air flow was measured by the heated thermocouple anemometer. This was mounted as shown in fig. 3.11. The air velocity was measured at regular intervals along the drum length. The results of the first series is shown in fig. 3.12. It shows that the distribution is uneven, the velocity being a maximum at one end varying to a negative value at the other end of the drum.

The first adjustments made were the installation of concentric tubes to divide up the total air throughput equally over three sections of the drum length. The number of tubes which could be installed was limited by the thickness of the tube wall. The separation of the tubes was ensured by the inclusion of splines on the tube walls. A further refinement was the inclusion of a cone at the end of the drum to improve the free flow of the air. The distribution of air was again checked and is shown in fig. 3.13. The variation was now much less pronounced than in fig. 3.12 showing three maximums and a positive value at all positions along the drum. From this it was concluded that further modifications would have to be made to each of the three sections. The three sections are not of equal length as the velocity of the air had the distribution shown in fig. 3.12. Since the separation of the tubes was achieved by the use of splines the positions of the two tubes could be adjusted easily. The magnitude of the variations could only be reduced by decreasing the

AIR VELOCITY DISTRIBUTION (III)

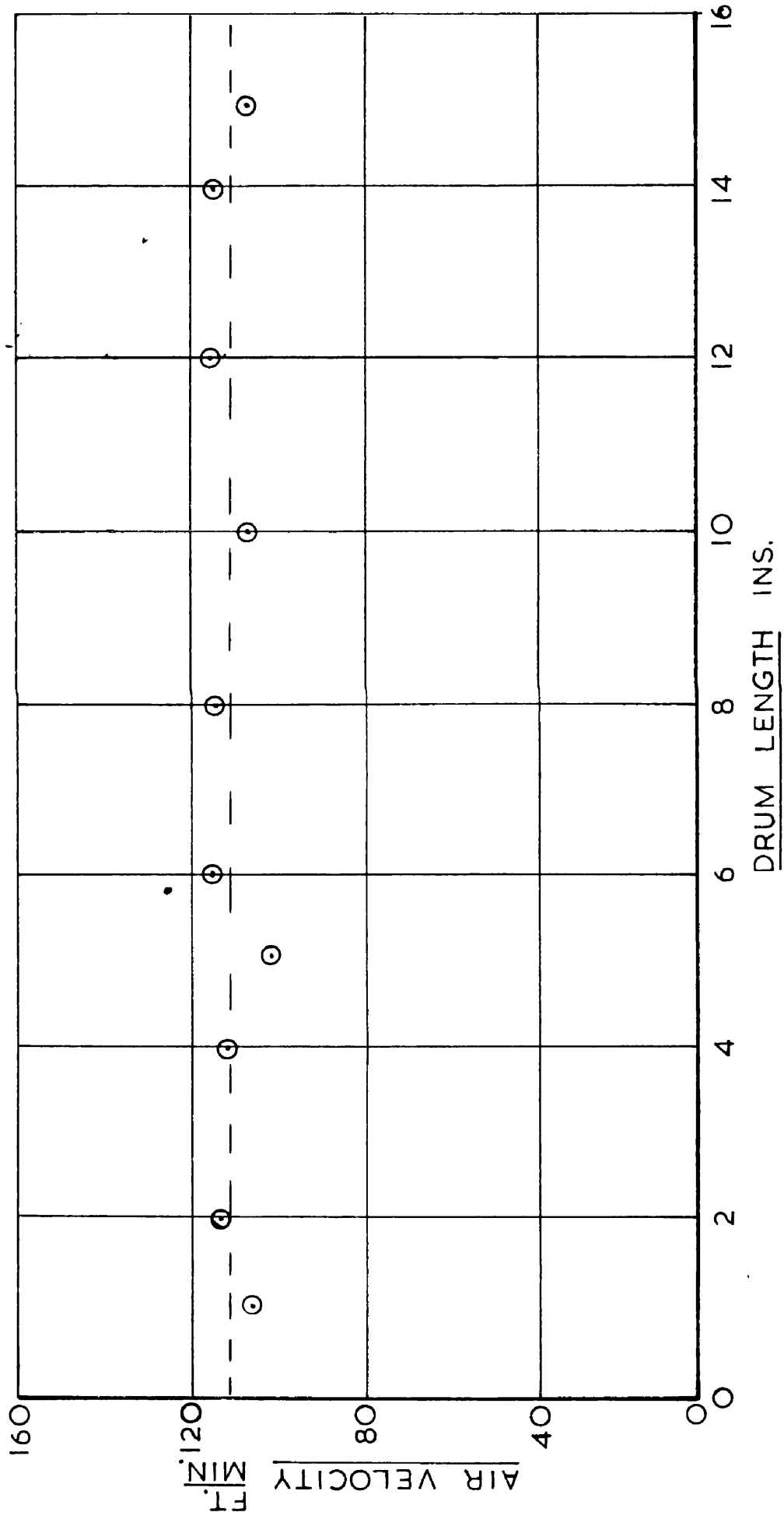


FIG. 3.14.

amount of air available in those particular sections. Hence pieces of angled blading were inserted in each of the holes in the circumference at varying depths according to their position in the section of the tube wall. The blading was made of aluminium which is resilient enough to be pressed into position and remain firmly fixed for a considerable time. However it was found unsatisfactory to use the same piece of blading after it had become loose. Another modification was to place baffle plates at regular intervals along the drum. In addition a wire mesh casing was wound round fourteen inch wooden formers. The effect of these modifications on the air distribution is shown in fig. 3.14. As the variation is within ± 10 per cent these modifications were accepted as within the accuracy of the other variables.

RESULTS - PART I

Evaporation of liquids
during the Constant Rate
Period of Drying.

4.1 Introduction - The Drying of Continuous Fibre Tows.

The work described in this section deals with the drying of continuous, multi-filament tows of Ardil and Terylene during the constant rate period of drying. These two types of fibre were chosen because of the wide difference in their physical properties, especially with respect to their affinity to water. As a result of experiments, it was concluded that the properties of the fibre do not appear to influence the rate of drying during the constant rate period. A summary of the results of these experiments is shown in table 4.1. The table shows the rates of evaporation of water from fibre tows of Ardil and Terylene under similar conditions at four different levels of temperature.

Table 4.1

Temp. °F.	194	167	122	95
Ardil $\frac{dw}{de} \frac{lb}{min ft^2} \times 10^3$	16.8	10.4	6.44	3.85
Terylene $\frac{dw}{de} \frac{lb}{ft^2 min} \times 10^3$	16.68	10.78	6.67	3.59

This is in general agreement with the work of Gilliland⁽⁵⁰⁾ who compared the rates of drying of various materials, sand, clay, etc. and showed that during the constant rate period the rates of evaporation, under similar conditions, were substantially the same as shown by his

results tabulated on page 22. Hence it was decided to carry out most of the experiments using Ardil, a fibre which is much easier to handle as it has a much lower tensile strength.

The initial work was carried out evaporating water from the fibre tows. Later the work was extended to include methanol, ethanol, propanol, butanol and trichloroethylene. The reason for extending the work to include the latter group was to vary the Schmidt number and so investigate its effect on the rate of mass transfer, thus enabling equation 1.19 to be fully investigated. The above liquids were chosen because they have the desired variations in the physical properties and can be handled in comparative safety in the quantities necessary in a drier of this size.

The experimental work was designed to determine the rates of heat and mass transfer over as wide a range of conditions as possible in the plant used. An additional object was to accumulate data suitable for use in the design of driers of this type.

The method of determining the effects of the variables was to separate them by plotting the results in log-log form, thus revealing the occurrence of any interactions between the variables⁽⁷⁷⁾.

4.2. Mass Transfer.

4.2.1. Evaporation of Water.

4.2.1.1. Procedure.

The procedure was as described on page 46. Care was taken to keep the inlet moisture content to below 120 per cent dry

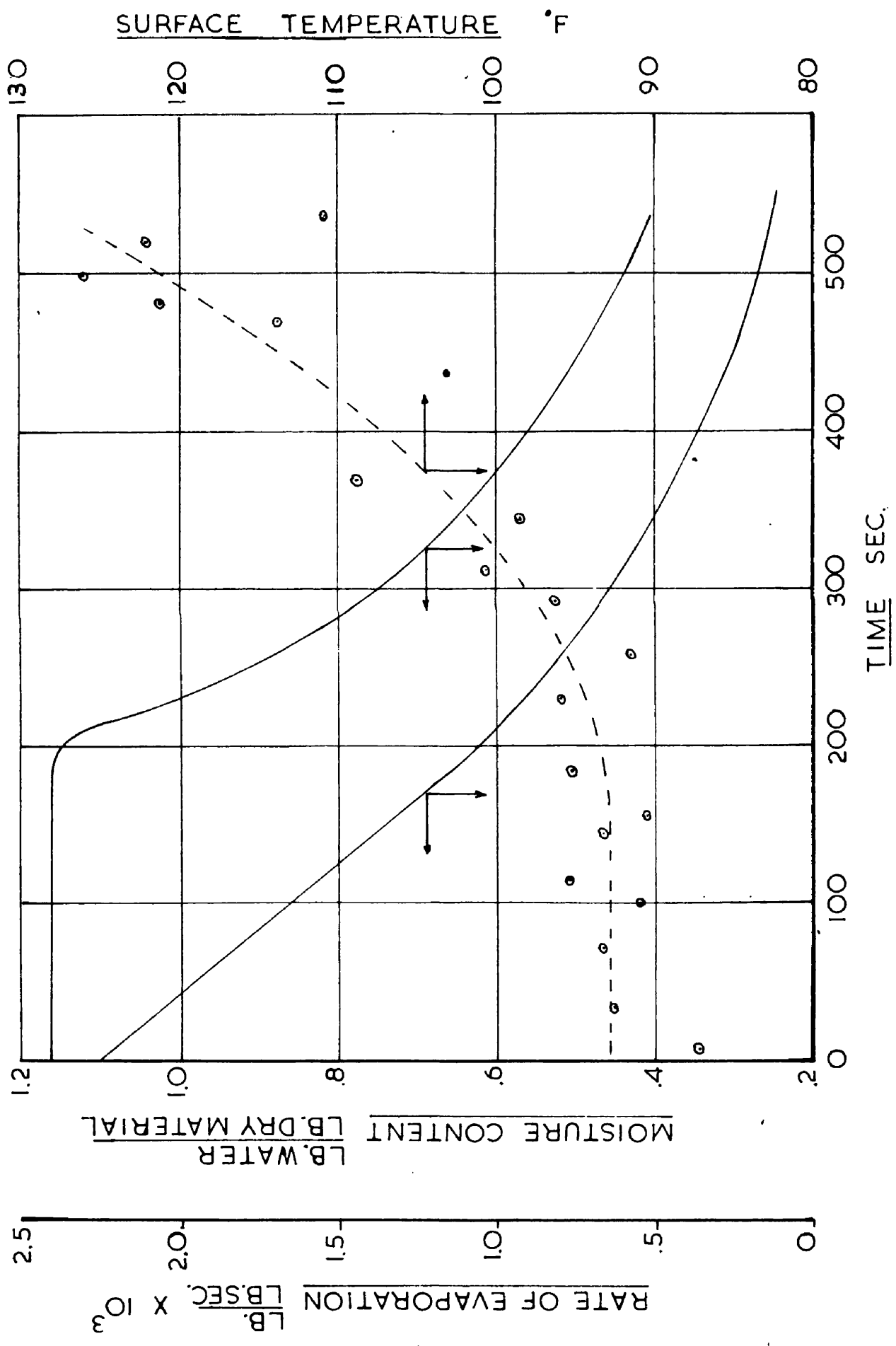


FIG. 4.1.

fibre. It was found that if the inlet moisture content was allowed to rise above this figure the drying characteristics of the machine were altered and that reproducibility of results was extremely difficult. This was due to liquid migration along the fibre caused mainly by gravity as the drum rotates. Thus as the tow is moving downwards the moisture from the very wet section of the tow tends to move forward wetting further the section immediately in front. This effect is negligible when the associated liquid is below the value given above which is for Ardil. With the other fibre, Terylene, which has a negligible percentage as bound liquid, the effect above is even more marked and the inlet moisture content normally used was below 100 per cent.

4.2.1.2. Initial Tests.

Before the main experimental work could be carried out a series of runs were conducted to determine the critical moisture contents. An example of one of the drying curves is shown in fig. 4.1. Also plotted on the same figure is the rate of evaporation and graph of fibre surface temperature with time corresponding to the drying curve. The temperature-time graph shows the tendency for a constant value of temperature during the constant rate period of drying with the temperature gradually rising thereafter as the moisture content of the fibre decreases. The rather scattered curve for the temperature time graph indicates the difficulty which was encountered in measuring the temperature of the moving tow within the drier itself.

4.2.1.3. Repeatability.

Several runs were carried out to determine the repeatability of the method in determining the rate of evaporation. Two sets of conditions were chosen, the value of air velocity being kept constant, such that the values of air temperatures were widely separated. Four runs were carried out under each set of conditions and the results within each group compared by calculating the mean value of rate of evaporation and assessing the deviation from it for each result. In calculating the rate of evaporation from the moisture content-time graph it was found that much more consistent results were obtained if values on the moist-time graph which were abnormally low were omitted. The occurrence of these points was investigated and attributed to errors caused by the sample being in contact with metal of the drying drum for a short time during the sampling operation. Hence it was thought justifiable to ignore them when calculating the gradient of the line. The results of the two series are compared below in table 4.2.

Table 4.2

Air Temperature 167°F		Air Temperature 122°F	
$\frac{dw}{de} \frac{lb}{ft^2 min.} \times 10^3$	Deviation per cent	$\frac{dw}{de} \frac{lb}{ft^2 min.} \times 10^3$	Deviation per cent
10.36	+0.25	3.81	+1.0
10.62	+2.73	3.64	-3.7
10.04	-2.97	3.07	+2.7
10.35	+0.13	3.71	-1.7

WATER AIR

RATE OF EVAPORATION VS AIR VELOCITY

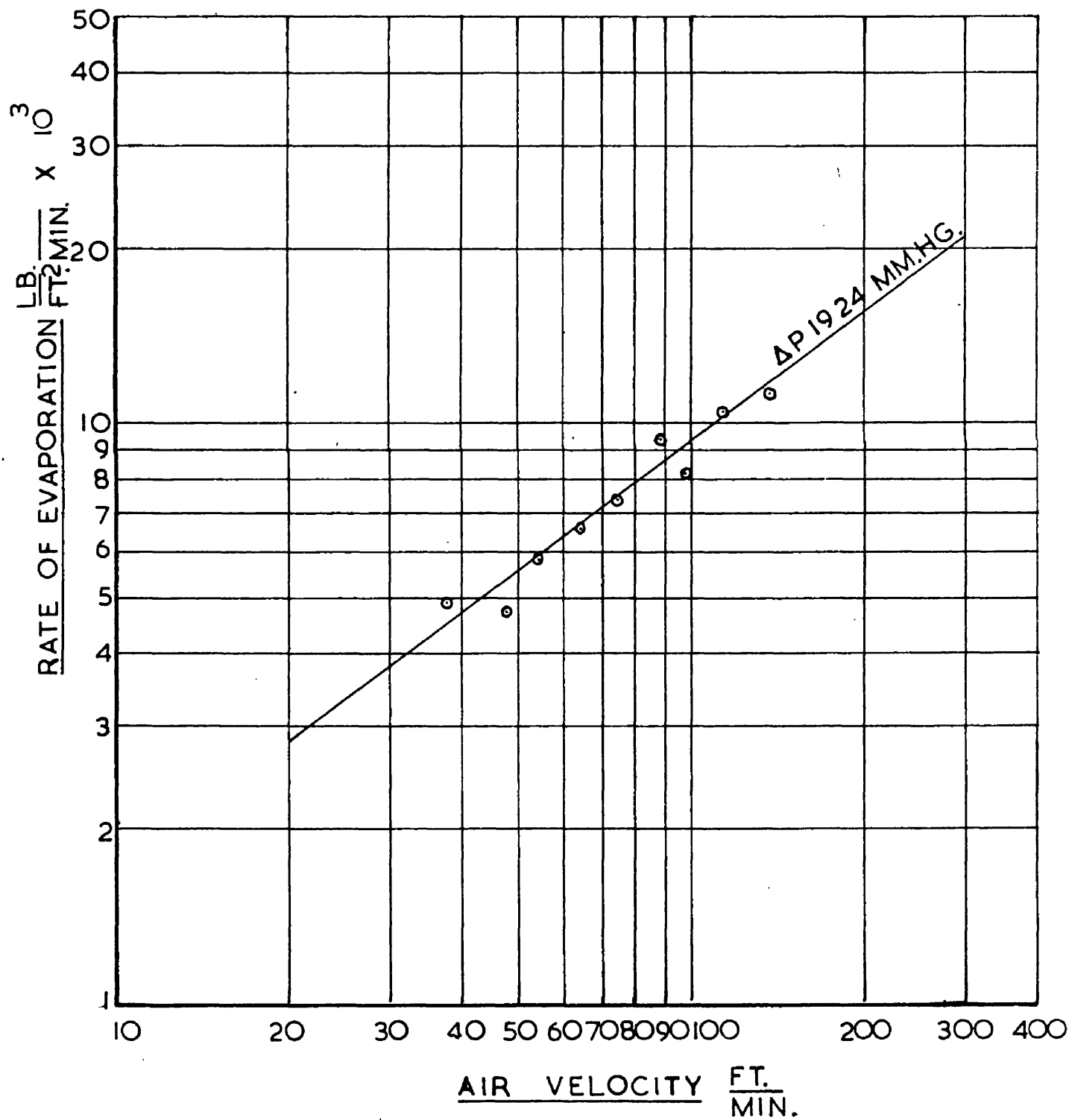


FIG. 4.2.

From table 4.2. it can be seen that at the higher value of temperature the maximum overall deviation (5.7 per cent) from the mean value is slightly less than the overall deviation at the lower value (6.4 per cent). The results indicated that the repeatability of the method is within the range ± 4.0 per cent.

4.2.1.4. Air Velocity.

To determine the effect of the air velocity on the rate of evaporation, a series of experiments were conducted at 167°F using a tow of standard width and maintaining a constant partial pressure difference between the liquid surface and the vapour in the recirculating air. The air velocity was varied as widely as possible. The effect is shown in fig. 4.2. with the rate of evaporation increasing with increase in air velocity. The effect of the increase in air velocity on the rate of evaporation is given by an equation of this type,

$$\frac{dw}{de} = k V^b \dots \dots \dots (4.1)$$

The exact relationship was calculated using the method of least squares. The general formulae and method are those outlined by Davies⁽⁷⁸⁾.

Table 4.3.

$\frac{dw}{de} \frac{lb \times 10^3}{ft^2 \min}$	$V \frac{ft}{min}$	$Y = \log \frac{dw}{de}$	$X = \log V$	$X + Y = T$
9.29	88.3	-2.0321	1.9460	-0.0861
10.38	114.0	-1.9837	2.0569	+0.0732
11.02	137.0	-1.9680	2.1367	+0.1687
8.05	98.7	-2.0935	1.9943	-0.0992
7.34	73.6	-2.1341	1.8669	-0.2672
6.58	64.0	-2.1818	1.8062	-0.3756
5.80	54.3	-2.2369	1.7348	-0.5021
4.93	37.0	-2.3070	1.5682	-0.7388
4.75	48.0	-2.3232	1.6812	-0.6420

$$\Sigma x = 16.7912 \quad ; \quad \Sigma y = -19.2603 \quad ; \quad \Sigma T = -2.4691 \quad ;$$

$$\Sigma x^2 = 31.60336276 \quad ; \quad \Sigma y^2 = 41.35812525 \quad ; \quad \Sigma xy = -35.74392559 \quad ;$$

The Regression Coefficient is given by the following expression,

$$\begin{aligned}
 b &= \frac{\Sigma xy - \frac{1}{n} (\Sigma x)(\Sigma y)}{\Sigma x^2 - \frac{1}{n} (\Sigma x)^2} \\
 &= \frac{-35.74392559 + 37.73355777}{31.60336276 - 31.32715510} \\
 &= \underline{0.698}
 \end{aligned}$$

WATER-AIR

RATE OF EVAPORATION VS AIR VELOCITY

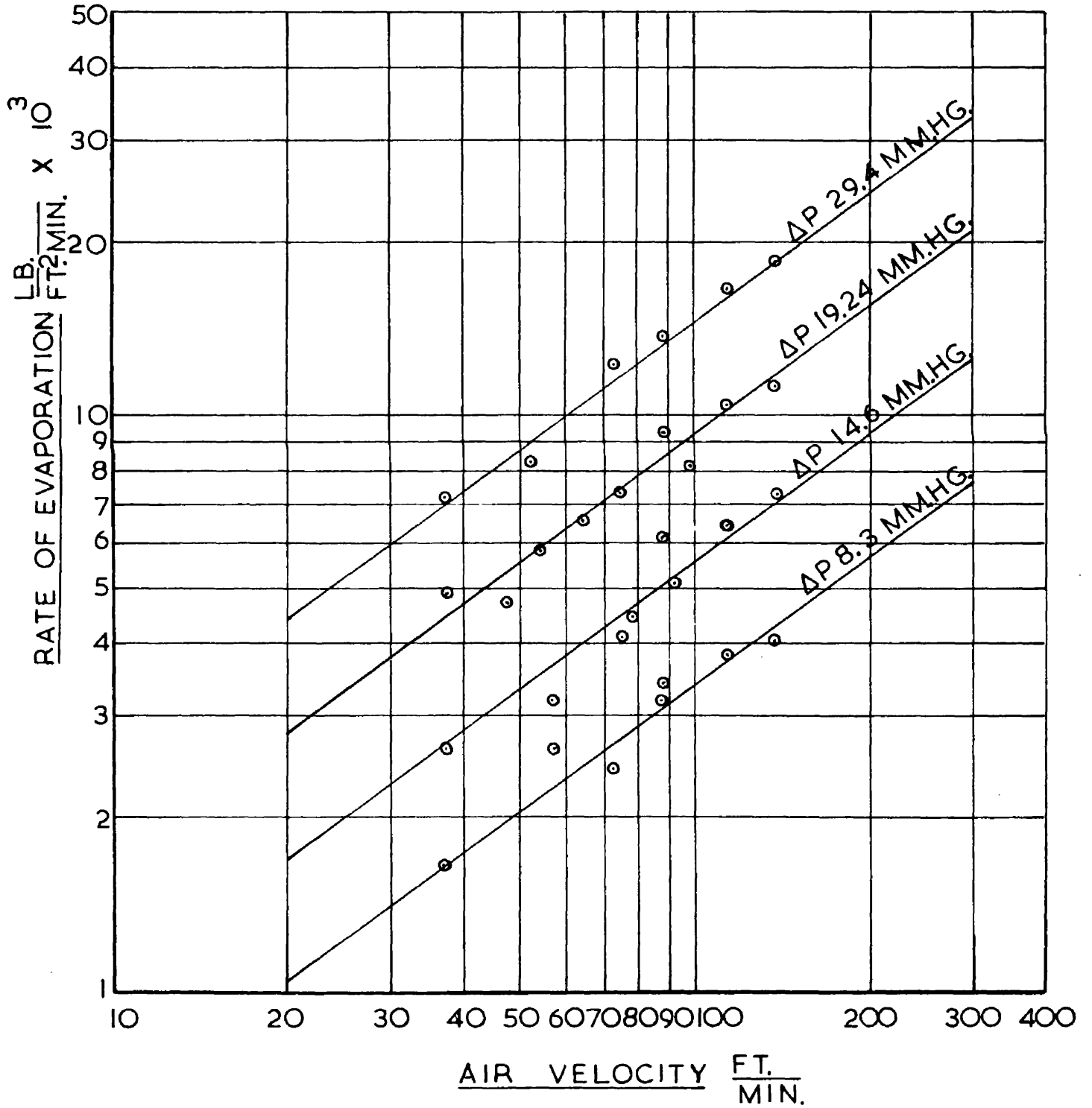


FIG. 4.3.

The significance of the value given above can be evaluated in the following manner,

$$\begin{aligned} b\Sigma(x-x) &= (0.698) (0.27585) = 13.43912 \\ \Sigma(y-y) &= \Sigma y - \frac{1}{n} (\Sigma y) = 45.5940424 - 45.45006945 \\ &= 0.14397079 \\ \text{Residual} &= 0.14397079 - 0.1343912 \\ &= 0.0104783 \\ F &= \frac{0.13439412}{0.01047830} = 12.83 \end{aligned}$$

The value given for $n_1 = 1$, $n_2 = 7$, by the F-distribution table, 1 per cent level, was 12.25, hence the gradient b is highly significant.

4.2.1.5. Partial Pressure Difference.

In order to find the effect of the partial pressure difference on the rate of evaporation, and investigate the possibility of interaction between the air velocity and partial pressure difference, three series of runs were carried out similar to the one above, varying the partial pressure difference in each series.

The results are shown in Fig. 4.3 as a family of lines of the type shown on page 55. The gradients were calculated using the same method and were found to reveal sufficient variations to make interactions a possibility. The significance of the variations was tested by comparing the highest and lowest values.

Table 4.4.

Gradient	Partial Press. Diff. m.m. hg.
0.702	8.30
0.773	14.60
0.698	19.24
0.783	29.40

4.2.1.6. Comparison of Gradients.

Let s^2 be the combined variance about the two regressions, i.e. if s_1^2 = variance about b_1 with ϕ_1 degrees of freedom and s_2^2 = variance about b_2 and ϕ_2 degrees of freedom.

$$s^2 = \frac{\phi_1 s_1^2 + \phi_2 s_2^2}{\phi_1 + \phi_2}$$

$$s_1^2 = 0.0105 \qquad \phi_1 = 7$$

$$s_2^2 = 0.0127 \qquad \phi_2 = 4$$

$$s^2 = \frac{0.0735 + 0.0508}{4 + 11} = 0.00113$$

$$s = \underline{0.0362.}$$

$$\begin{aligned}
 t &= \frac{b_1 - b_2}{\sqrt{\left(\frac{1}{\sum_1 (x - \bar{x})^2} + \frac{1}{\sum_2 (x - \bar{x})^2} \right)}} \\
 &= \frac{0.783 - 0.698}{0.036 \times 2.92} \\
 &= \underline{0.804}
 \end{aligned}$$

From the value of $t = 0.804$ and $n = 11$, the t - distribution tables indicate that the difference in the values of gradient is not significant. Hence there is no significant interactions between the effect of velocity and partial pressure difference on the rate of evaporation.

Hence the equation becomes $\frac{dw}{d\theta} = K V^b \Delta p.$

In order to evaluate the power n , the gradient of the family of lines, it is necessary to calculate a weighted mean gradient taking into consideration the different number of points used to calculate the original gradients and their different distributions about the chosen lines. Williams⁽⁷⁹⁾ has shown that the weighted mean gradient can be calculated using the following equation,

$$b = \frac{\sum \frac{b_r}{s_r^2}}{\sum \frac{1}{s_r^2}} \dots \dots \dots (4.2)$$

where $s_r^2 = \sum x^2 - 1/n (\sum x)^2$

WATER-AIR

RATE OF EVAPORATION VS PARTIAL PRESSURE DIFFERENCE

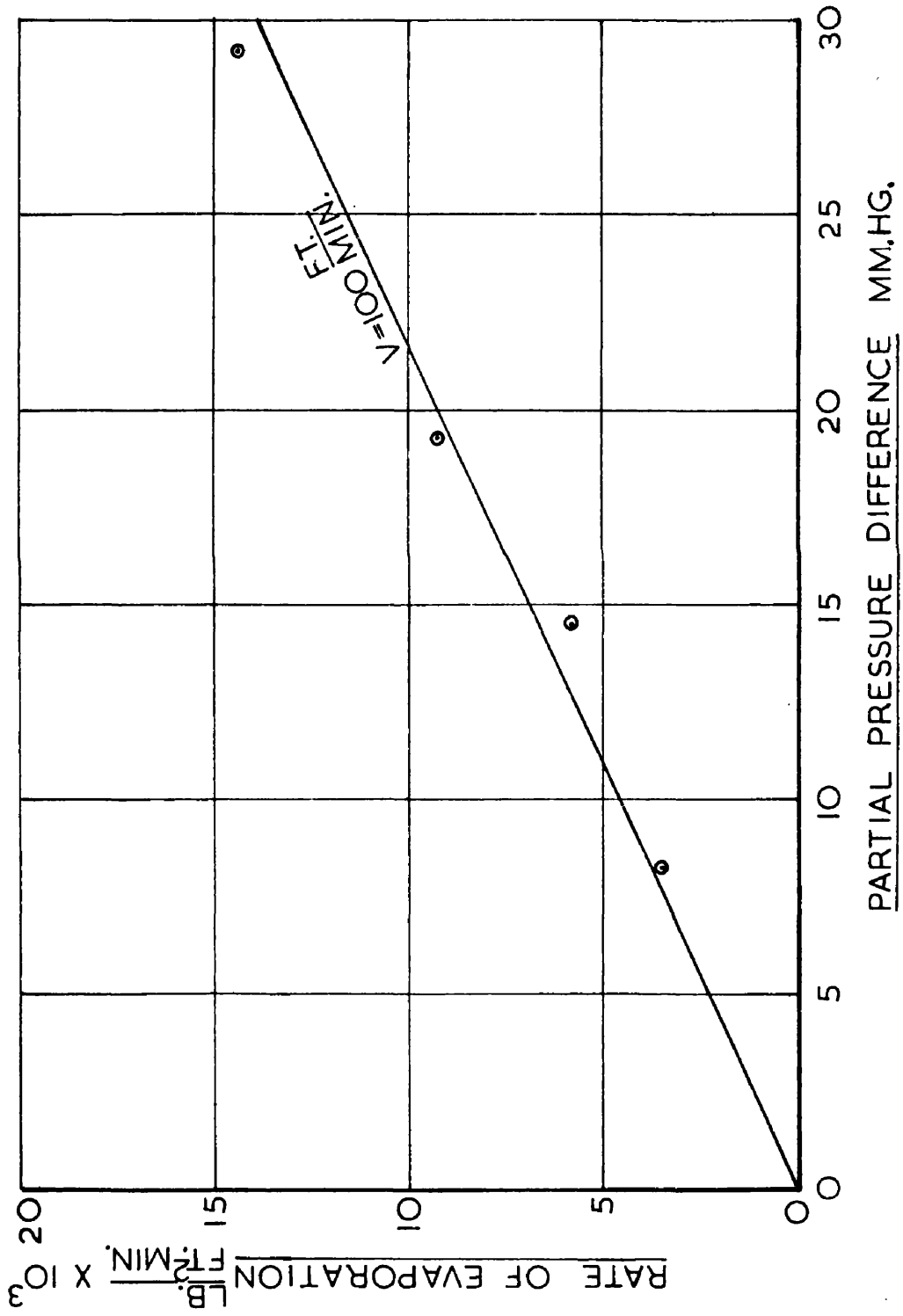


FIG. 4.4.

Table 4.5

	b_r	$\frac{1}{s_r^2}$	$\frac{b}{s_r^2}$
1	0.702	4.9915	3.50403
2	0.773	4.8039	3.71343
3	0.698	3.6251	2.53032
4	0.783	4.8835	3.75874

$$\bar{b} = \frac{13.50652}{18.2240} = 0.741.$$

The equations of the family of lines were then calculated using the weighted mean value of the gradient, 0.741, and the values of \bar{x} and \bar{y} as calculated in the original analyses. The values of the rate of evaporation at a fixed value of velocity were then related to the partial pressure differences as shown in Fig. 4.4.

Hence the relationship between the rate of evaporation velocity of the gas stream, and partial pressure difference is given by the equation,

$$\frac{dw}{dG} = K \cdot V^{0.741} \cdot \Delta p. \quad \dots \dots \dots (4.3)$$

4.2.1.7. Tow Width.

In the preceding experimental work the tow width has been constant. Since by analogy with the system of a gas flowing

$d \frac{dw}{d\theta}$ vs v_d

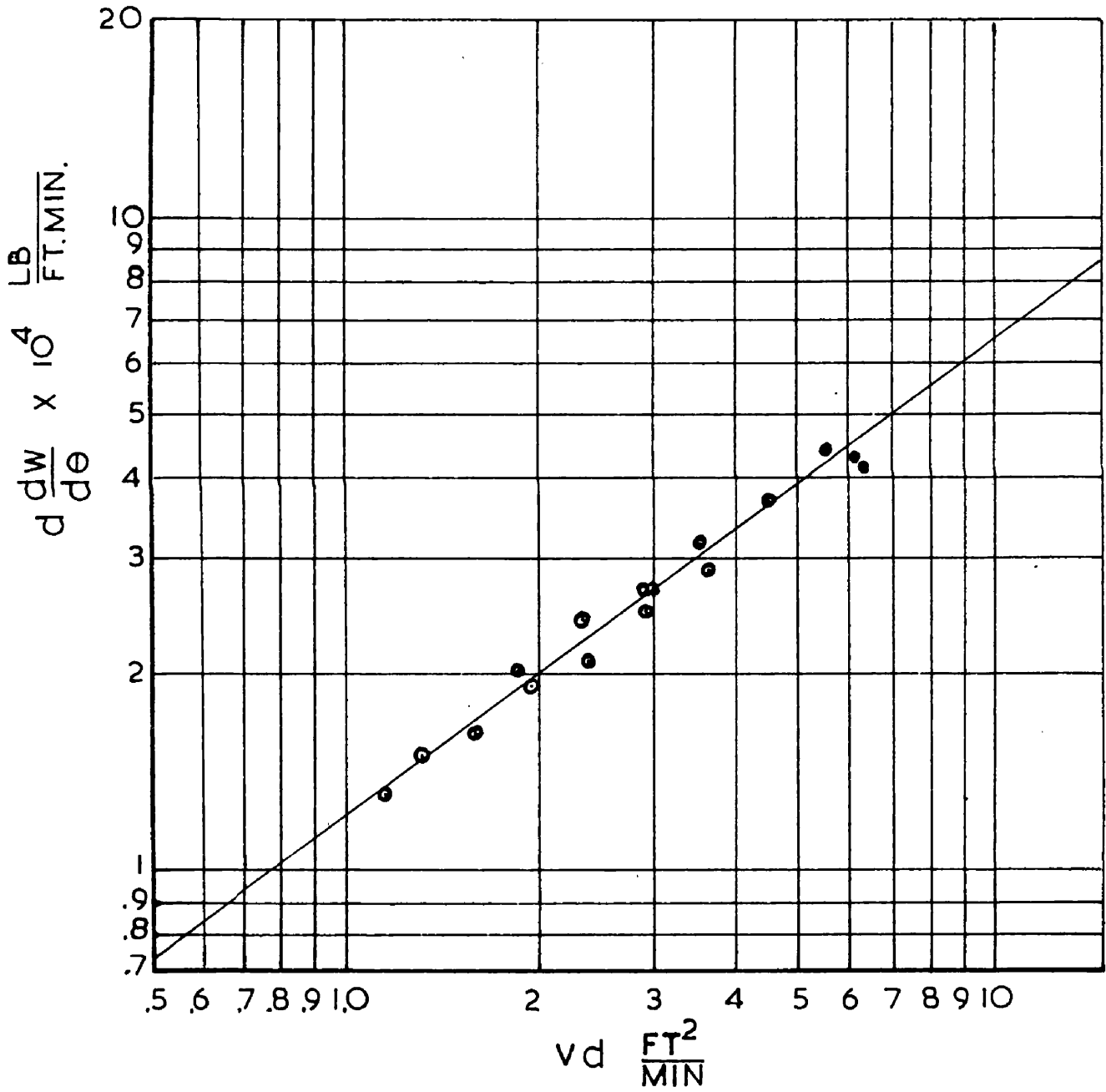


FIG. 4.5

over a cylinder it would appear that the rate of evaporation would be influenced by the variations of the tow width a series of experiments were carried out to correlate them. The range of the experimental work was limited by ability of the drier to handle a wide range of tow widths.

A series of experiments were carried out at an air temperature of 167°F. using three different tows and varying the air velocity over a range of 100 ft/min. The results are shown in fig. 4.5 and correlated by the following equation,

$$d. \frac{dw}{de} \propto (Vd)^{0.74} \dots \dots \dots (4.4)$$

Powell obtained the following expression,

$$d. \frac{dw}{de} \propto (Vd)^{0.69} \dots \dots \dots (4.5)$$

when investigating the rate of evaporation of water from rectangular surfaces in a small wind tunnel. This is slightly lower than the value of the power in equation 4.4. but comes within the range of values contained in table 4.5.

The effect of varying the width of the spaces adjacent to the tow was also investigated. The number of turns of tow on the drying drum were varied, a series of runs being conducted at each value. The conditions were constant throughout except for air velocity which was varied over a range in each of the series. Although slight variations in the rate of evaporation were noted, they were ignored since they were within the experimental error of the method.

WATER AIR

$\frac{K_G^{MPBM}}{\rho V}$ VS REYNOLDS NUMBER

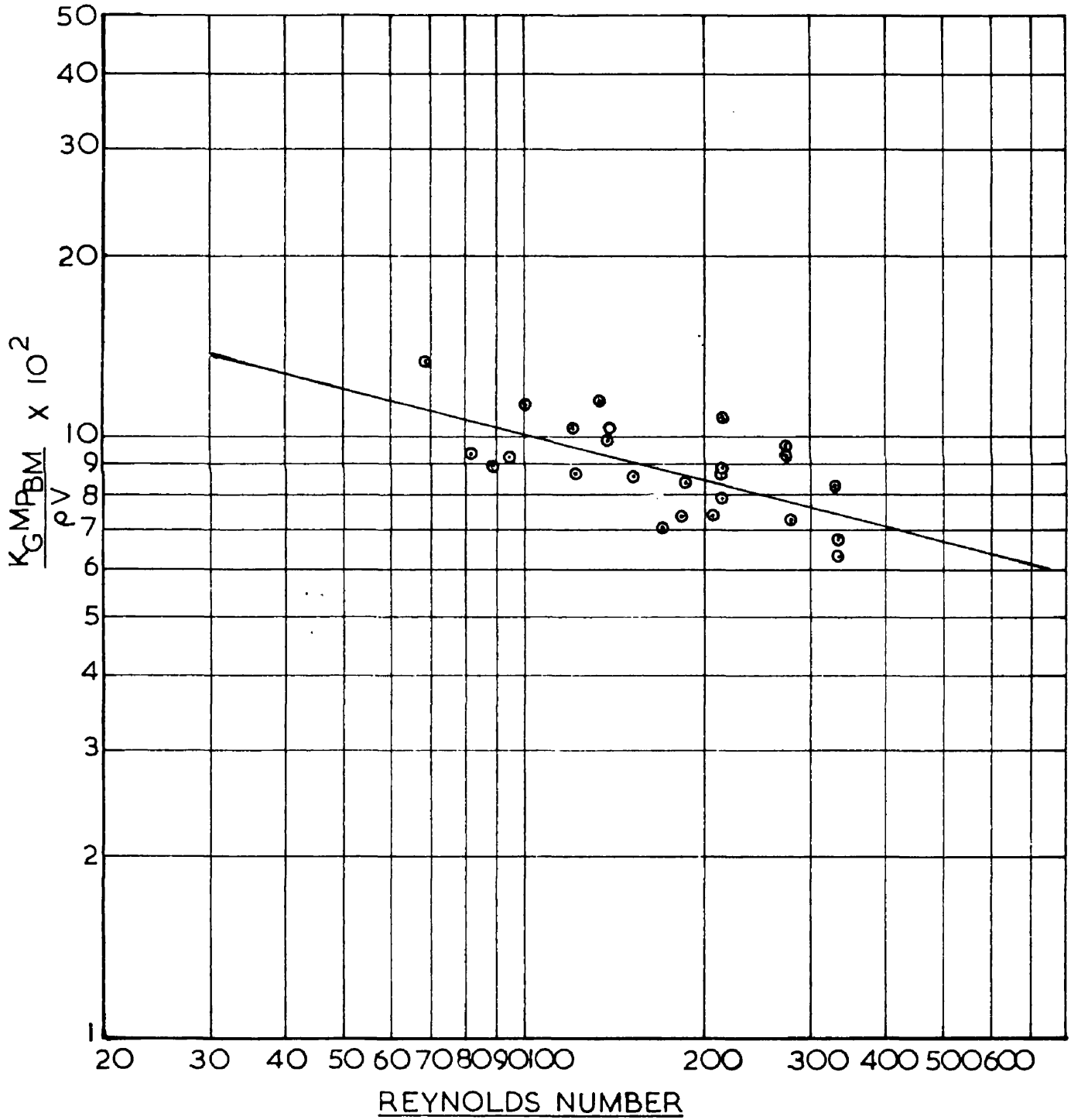


FIG. 4.6.

The relationship between the rate of evaporation and three variables can be expressed by the following expression,

$$\frac{dw}{d\theta} = 5.58 \times 10^{-6} \frac{V^{0.74}}{d^{0.26}} \Delta p. \quad \dots \dots \dots (4.6)$$

If the data used in the previous work is converted into the form of dimensionless groups, the effect of Reynolds number on the rate of mass transfer can be assessed. In Fig. 4.6 the relationship between the group $\frac{k_g M_{av} P_{bm}}{\rho V}$ and Reynolds number is shown to be of the type,

$$\frac{k_g M_{av} P_{bm}}{\rho V} = 0.33 \text{ Re}^{-0.26} \quad \dots \dots \dots (4.7)$$

4.2.2. Evaporation of Alcohols from a Fibre Tow.

In order to extend the scope of the investigation, particularly the range of Schmidt numbers, the liquid evaporated from the fibre tow was varied. This was thought to be advisable to assess the effect of the variation of the diffusion (air/vapour) coefficient on the rate of mass transfer. Previous workers have assessed this effect in terms of Schmidt numbers with a certain measure of success for similar types of systems as stated on page 14. The liquids chosen, the lower members of the alcohol series, have no practical significance in connection with artificial fibres, however they give a range of diffusion coefficients wide enough to cover the range of data likely to be required in the event of some liquid other than water being

removed from a fibre tow in a drier of this type. The regular increase in the value of their diffusion coefficients was desirable for the purpose of the present investigation. Their use in fairly large quantities presented a number of difficulties with regard to the danger of explosion. The plant, being open, resulted in fairly large quantities of vapour surrounding the plant. These fumes were removed by installing an extractor fan immediately above the plant. The main hazard was from the possibility of a build up of vapour in the recirculating air, possibly ignited by a static discharge in the drier. The vapour concentration in the circulating air was kept well below the explosive limits by careful checking of the dew-point at regular intervals during the running of the plant.

4.2.2.1. Procedure.

The experimental runs were carried out using the procedure described on page 46. The effect of the change of liquid was to alter the characteristics of the running of the plant. The Ardil after immersion in the alcohol was no longer so elastic as it had been after immersion in water. As a result the tendency for the fibre to slide along the cage was not so pronounced and greater care had to be taken with the initial tensioning to ensure the smooth running of the plant. Due to the increase in rate of evaporation the machine was run at a slightly higher speed than previously to ensure that the drying was within the constant rate period. This resulted in an increased risk of the fibre becoming entangled with the first

pair of rollers. The latter risk was accentuated by the fact that the liquid was not used to spray the fibre tow as it had during the previous runs. The reason for this was to attempt to restrict the amount of vapour around the plant. The spray was found to add considerably to this and it was found by experience that when the spray was used the extractor fan was not sufficient to remove the amount surrounding the plant. This was not so serious with methanol or ethanol but with butanol it meant that a gas mask had to be worn for any run of reasonable length. During the runs using butanol a gas mask had to be worn when samples were taken or any other time when the window of the drying compartment was open. This tended to hamper the taking of the samples causing a slight decrease in the accuracy of the sampling. In several instances the runs were disregarded where the liquid content time graph was not satisfactory.

4.2.2.2. Methanol.

An initial run was carried out at 167°F. to ensure that the drying curve for the evaporation of methanol was similar to that for water and to assess the approximate value of the critical moisture content and in general to find the running conditions to ensure that the runs would be carried out under the required conditions. The ratio liquid to solid vs. time graph shows similar characteristics to that of water in fig. 4.1.

4.2.2.2.1. Air Velocity.

A series of runs were conducted at an air temperature of 167°F using a standard tow and keeping the vapour pressure of the methanol in the circulating air constant. The rates of evaporation were measured at four different velocities. The rate of evaporation was calculated as previously by plotting the methanol associated with fibre against the corresponding time and measuring the gradient of the linear relationship. The distribution of points about the line is less varied than with the water experiments as there was less tendency for the tow to contract suddenly during sampling.

Table 4.6.

$\frac{dw}{de} \frac{lb}{ft^2 min.} \times 10^2$	V ft./min.	Y = $\log \frac{dw}{de}$	X = $\log V$
3.31	137.0	-1.4802	2.1367
2.78	114.0	-1.5560	2.0569
2.45	88.3	-1.6108	1.9460
2.09	72.0	-1.6799	1.8573

$$\Sigma x = 7.9969 \quad \Sigma y = -6.3269 \quad \Sigma xy = -12.61797481$$

$$\Sigma x^2 = 16.03280379 \quad \Sigma y^2 = 10.02886869$$

$$b = \frac{\Sigma xy - \frac{1}{N}(\Sigma x)(\Sigma y)}{\Sigma x^2 - \frac{1}{N}(\Sigma x)^2}$$

$$= 0.706$$

METHANOL-AIR

RATE OF EVAPORATION VS AIR VELOCITY

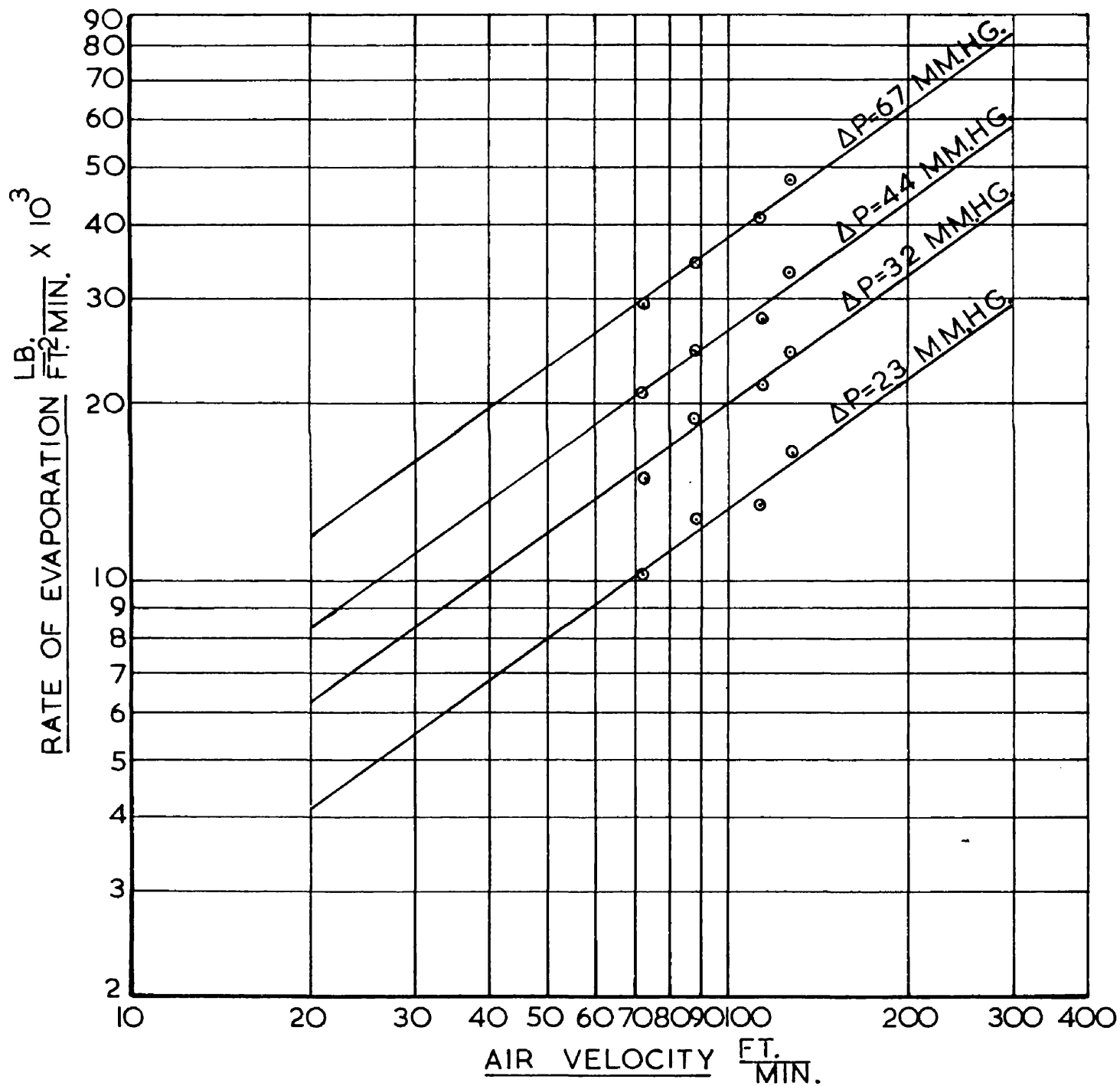


FIG. 4.7.

Hence the relationship between the rate of evaporation and air velocity is given by

$$\frac{dw}{de} \propto v^{0.706} \dots \dots \dots (4.8)$$

which compares with the value 0.74 obtained in the previous set of results for water.

4.2.2.2.2. Partial Pressure Difference.

To evaluate the effect of partial pressure difference, three additional series of runs were carried out at different values of partial pressure difference. The regression coefficients of each series were calculated using the method of least squares as previously.

Table 4.7.

Gradient	Partial Pressure Diff. m.m. hg.
0.731	67
0.706	44
0.758	32
0.698	23

The weighted mean gradient is given by

$$b = \frac{\sum \frac{b_r}{s_r^2}}{\sum \frac{1}{s_r^2}} = 0.723$$

In fig. 4.7 a family of parallel lines was constructed of gradient 0.723

METHANOL-AIR

RATE OF EVAPORATION VS PARTIAL PRESSURE DIFFERENCE

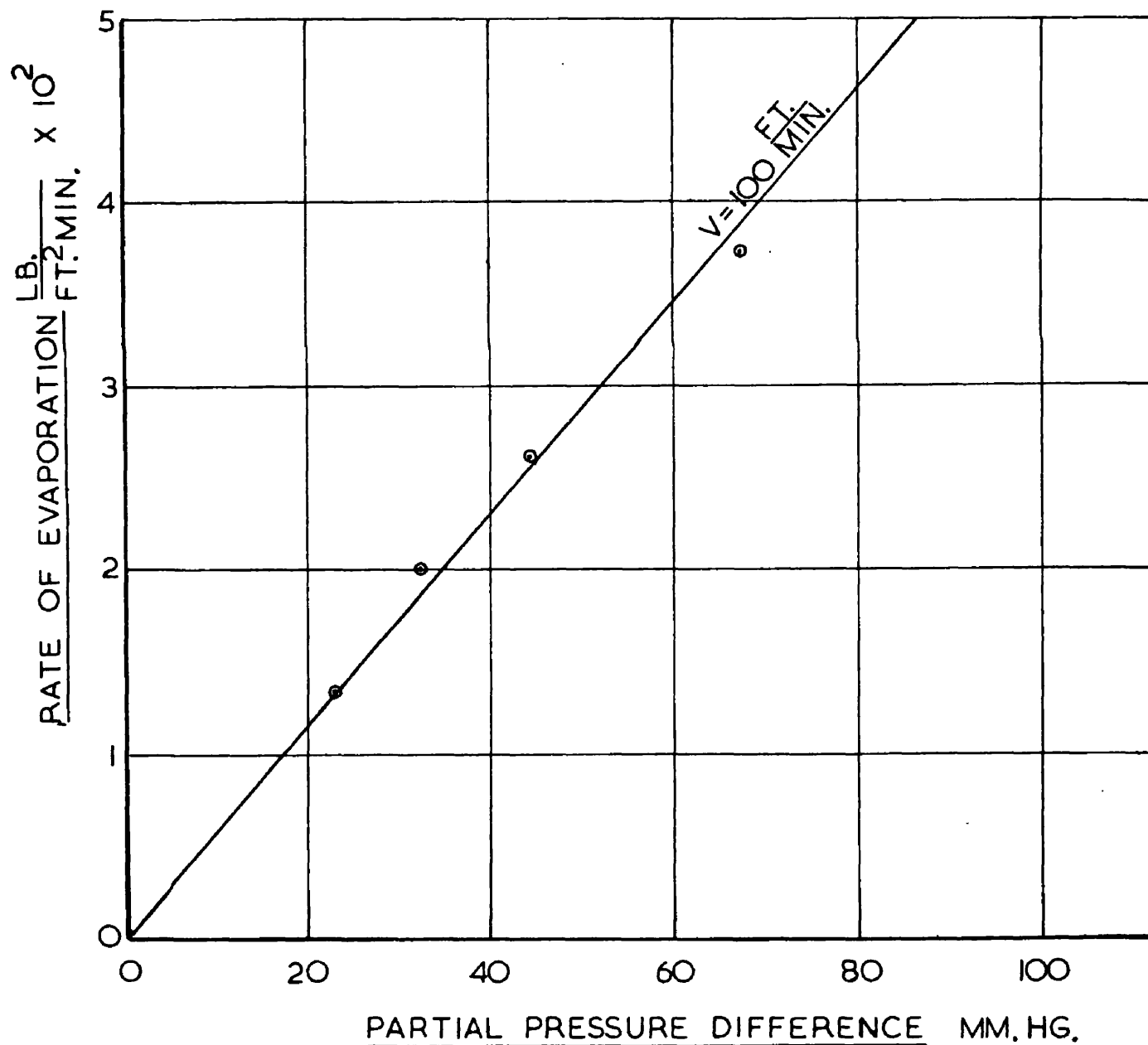


FIG. 4.8.

passing through the centroids of each of the groups of points. The intercepts, at a fixed value of velocity (100 ft/min.), were related to the corresponding value of partial pressure difference giving a linear relationship as shown in fig. 4.8.

The effects of the variables are combined to give the following equation,

$$\frac{dw}{de} = 0.782 \times 10^{-6} V^{0.72} d^{-0.28} \Delta p \dots \dots (4.9)$$

4.2.2.3. Ethanol.

4.2.2.3.1. Air Velocity.

A series of four runs at air velocities ranging from 57 to 137 ft/min. were carried out using a standard tow at a circulating air temperature of 167°F. The partial pressure of the ethanol in the circulating air was kept constant. The ethanol-fibre ratio, at inlet, was maintained at one or slightly above in order to prevent undue migration of the liquid along the fibre during the initial period in the drying drum giving poor associated liquid-time graphs. The rate of evaporation was calculated from the gradient of this graph as previously.

ETHANOL-AIR

RATE OF EVAPORATION VS AIR VELOCITY

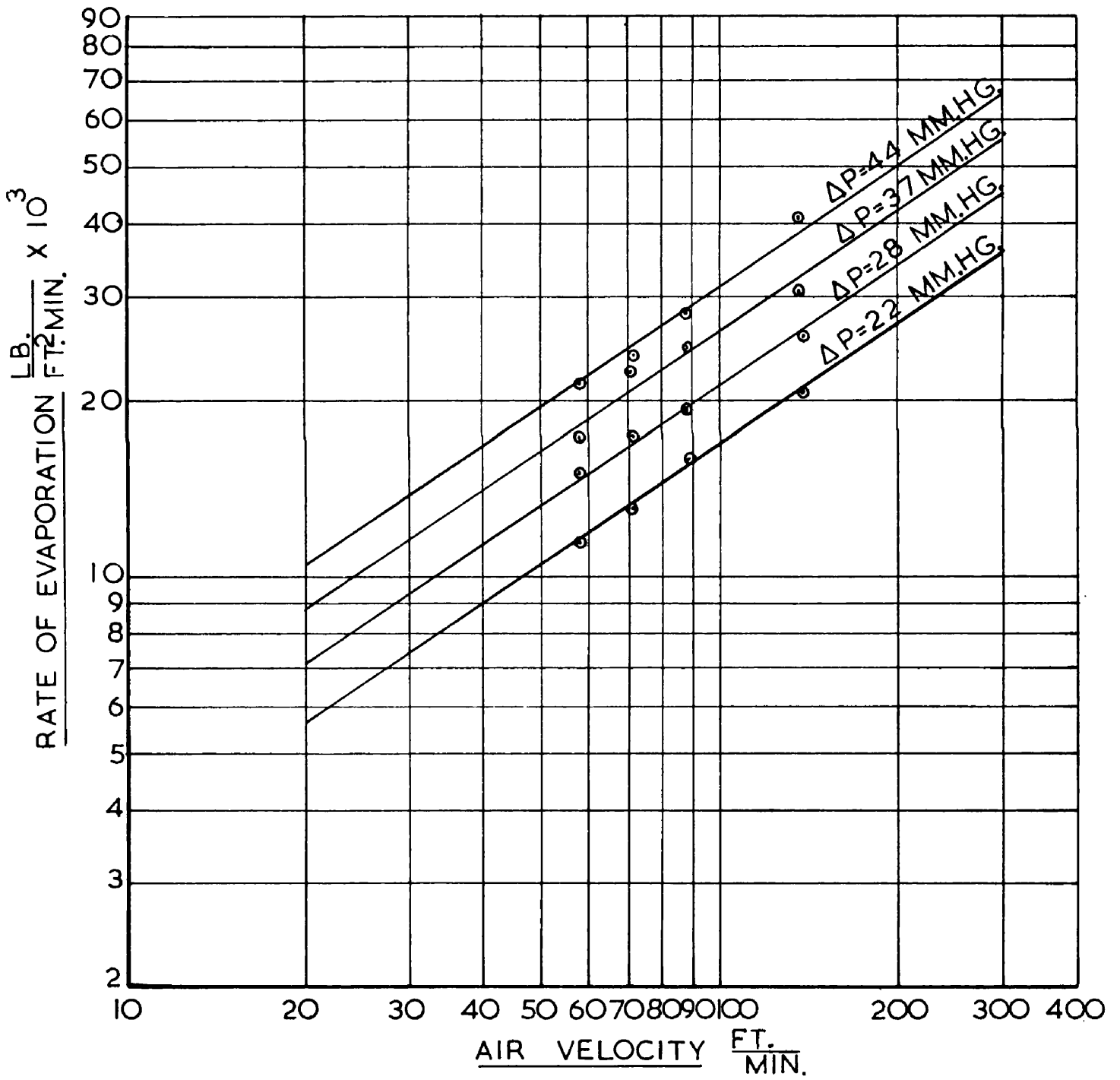


FIG. 4.9.

Table 4.8.

$\frac{dw}{de} \frac{lb}{ft^2 min.} \times 10^2$	$V \frac{ft}{min.}$	$Y = \log \frac{dw}{de}$	$X = \log V$
3.03	137.0	-1.5186	2.1367
2.45	88.0	-1.6108	1.9445
2.23	70.0	-1.6517	1.8451
1.73	57.0	-1.7620	1.7559

Hence the correlationship is given by

$$\frac{dw}{de} \propto v^{0.69} \dots \dots \dots (4.10)$$

4.2.2.3.2. Partial Pressure Difference.

Three runs similar to the one above were carried out to evaluate the effect of partial pressure difference on the rate of evaporation, the partial pressure difference being altered for each series as was done in the experiments with the liquids used previously. The results are shown in graphical form in fig. 4.9. The gradient of each correlation, rate of evaporation against time, was calculated using the method of least squares and are tabulated below. From these the weighted mean gradient was calculated.

ETHANOL-AIR

RATE OF EVAPORATION VS PARTIAL PRESSURE DIFFERENCE

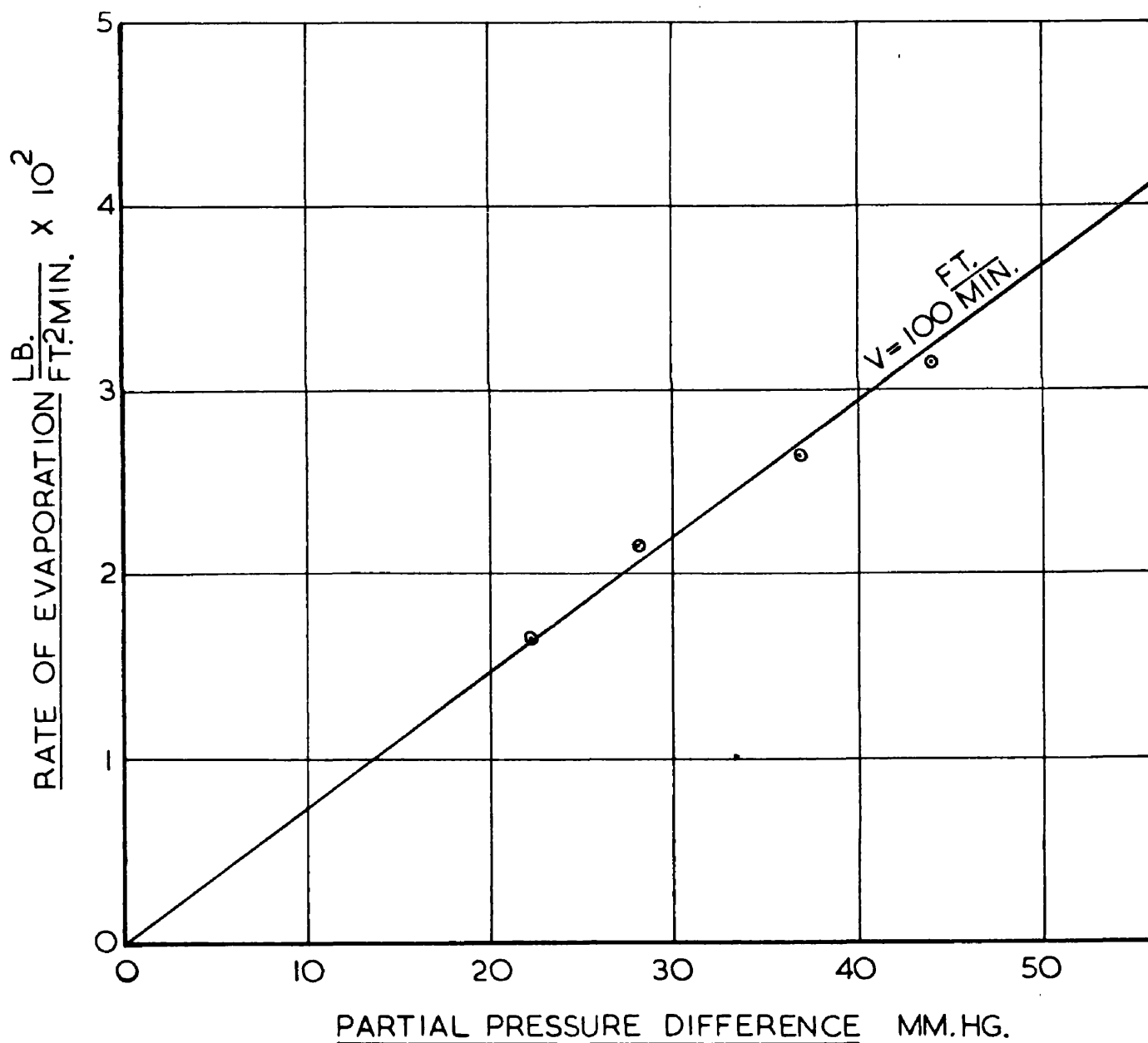


FIG. 4.10.

Table 4.9.

Gradient	Partial Pressure Diff. m.m. hg.
0.751	44
0.690	37
0.640	28
0.695	22

The weighted mean gradient is given by

$$b = \frac{\sum \frac{b_r^2}{s_r^2}}{\sum \frac{1}{s_r^2}} = 0.694$$

After constructing a series of parallel lines through the groups of points of gradient 0.694 the intercepts at a fixed value of velocity were correlated with the corresponding value of partial pressure difference. This is shown in graphical form in fig. 4.10. Hence the rate of evaporation is correlated by the following equation

$$\frac{dw}{de} = 0.985 \times 10^{-6} \frac{V^{0.69}}{d^{0.31}} \Delta p. \quad \dots \dots \dots (4.11)$$

4.2.2.4. Propanol.

4.2.2.4.1. Air Velocity.

As in the previous experimental work the investigation into the effect of air velocity was a series of four runs conducted

at an air temperature of 167°F under standard conditions of tow width and constant partial pressure difference between the fibre surface and the circulating air. The air velocity was varied over a range from 70 to 137 ft/min. The rate of evaporation was calculated as previously.

Table 4.10.

$\frac{dw}{de} \frac{lb}{ft^2 \cdot min.} \times 10^2$	V ft/min	Y = log. $\frac{dw}{de}$	X = log. V
3.82	137	-1.4179	2.1367
3.31	114	-1.4802	2.0569
2.59	88	-1.5867	1.9445
2.31	70	-1.6364	1.8451

Hence the equation of the relationship is given by

$$\frac{dw}{de} \propto V^{0.77} \dots \dots \dots (4.12)$$

4.2.2.4.2. Partial Pressure Difference.

Three series of runs at different values of partial pressure difference were carried out similar to the one above. The gradients were evaluated by the same procedure and are compared in the following table

N-PROPANOL-AIR

RATE OF EVAPORATION VS AIR VELOCITY

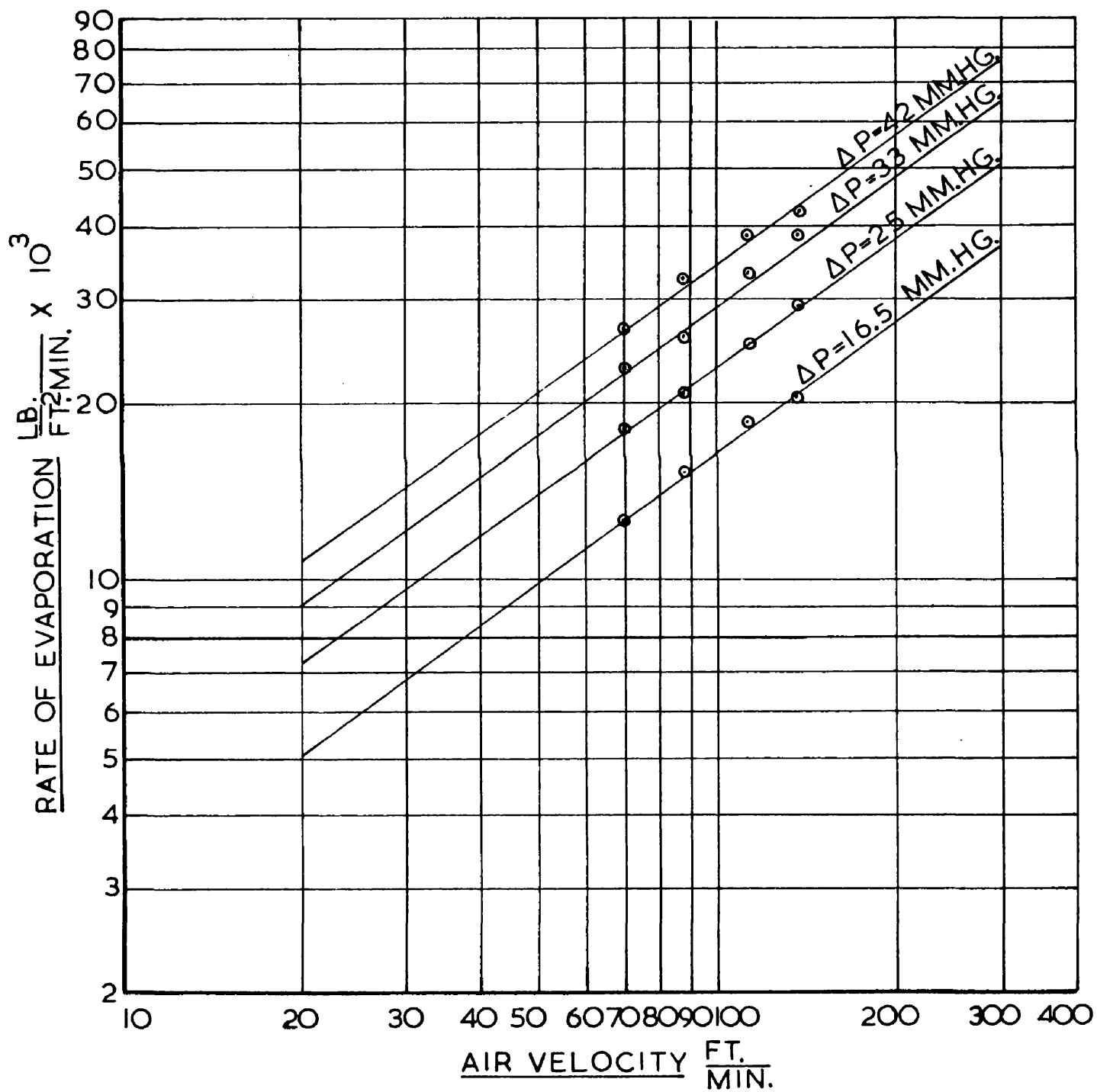


FIG. 4.11.

N-PROPANOL—AIR

RATE OF EVAPORATION VS PARTIAL PRESSURE DIFFERENCE

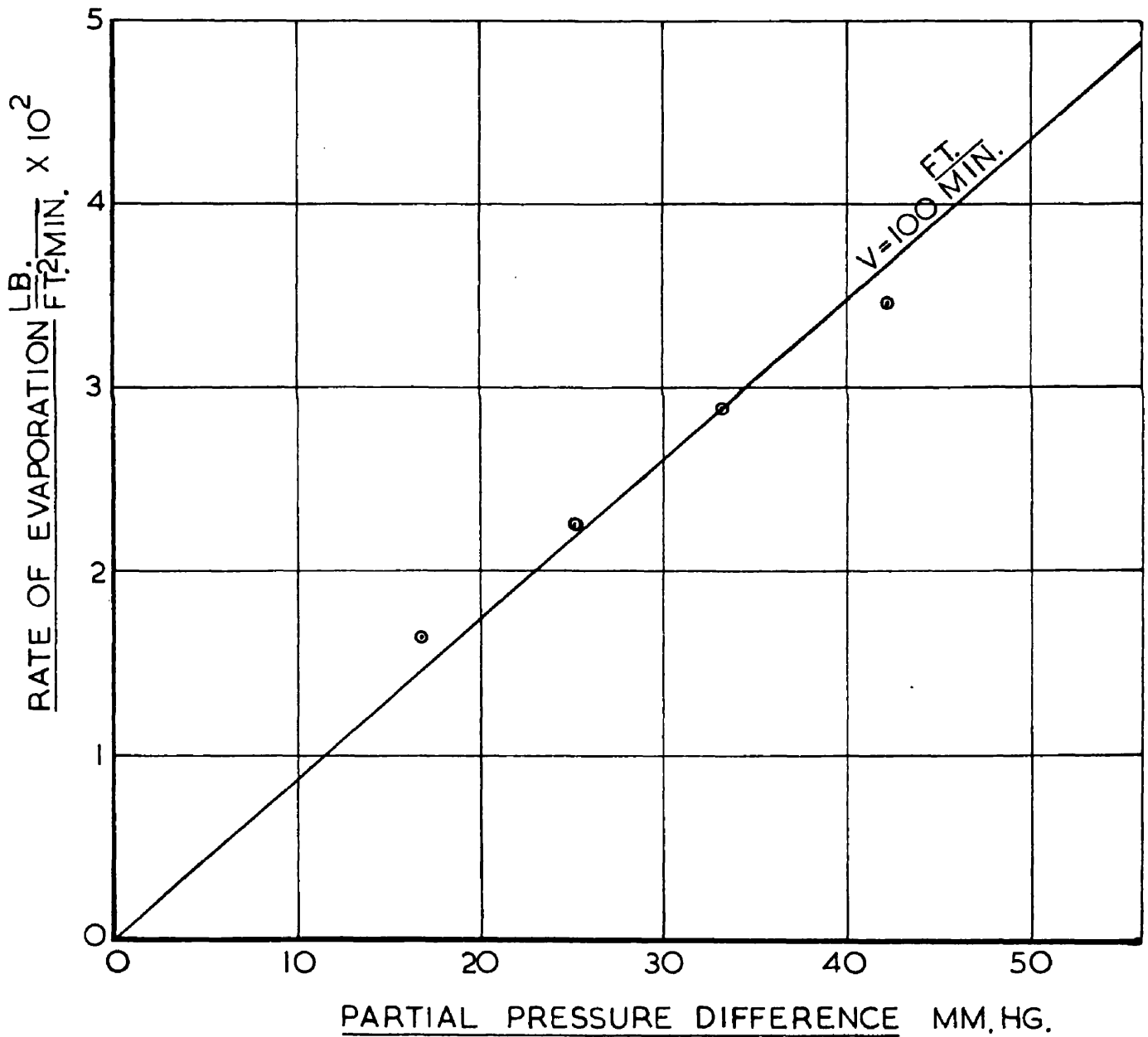


FIG. 4.12.

Table 4.11.

Gradient	Partial Pressure Diff. m.m. hg.
0.69	42
0.77	33
0.72	25
0.76	16.5

The weighted mean gradient is given by

$$b = \frac{\sum \frac{b_r}{s_r^2}}{\sum \frac{1}{s_r^2}} = 0.735$$

A series of parallel lines were constructed of gradient 0.735 as shown in fig. 4.11. The intercepts at a fixed value of velocity were graphed against the corresponding values of partial pressure difference, giving a linear relationship (fig. 4.12).

Hence the rate of evaporation of propanol is given by

$$\frac{dw}{de} = 1.12 \times 10^{-6} v^{0.74} d^{-0.26} \Delta p. \dots (4.13)$$

4.2.2.5. n-Butanol.

4.2.2.5.1. Air Velocity.

A series of runs were carried out at 167°F with fixed

values of tow width and partial pressure difference, the air velocity being varied from 55 to 137 ft/min. The ratio butanol-fibre was plotted against time and the gradient, the rate of evaporation, was calculated.

Table 4.12.

$\frac{dw}{de} \frac{lb}{ft^2 min.} \times 10^2$	V ft/min.	Y = log $\frac{dw}{de}$	X = log V
3.46	137	-1.4609	2.1367
3.02	114	-1.5200	2.0569
2.45	88	-1.6108	1.9445
1.84	55	-1.7352	1.7404

The relationship is given by,

$$\frac{dw}{de} \propto V^{0.68} \dots \dots \dots (4.14)$$

4.2.2.5.2. Partial Pressure.

Three series of runs, similar to the one above, were carried out at different values of partial pressure difference. The gradients of the log-log plots of rate of evaporation and air velocity were evaluated, using the method of least squares, and compared.

N-BUTANOL-AIR

RATE OF EVAPORATION VS AIR VELOCITY

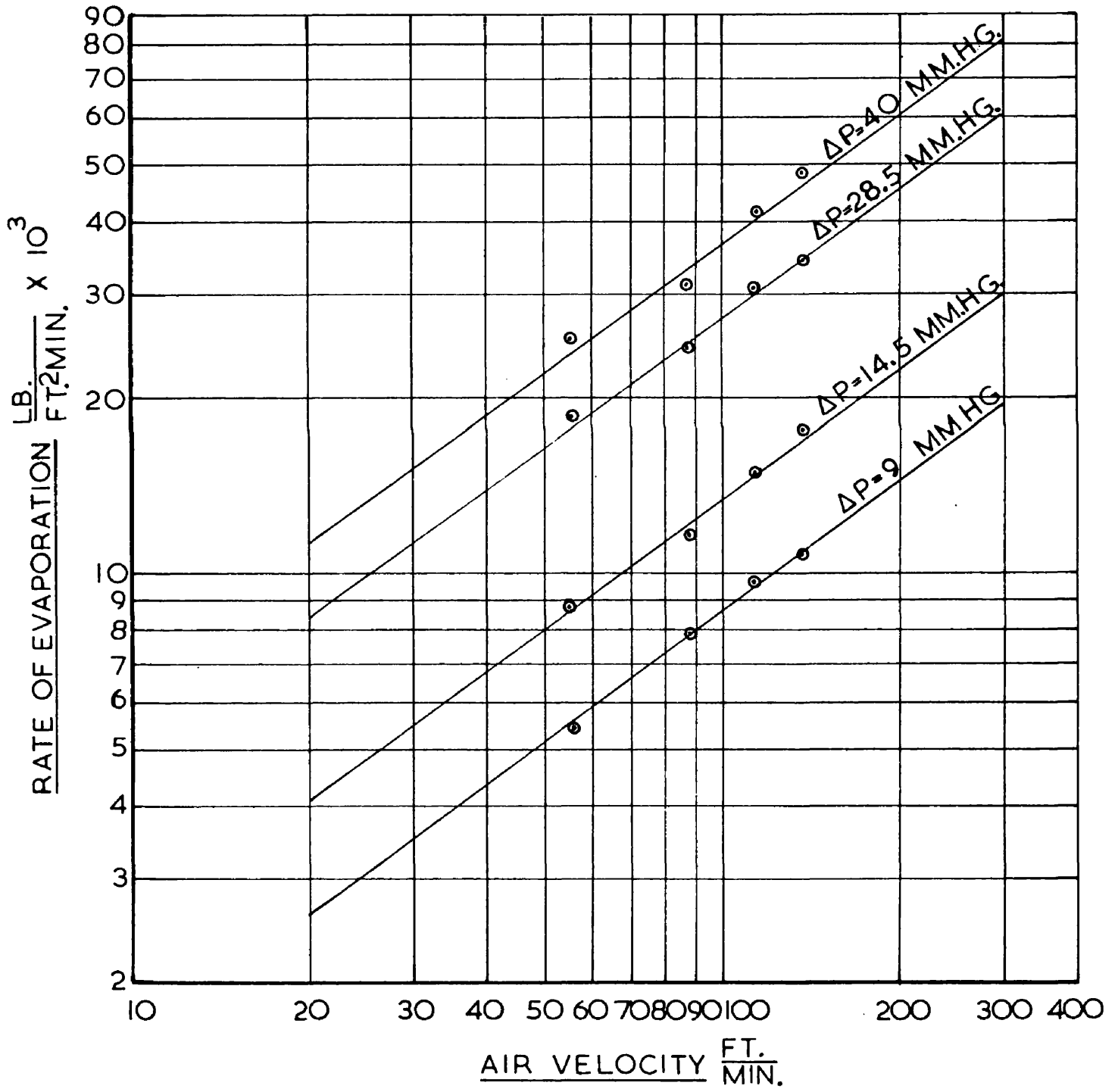


FIG. 4.13.

N-BUTANOL—AIR

RATE OF EVAPORATION VS PARTIAL PRESSURE DIFFERENCE

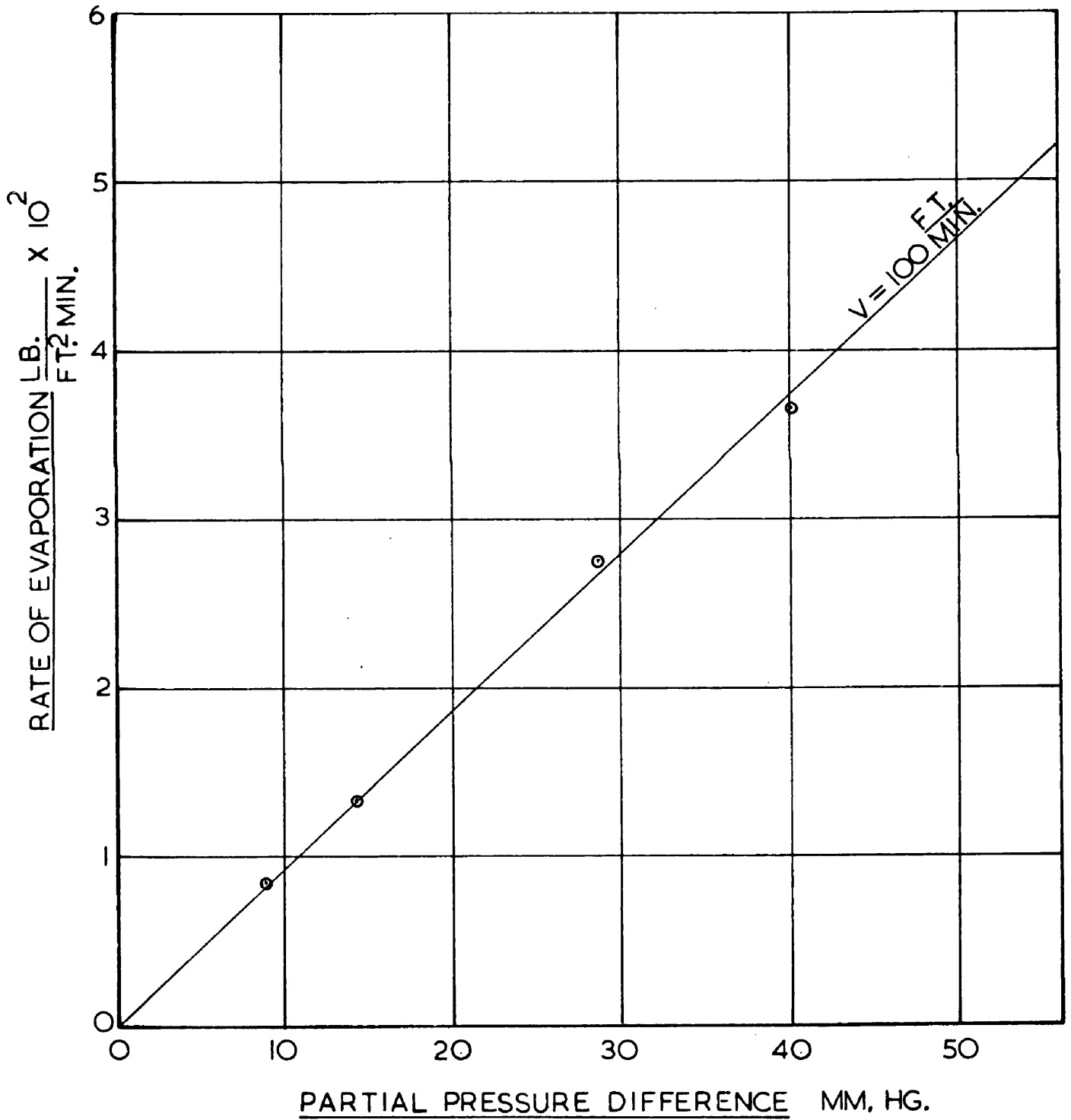


FIG. 4.14.

Table 4.13.

Gradient	Partial Pressure Diff. m.m. hg.
0.754	40.0
0.68	28.5
0.76	14.5
0.771	9.0

The weighted mean gradient = 0.741.

A series of parallel lines were constructed of gradient 0.741 as shown in fig. 4.13. The intercepts at a fixed value of velocity, 100 ft/min. were related to the corresponding values of partial pressure difference. This resulted in a linear relationship which is shown in fig. 4.14.

Thus the rate of evaporation of butanol from a fibre tow width d is given by

$$\frac{dw}{de} = 1.205 \times 10^{-6} \frac{v^{0.74}}{d^{0.26}} \Delta p. \quad \dots \dots (4.15)$$

4.2.3. Evaporation of Trichloroethylene.

Trichloroethylene was chosen for its low diffusion coefficient and general inertness. The main disadvantage of using it in a plant of this type is the danger of the vapour accumulating in quantity around the plant. Even in small concentrations the vapour has anaesthetic properties.

4.2.3.1. Procedure.

The procedure was as described on page 46. Throughout

the experimental work a gas mask had to be worn to overcome the effects of the gas mentioned above. The effect of wetting the fibre with trichloroethylene was similar to that of the alcohols.

4.2.3.2. Air Velocity.

A series of runs were carried out at a constant temperature of 167°F, using a standard tow width and also keeping the partial pressure difference constant. The air velocity was varied from 55 to 137 ft/min. The rate of evaporation of the liquid from the tow was evaluated from the graph of trichloroethylene/fibre against time.

Table 4.14

$\frac{dw}{de} \frac{lb}{ft^2 min.} \times 10$	V ft/min.	Y = $\log. \frac{dw}{de}$	X = $\log. V$
0.8	72.0	-1.0969	1.8573
1.03	88.3	-0.9872	1.9460
1.18	114.0	-0.9281	2.0569
1.37	137.0	-0.8633	2.1367
0.735	55.0	-1.1337	1.7404

The relationship between the rate of evaporation and the air velocity is given by,

$$\frac{dw}{de} \propto V^{0.71} \dots \dots \dots (4.16)$$

TRICHLOROETHYLENE-AIR

RATE OF EVAPORATION VS AIR VELOCITY

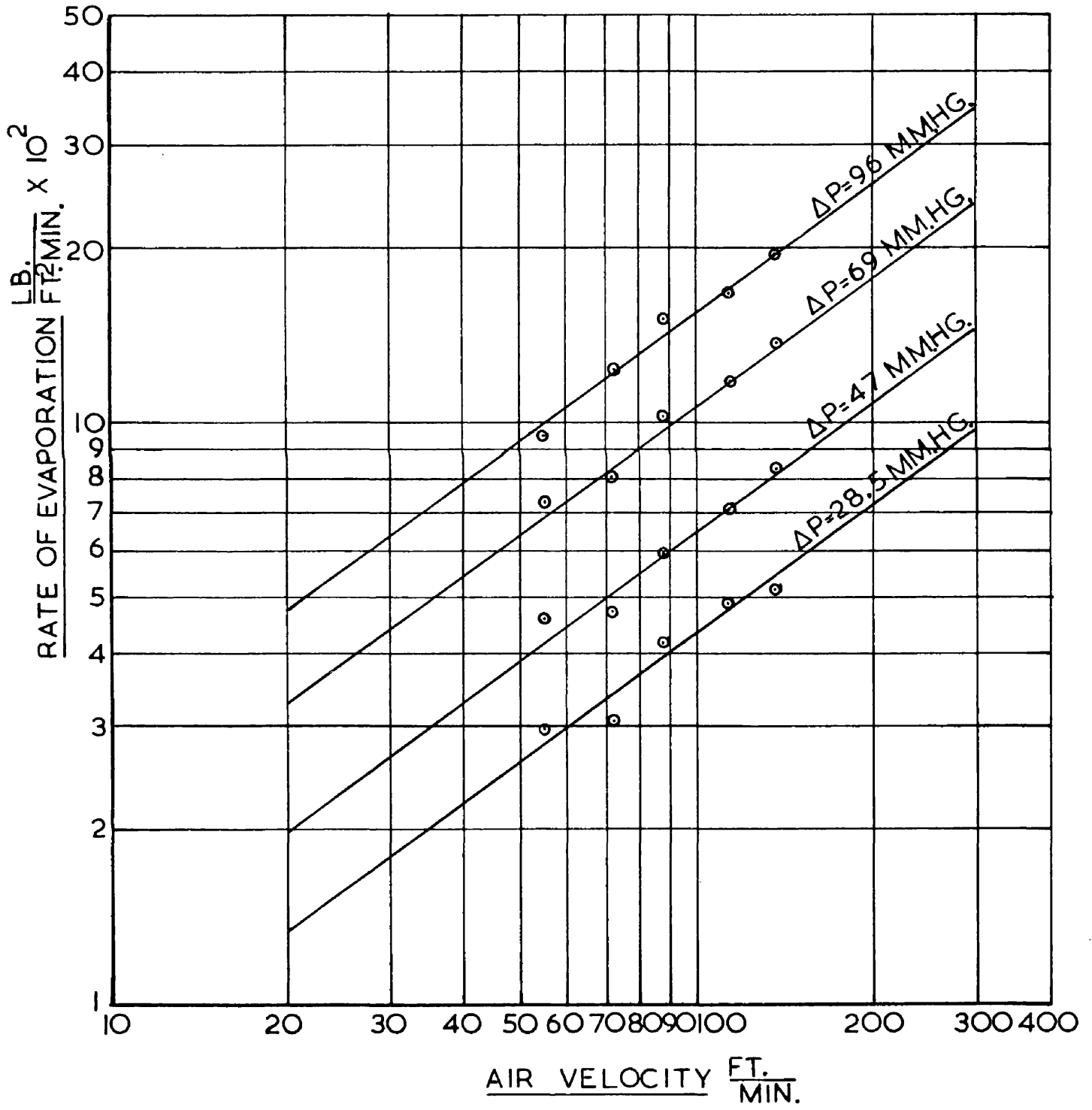


FIG. 4.15.

TRICHLOROETHYLENE-AIR

RATE OF EVAPORATION VS. PARTIAL PRESSURE DIFFERENCE

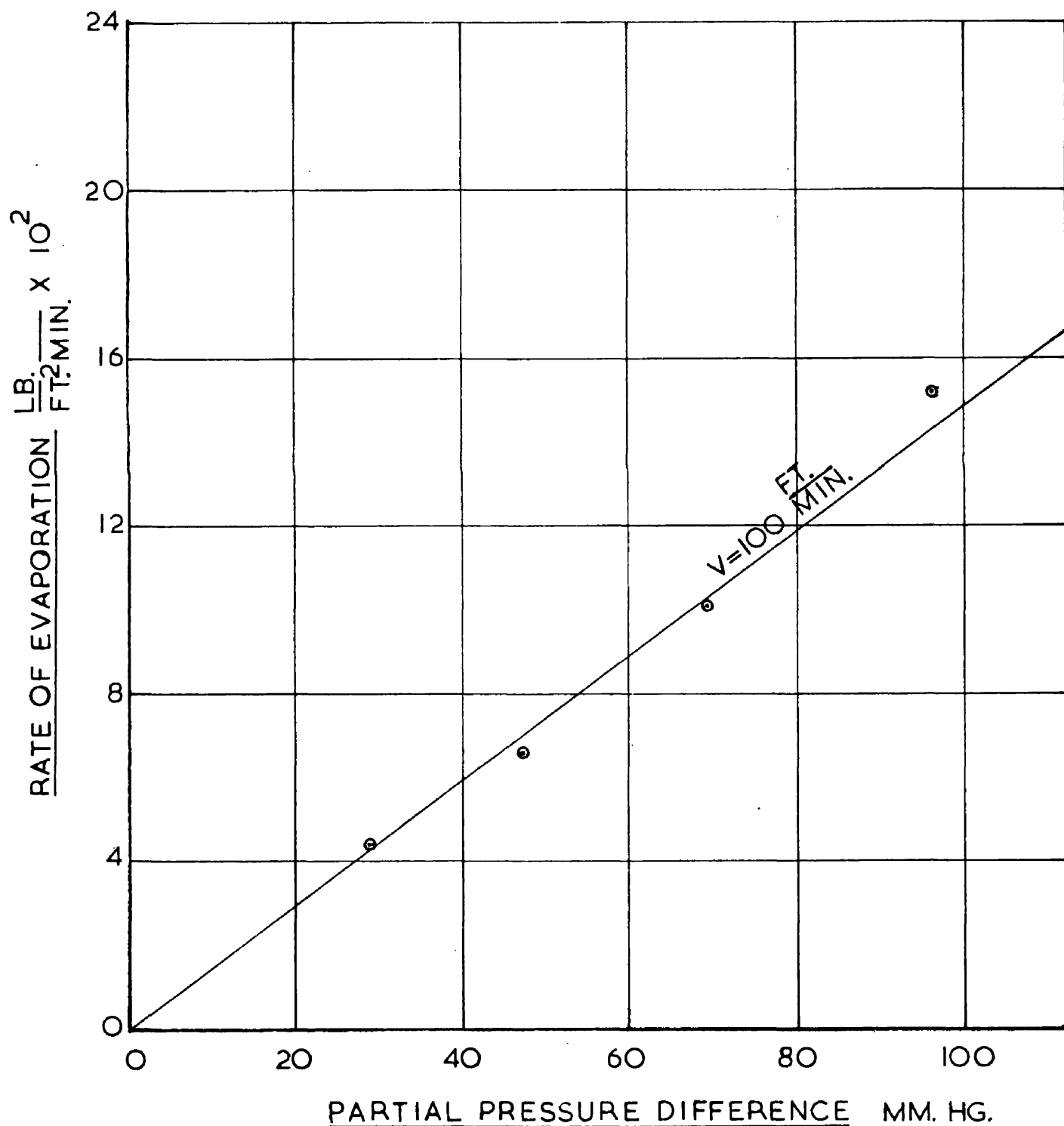


FIG. 4.16.

which, including the effect of tow width becomes,

$$\frac{dw}{de} \propto v^{0.71} d^{-0.29} \dots \dots \dots (4.17)$$

4.2.3.3. Partial Pressure Difference.

A series of three runs similar to the one above were carried out at different values of partial pressure difference. The gradients of the log-log plots of rate of evaporation against air velocity were evaluated and are tabulated with the corresponding values of partial pressure difference in table 4.15.

Table 4.15

Gradient	Partial Pressure Diff. m.m. hg.
0.766	96
0.710	69
0.676	47
0.691	28.5

The weighted mean gradient is 0.711.

Hence fig.4.15 shows a series of parallel lines of gradient 0.711 the intercepts being related to the partial pressure difference. This relationship is shown in fig.4.16 to be linear.

The relationship established for the rate of evaporation of trichloroethylene from a fibre tow is

$$\frac{dw}{de} = 1.94 \times 10^{-6} \frac{v^{0.71}}{d^{0.29}} \Delta p. \dots \dots \dots (4.18)$$

4.2.4. Comparison of Results.

The results were found to be satisfied by the general equation,

$$\frac{dw}{de} = k \cdot V^b \cdot d^{b-1} \cdot \Delta p \quad \dots \dots \dots (4.19)$$

where the values of b and k for the various liquids are shown in table below.

Table 4.16

Liquid	k x 10 ⁶	b	D cm ² /sec. (80)
Water	0.558	0.74	0.256
Methanol	0.782	0.72	0.159
Ethanol	0.985	0.69	0.119
Propanol	1.12	0.74	0.100
Butanol	1.205	0.74	0.090
Trichloroethylene	1.94	0.71	0.073 *

The diffusion coefficient was included to indicate the tendency for the rate of evaporation to be influenced by the diffusion coefficient.

* Calculated from equation.
$$D = \frac{0.0043 T^{\frac{3}{2}}}{P(V_A^{\frac{1}{3}} + V_B^{\frac{1}{3}})^2} \sqrt{\frac{1}{M_A} + \frac{1}{M_B}}$$

$\frac{K_G^M P_{BM}}{\rho V}$ VS REYNOLDS NUMBER

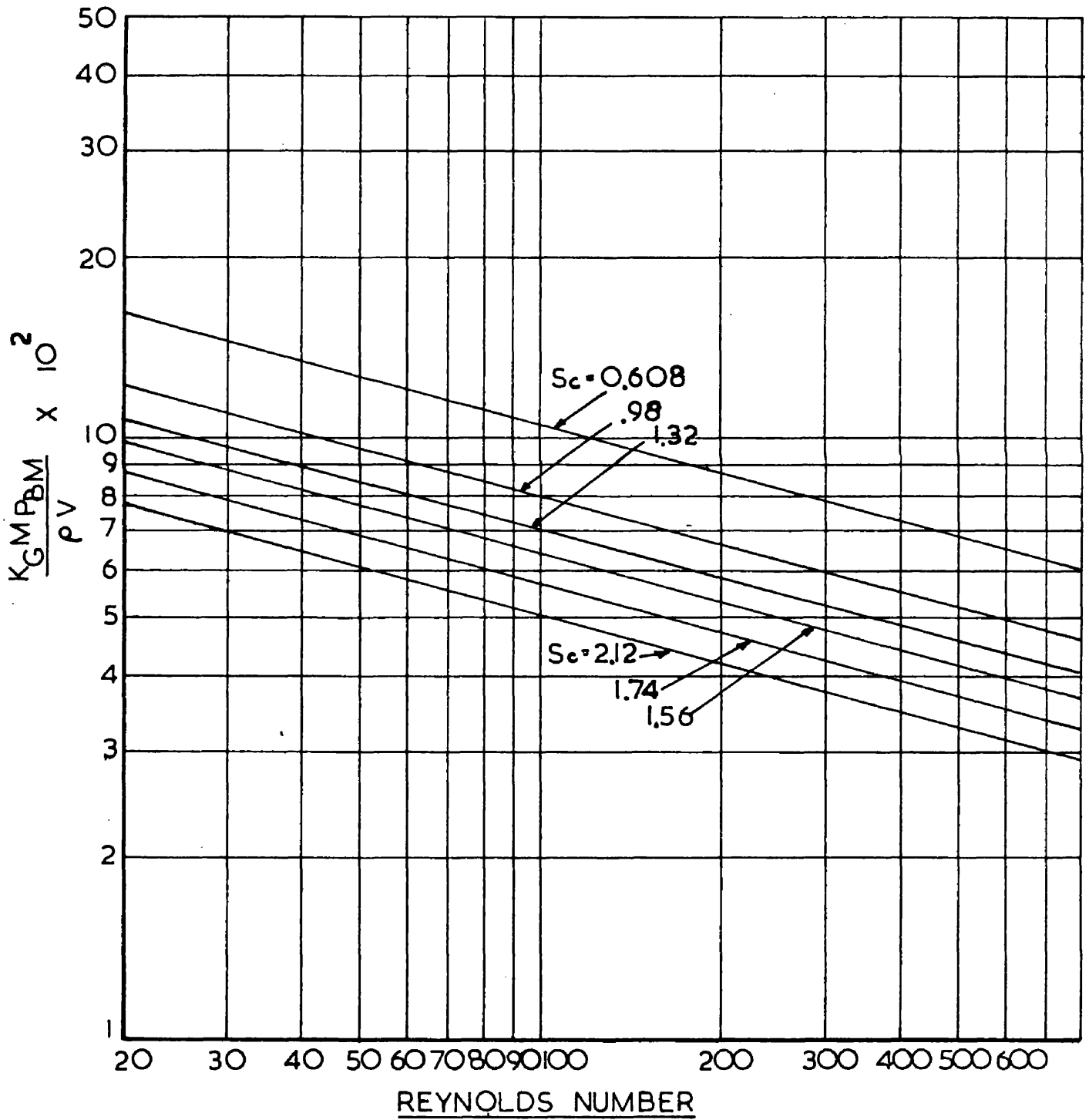


FIG. 4.17.

In forming a general equation for mass transfer the significance of the variations in the power b were investigated and found to be insignificant. Hence a weighted mean value of b was used and appropriate adjustments made to the values of k, the new values are given in table 4.17.

Table 4.17

Liquid	k x 10 ⁶	b
Water	0.613	0.72
Methanol	0.856	0.72
Ethanol	1.08	0.72
Propanol	1.23	0.72
Butanol	1.32	0.72
Trichloroethylene	2.13	0.72

In order to determine the effect of the Schmidt number, or diffusion coefficient, the mass transfer data was rearranged in the form

$$\frac{KgM_{p_{bm}}}{\rho V} = A. Re^n \dots \dots \dots (4.20)$$

4.2.4.1. Effect of the Schmidt Group.

In determining the effect of the Schmidt group, the data was plotted as in fig. 4.17, $\frac{kgM_{p_{bm}}}{\rho V}$, vs. Re. Thus a series of parallel lines were constructed using a weighted mean gradient, the

$\frac{K_{G MP_{BM}}}{\rho V}$ VS SCHMIDT NUMBER

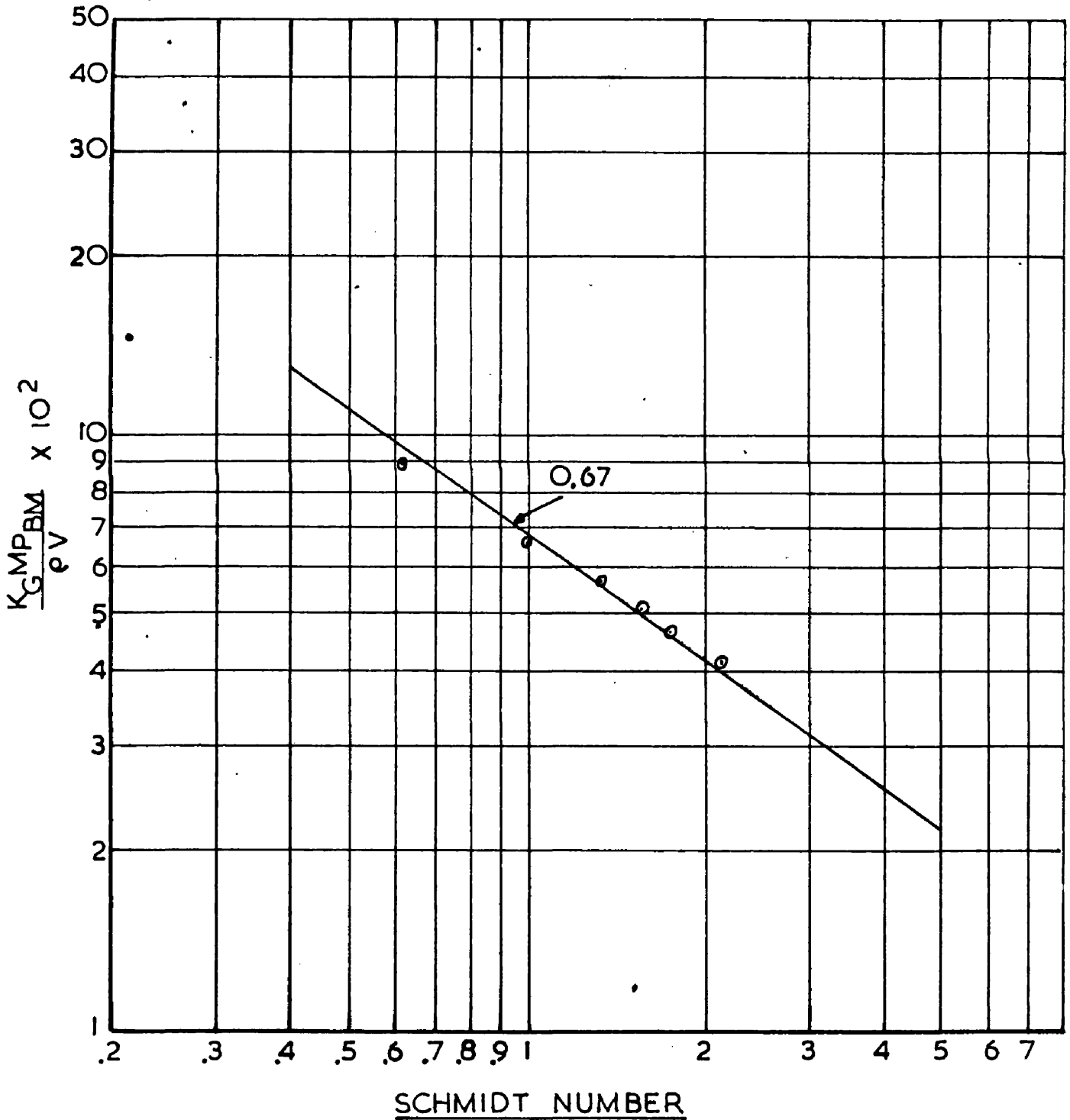


FIG. 4.18.

parameter being the Schmidt group. The intercepts, at a fixed value of Reynolds number, were plotted vs the corresponding values of the Schmidt number. The range of the Schmidt numbers is not very wide, hence the line of gradient 0.67 was drawn for comparison. The agreement is satisfactory considering the range of Schmidt number. Hence the mass transfer data can be correlated by the general equation,

$$\frac{K_g M_p b_m}{\rho V} = 0.24 \text{ Re}^{-0.24} \text{ Sc}^{-0.67} \dots \dots \dots (4.21)$$

4.3. Heat Transfer.

The rate of heat transfer to the fibre tow was calculated from the formula derived below.

4.3.1. Heat Transfer to a Continuous Tow.

Consider a small element of the fibre tow of the length dl . Let the temperature of the fibre vary from T_f 'F to $(T_f + dT_f)$ 'F and the associated liquid from x to $(x - dx)$. Thus if the throughput of dry fibre is W lb/hr. the rate of evaporation becomes Wdx lb/hr. The temperature of the ambient air stream is assumed to be constant at t_a 'F.

Heat Balance on Element per unit time.

$$\begin{aligned} ha dl \left[t_a - \left(T_f + \frac{dT_f}{2} \right) \right] &= \lambda dx \cdot W + WC_f dT_f + WC_s T_f dx + Wdx \left(\frac{dT_f}{2} \right) \\ &\quad - C W(x - dx)(T_f + dT_f) - C_s W x T_f \\ &= Wdx + WC_f dT_f + WC_s dT_f \\ \frac{ha dl}{W} (t_a - T_f) &= \lambda dx + (C_f + x C_s) dT_f \end{aligned}$$

Integrate both sides of the equation,

$$\frac{ha}{W} \int_0^L (t_a - T_f) dl = \lambda \int_{x_1}^{x_2} dx + \int_{T_1}^{T_2} (C_f + C_s x) dT_f$$

During the Constant Rate Period the fibre temperature remains constant.

$$\text{Hence } \frac{ha}{W} (t_a - T_f) l = (x_2 - x_1)$$

$$h = \frac{(\lambda) \cdot (x_2 - x_1)}{al (t_a - T_f)} \dots \dots \dots (4.22)$$

WATER AIR

HEAT TRANSFER COEFFICIENT VS AIR VELOCITY

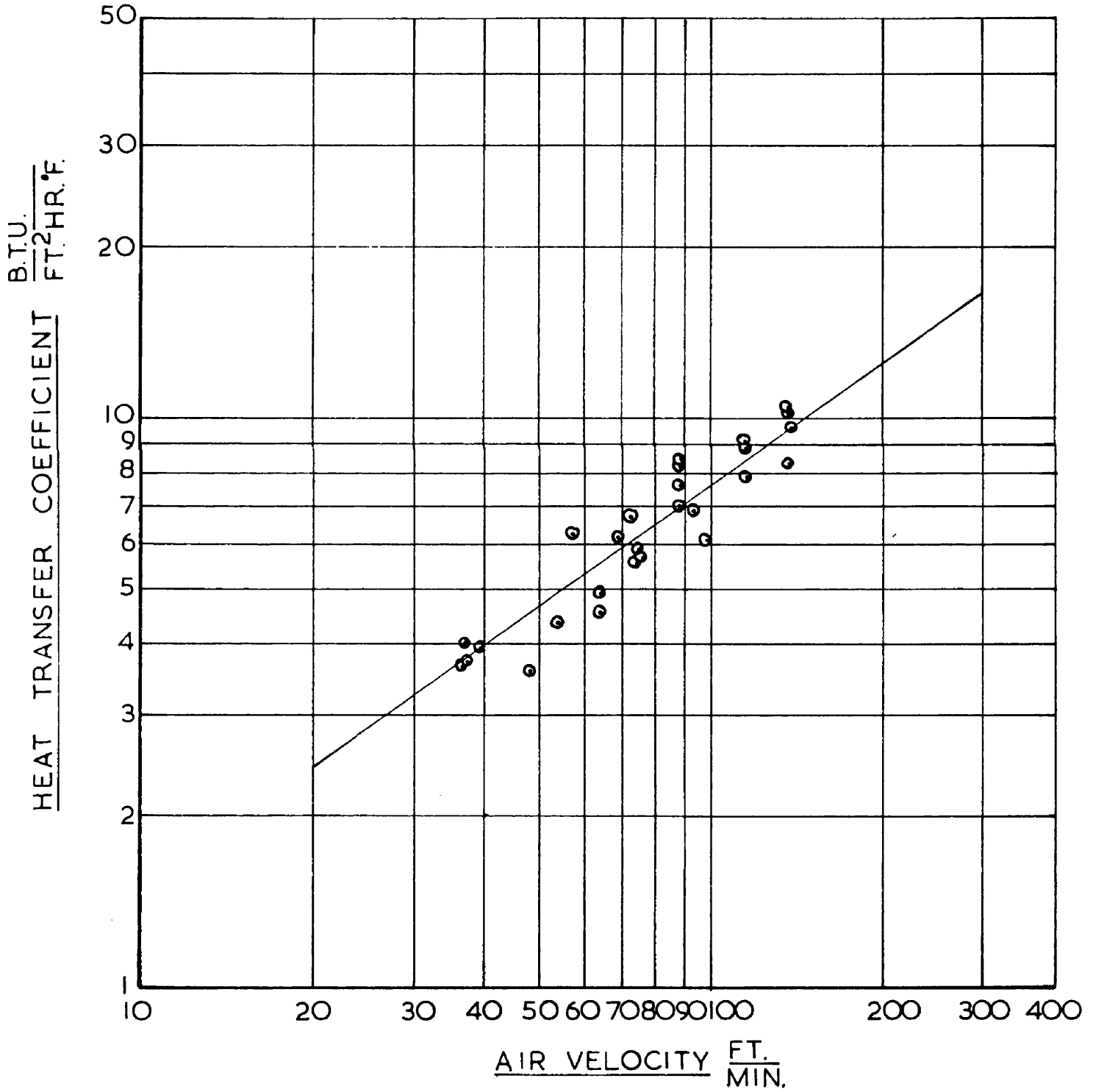


FIG. 4.20.

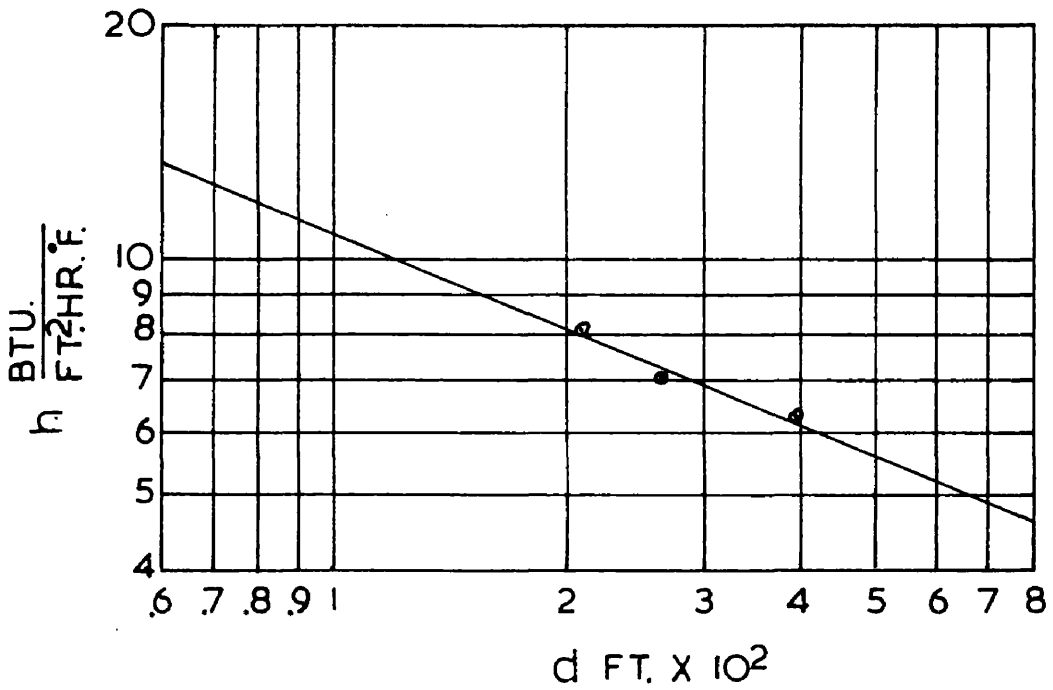
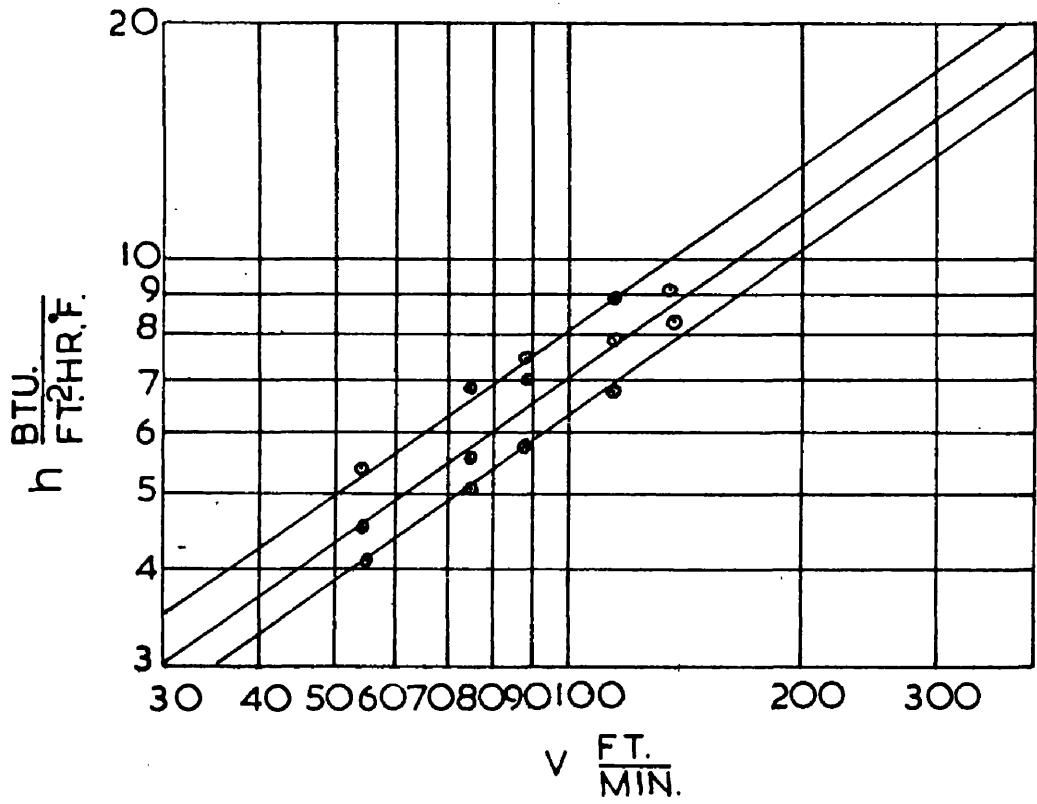


FIG. 4.21

4.3.2. Evaporation of Water.

4.3.2.1. Air Velocity.

The rate of heat transfer is influenced by several variables, one of which is the velocity of the air. To find the effect of the air velocity in the present system, the rates of heat transfer were calculated for the series of runs described on pages 55-57. The results are plotted in Fig. 4.20, showing a relationship of the type

$$h = A \cdot V^n \quad \dots \dots \dots (4.23)$$

However all these runs were carried out using the same tow width, hence the effect of the tow width is unknown.

4.3.2.2. Tow Width.

The effect of the tow width can be assumed to be important since the velocity profile is affected by it. The study of the effect of the tow width, d , on heat transfer was restricted by the limitations imposed by the drier. The results which are shown in fig. 4.21 were calculated from the same experimental runs as the mass transfer results in fig. 4.5. The resulting expression was

$$h \propto d^{-0.3} \quad \dots \dots \dots (4.24)$$

The combined effects of velocity and tow width are a measure of the degree of turbulence in the air stream and can be expressed in terms of Reynolds number.

$$hd \propto Re^{0.68} \quad \dots \dots \dots (4.25)$$

If the physical properties of the air stream are included in the form of dimensionless groups, the expression becomes

$$Nu = 0.34 Re^{0.68} Pr^{0.33} \dots \dots \dots (4.26)$$

4.3.3. Evaporation of Other Liquids.

The rates of heat transfer were calculated for each of the runs where the liquid evaporated was a liquid other than water. The relationship between rate of evaporation and air velocity was assessed in a similar manner to that for water giving a correlation of the type,

$$h = A. V^n \dots \dots \dots (4.23)$$

The data was then correlated in the following manner to compare with the similar data for water.

$$Nu = k Re^m Pr^{0.33} \dots \dots \dots (4.27)$$

4.3.4. Comparison of Results.

The results of all the liquids were compared using the form of equation 4.27. The various values for k and m are tabulated below.

Table 4.18

Liquid	k	m
Water	0.34	0.68
Methanol	0.25	0.73
Ethanol	0.28	0.68
Propanol	0.32	0.71
Butanol	0.38	0.67
T.C.E.	0.30	0.71

The significance of the differences of the powers was investigated by comparing the highest and lowest values, 0.73 and 0.67. The difference was found to be insignificant and hence a weighted mean value was calculated by the method described on page 58. The corresponding values of k were evaluated and are tabulated below.

Table 4.19

Liquid	k	m
water	0.31	0.70
methanol	0.30	0.70
ethanol	0.25	0.70
propanol	0.28	0.70
butanol	0.32	0.70
T.C.E.	0.32	0.70

The above table reveals slight variations in the values of k for the various liquids. A mean value was calculated to be 0.30. The maximum and minimum values of k are 0.32 and 0.25. The percentage deviation from the calculated mean value was found to be 6.7 for the higher value, and 17.7 per cent for the lower. Although the deviation in the latter case is considerable it can be seen from table 4.19 that this deviation is not typical, being much greater than the others.

In order to calculate an overall correlation the method of least squares was used to correlate the individual values.

This resulted in the following correlation.

$$\text{Nu} = 0.32 \text{Re}^{0.70} \text{Pr}^{0.33} \dots \dots \dots (4.28)$$

4.4. Discussion.

4.4.1. Introduction.

In the investigation into the processes of simultaneous heat and mass transfer, the system which has been used as the basis for all investigations is the evaporation of liquids from a surface. Usually pure liquids are used, thus diffusion through one resistance layer only has to be considered, that of the gas. In order to assess the effect of different velocity profiles, etc. many systems have been devised, most of which have inherent disadvantages. If one considers, as an example, the flow of a gas up a wetted wall column, the continually changing value of the partial pressure difference as the gas flows upwards presents a problem in assessing the effect of the partial pressure difference as, depending on the gas throughput, this variation may be considerable. This disadvantage is not so pronounced in the system of a gas flowing past a wetted object, say a cylinder at right angles to the gas flow, where the contact time between the gas and the surface is usually negligible compared to the previous system. The main problem in the cylinder type of experiments is the difficulty in maintaining a uniformly wetted surface, as the effect of gravity tends to cause a certain amount of liquid migration within the cylinder. In some instances a constant liquid feed system is used and in this case the danger is the excessive wetting of the surface coupled with uneven distribution as previously. It was with

these difficulties in mind that the present system was devised, initially to overcome them and latterly as a compromise between them. It also enabled the effect of a new geometry to be studied.

4.4.2. Present System.

As in the previous systems certain disadvantages arose, some of which were inherent in the system, others which were related to the plant used. Of the latter type was the restricted range of air velocity which was mainly due the modifications which had to be carried out to improve the air distribution along the drying drum as described on page 49. This had the effect of considerably increasing the pressure drop across the drum with the resultant decrease in air throughput. In order to mitigate the effect of lack of range of air velocity a statistical check was used to evaluate the significance of the results, the method was that shown on page 57. If after a series it was found that the significance of the correlation was less than 95 per cent further runs were carried out to obtain a more significant correlation. This was the case with the trichloroethylene results which, due to the high rate of evaporation and the physical difficulties involved, were found to be more scattered than those in the other series. The problem of liquid migration was reduced to negligible dimensions by keeping the overall liquid to solid ratio at inlet within strict limits determined by experiment. The rotary motion of the drier tends to balance the migration due to

gravity from one surface to another over a complete cycle. Throughout the experimental work this migration could not be detected and presented no major difficulties except with some of the more volatile liquids where the tendency was to increase the liquid to solid ratio to obtain a longer constant period of drying. On balance the advantages gained make it a useful method of investigating the processes of heat and mass transfer.

4.4.3. Mass Transfer.

The method of investigation used was to vary one of the variables at a time keeping the other variables constant, repeating the process for each of the variables in turn. The method of analysing the results e.g. air velocity and partial pressure difference, was to graph the rate of evaporation against air velocity with partial pressure difference as the parameter using a log-log plot. By using this method the possibility of interactions between any two of the variables was accounted for although in this case no such interactions were detected. The form of the equation which was found to satisfy the main variables was

$$\frac{dw}{de} = k \cdot V^b \cdot d^{b-1} \cdot \Delta p \quad (4.29)$$

where the values of b and k for the various liquids are shown in tables, 4.16 and 4.17. In comparing the values given in these two tables with the work of Powell consideration should be given to the fact that his

results are based on the rates of evaporation from the individual surfaces whereas the present work uses the total surface area as the basis for calculating the rates of evaporation. Powell found that the rate of evaporation from the down stream surface was lower than that from the upstream surface but that the effect of velocity on both surfaces was similar. This is in agreement with the assumption that the flow pattern is as shown in fig. 2.2. The flow patterns near the surface on either side are similar, the vortex being distorted near the down stream surface into a pattern similar to that on the upstream surface caused by the fluid impinging on the surface at right angles to it then breaking into two paths, each following the contours of the object as shown in fig. 2.2. The dissimilar rates of evaporation may be caused by the fluid in the vortex on the downstream side having a higher contact time with the surface and hence a lower partial pressure difference. Similar problems have arisen in investigations into the rates of mass transfer from cylinders and spheres. In both these cases, the rates of evaporation have been based on total surface area and satisfactory correlations established.

4.4.3.2. Schmidt Group.

In establishing the effect of the Schmidt number, the limited range of the values obtained was considered to be such that only comparison with suggested values, i.e. 0.67 by Chilton and Colburn and 0.56 by Gilliland, was attempted. The results from present

investigation indicated that 0.67 was a better correlation than 0.56. The values are compared in fig. 4.18

Hence it was found that all the mass transfer data could be correlated by the correlation

$$\frac{K_g M_p \rho_{bm}}{\rho V} = 0.24 \text{ Re}^{-0.24} \text{ Sc}^{-0.67} \dots \dots \dots (4.21)$$

This correlation was obtained by using the individual results from all the experimental work, assuming the power of the Schmidt number to be 0.67, and correlating them using the method of least squares.

Statistical investigation of the significance of the correlation revealed that it was significant but just within the limits normally accepted, i.e. the 10 per cent level of significance. Thus the correlation could only be improved by extending the range of Reynolds number. This is not possible using the plant in its present form as the range at the lower limits is restricted by the tendency for the distribution of air along the drum to deteriorate markedly at such low velocities.

4.4.3.3. Comparison with Correlations from similar Systems.

The systems which most closely approximate to the one under consideration are flow past a cylinder and flow past a sphere. In these cases the flow patterns are of the same general form. The mass transfer data from each of the systems can be correlated by the general equation,

$$\frac{K_g M_p \rho_{bm}}{\rho V} \cdot \text{Sc}^m = k \cdot \text{Re}^n \dots \dots \dots (4.30)$$

The values of k, m, and n are tabulated below.

Table 4.20

System	k	m	n	Ref.
Cylinder	0.28	0.56	-0.40	37
Sphere	0.43	0.67	-0.44	43
Rectangular sectioned object	0.24	0.67	-0.24	Present

From the above comparison it can be seen that while two systems may appear to have very similar flow patterns the effect of the Reynolds may vary considerably.

4.4.4. Heat Transfer.

The heat transfer data calculated from the same experimental work as the mass transfer data of the previous section was found to be correlated by an equation of the type,

$$Nu = k Re^m Pr^n.$$

It was possible to correlate the data obtained from each of the individual series of experiments, i.e. each liquid used, in the above form. This approach led to several equations differing slightly in the values of k and m. When the differences in the values of m were analysed they were found to be insignificant and attributed to experimental error. Hence the data was grouped together to give one correlation.

$$Nu = 0.32 Re^{0.70} Pr^{0.33} \dots \dots \dots (4.28)$$

The above equation is compared with correlations of a similar type in the table below.

Table 4.21

System	Author	k	m	n
Flow past rect. sect. objects	Present	0.32	0.70	0.33
Flow past cylinders	Griffiths & Awbery ⁽⁸¹⁾	0.26	0.60	0.30
Flow through pipes	Colburn ⁽¹⁶⁾	0.023	0.80	0.33

Hence it appears that although the flow patterns around a rectangular sectioned object and a cylinder are very similar. The heat transfer equations for the two systems are not identical although they are of the same order.

4.4.5. Heat and Mass Transfer.

In order to compare the heat and mass transfer data, the results were correlated in the form of the Chilton and Colburn j-factors. The similarities between the processes were revealed by relating j_h and j_d to the Reynolds group. This resulted in equations of the following types.

$$j_h = k_1 Re^m \dots \dots \dots (4.31)$$

$$j_d = k_2 Re^n \dots \dots \dots (4.32)$$

The values obtained from the data for each of the various liquids are tabulated below.

Table 4.22

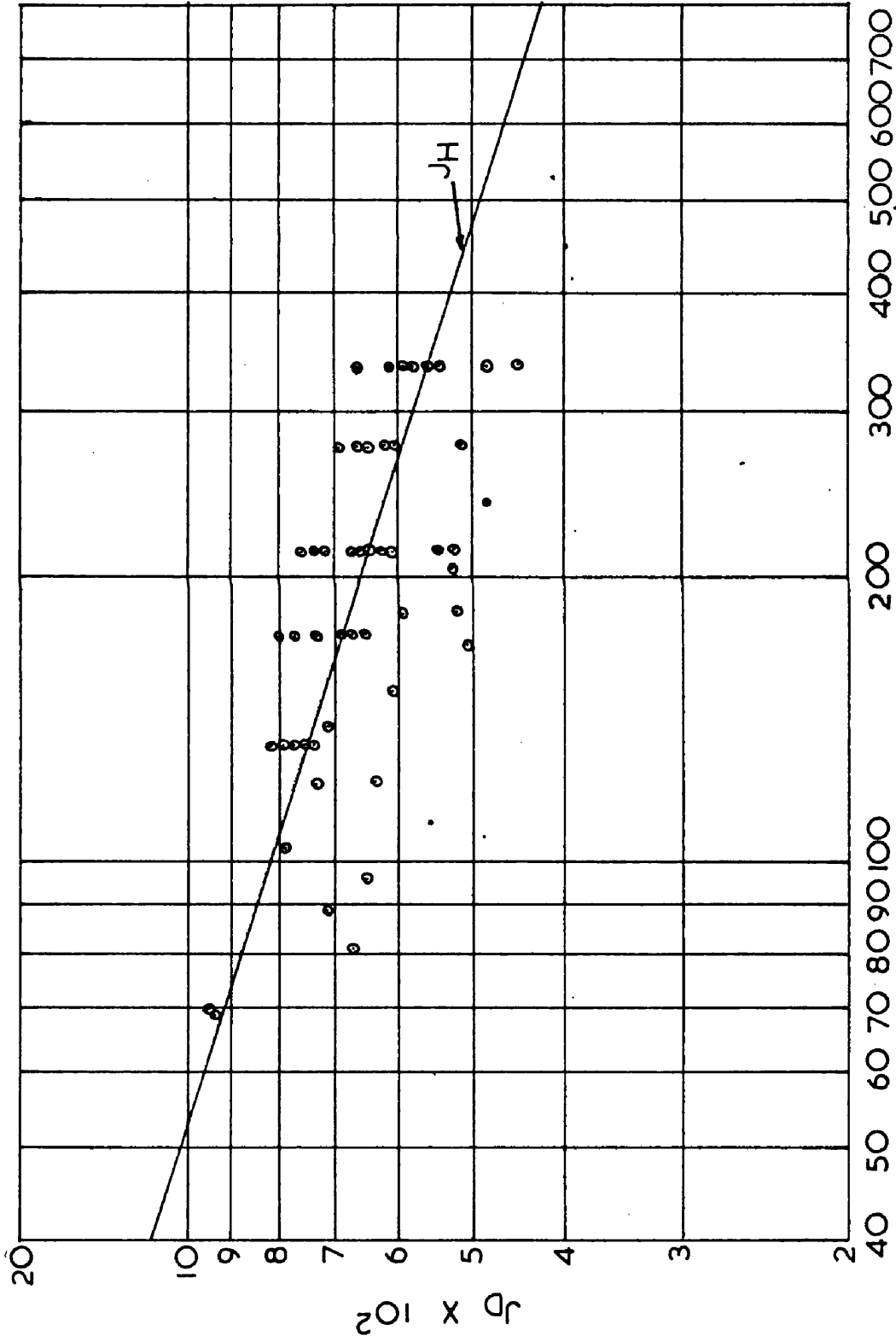
Liquid	k_1	m	k_2	n
Water	0.34	-0.32	0.23	-0.26
Methanol	0.25	-0.27	0.31	-0.29
Ethanol	0.28	-0.32	0.36	-0.31
Propanol	0.32	-0.29	0.21	-0.25
Butanol	0.38	-0.33	0.44	-0.35
Trichloroethylene	0.30	-0.29	0.36	-0.31

The variations in the corresponding values of m and n can be shown statistically to be insignificant when compared with the range of Reynolds numbers of the points used to form the correlations. Hence mean values were taken for each liquid and the corresponding values of k_1 and k_2 were adjusted and compared in the table below.

Table 4.23

Liquid	k_1	k_2	$\frac{k_2}{k_1}$
Water	0.304	0.300	0.99
Methanol	0.27	0.29	1.08
Ethanol	0.365	0.374	1.025
Propanol	0.277	0.300	1.08
Butanol	0.396	0.421	1.065
Trichloroethylene	0.318	0.342	1.08

J_D VS REYNOLDS NUMBER



REYNOLDS NUMBER

FIG. 4.22.

VELOCITY PROFILE

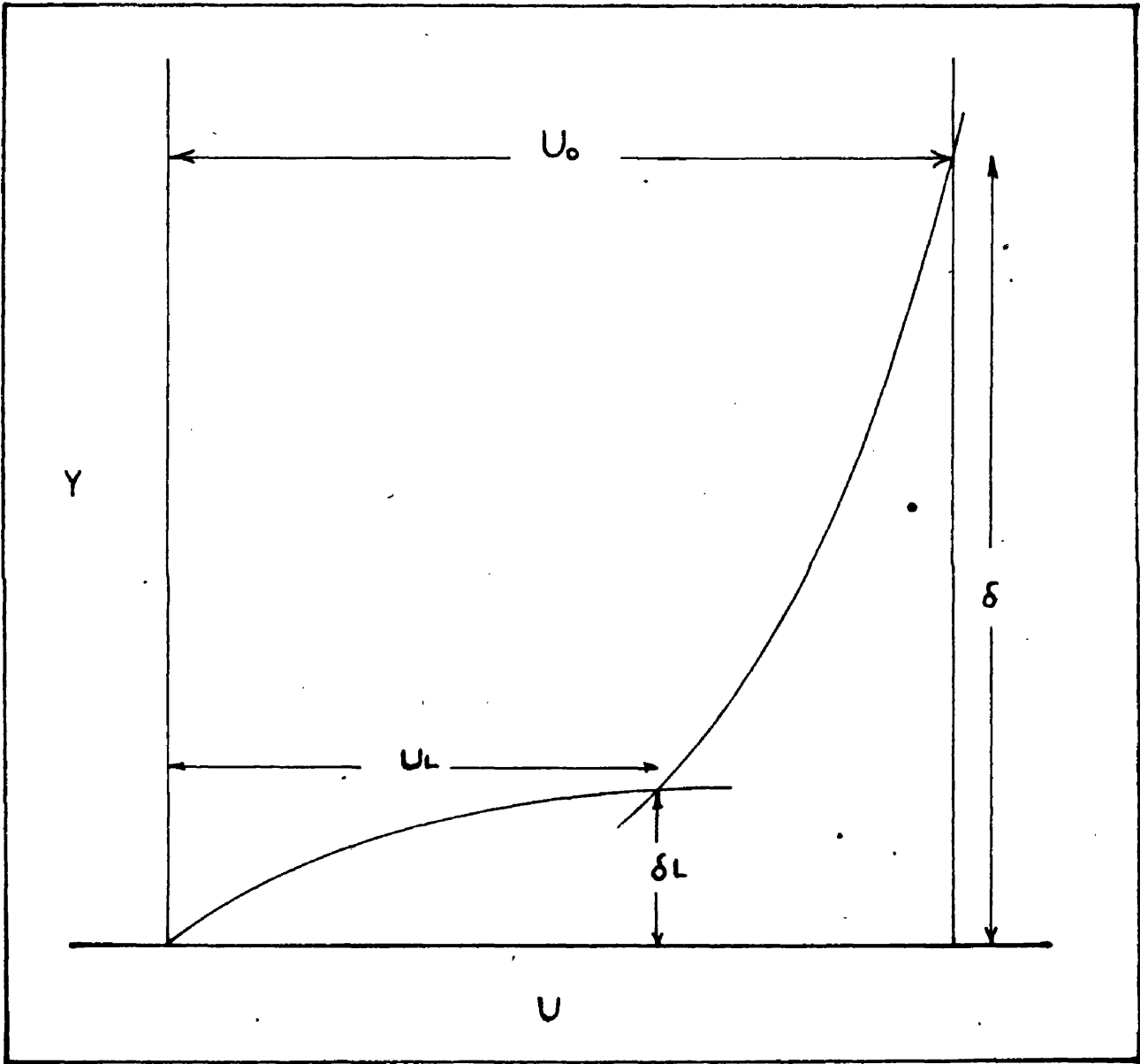


FIG. 4.23.

Mean value $\frac{k_2}{k_1} = \frac{j_d}{j_h} = 1.048$ when n is equated to m.

Alternatively the results may be analysed using all the individual values of j_h and j_d to evaluate correlations of the type in equations 4.31, 4.32. This resulted in the following correlations

$$j_h = 0.32 \text{ Re}^{-0.30} \dots \dots \dots (4.33)$$

$$j_d = 0.24 \text{ Re}^{-0.24} \dots \dots \dots (4.34)$$

In fig. 4.22 the values of j_d are compared with equation 4.33.

Since it can be shown statistically that the difference between the two powers is insignificant, the mean value was used and the constants were altered accordingly. Hence it can be shown that

$$\frac{j_d}{j_h} = 1.05$$

Hence both methods of analysis give approximately the same solution, j_d being slightly greater than j_h . This is within the limits claimed by Chilton and Colburn⁽¹²⁾ who claimed only an equality to within + or - 10 per cent. There are few other theoretical analyses with which the result can be compared, however Callaghan⁽⁸²⁾ has deduced an expression, a simplified version of which is shown below, for the case of fluid flowing over a flat plate. He assumed a profile of the type shown in fig. 4.23.

$$\frac{St_d}{St_h} = \frac{1 - \left[\frac{Re_L}{Re\delta} \right]^{\frac{1}{n+1}} (1 - Pr)}{1 - \left[\frac{Re_L}{Re\delta} \right]^{\frac{1}{n+1}} (1 - Sc)} \dots \dots \dots (4.35)$$

where St_d is the Stanton number for mass transfer
 St_h is the Stanton number for heat transfer
 Re is the Reynolds number based on the thickness
of the laminar layer.

Re is the Reynolds number based on the thickness
of the boundary layer.

n is the power exponent, $\frac{u}{u} = \frac{y}{\delta} \frac{1}{1+n}$

He estimated that, for the air-water system, the ratio of the Stanton numbers for mass and heat transfer would be slightly greater than unity, 1.05. This compares with the value obtained in the present investigation of 0.99 for the air-water system. Callaghan⁽⁸²⁾ obtained the value 1.05 assuming that $n = 4$ at transition and $n = 7$ at full turbulence. In table 4.24 are listed results from various types of experimental equipment involving air water systems only.

Table 4.24

Author	System	<u>Mass Transfer</u> Heat Transfer
Gamson et al.	Through circulation drying of spheres	0.93
Heertjees and Ringens	Evaporation from a porous block	0.91
Coles and Ruggeri.	Evaporation from flat surface.	0.94
Present.	Present.	0.99

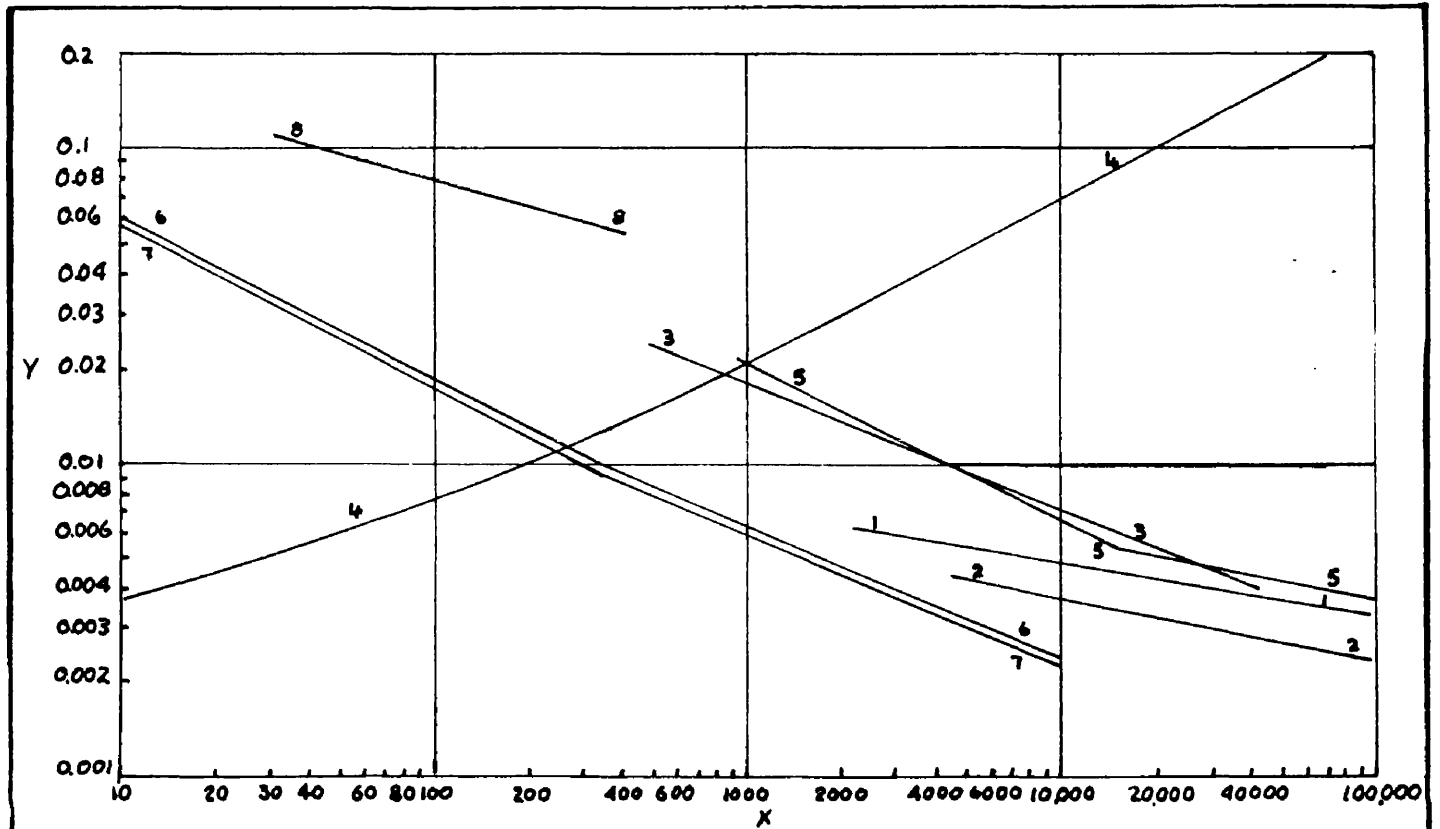
From the above it can be seen that the ratio tends to be less than unity. However when systems other than air-water are considered the reverse tends to be the case. For several experimental plants e.g. wetted wall columns, only mass transfer data was recorded and it has to be compared with the heat transfer data derived from similar systems when heat transfer only is taking place. This is justifiable as the differential equations for heat transfer without simultaneous mass transfer and that for heat transfer with mass transfer are identical, except in the case where there is a large partial pressure difference between the surface and the gas stream.

From fig. 1.2. it can be seen that when the data of Gilliland⁽²¹⁾ and other workers, obtained from investigations into mass transfer in wetted wall columns, was plotted in jd form and compared with the corresponding data for heat transfer,

$$jh = 0.023 Re^{-0.20}$$

the values of jd tend to be slightly above the corresponding values of jh , indicating that the ratio of mass to heat transfer to be greater than unity. This is in agreement with the results of the present investigation except in the case of the air-water system previously mentioned. The opposite tendency was noted by Ringens and Heertjecs⁽⁴⁷⁾ who obtained a value of 0.95 from their investigations into rates of evaporation of various liquids into air streams. However the variations from unity are small enough to be attributed to experimental error in most cases and for purposes of the design of chemical plant

HEAT AND MASS TRANSFER



LEGEND

No	SYSTEM	MEDIUM	X	Y
1	FLOW INSIDE PIPES	GASES LIQUIDS	Re	$J_d = \frac{k_g M P_{BM}}{\rho V} Sc^{0.67}$
2	FLOW INSIDE PIPES	GASES LIQUIDS	Re	$J_h = \frac{h}{c_p G} Pr^{0.67}$
3	FLOW PAST CYLINDERS	GASES	Re	$J_d = \frac{k_g M P_{BM}}{\rho V} Sc^{0.82}$
4	FLOW PAST SINGLE SPHERES	GASES	$Re Sc^{2/3}$	$\frac{k_c d_p}{D} (10^{-3})$
5	FLOW PARALLEL TO PLATES	GASES	Re	$J_d = \frac{k_g M P_{BM}}{\rho V}$
6	FLOW THROUGH PACKED SOLIDS	GASES	Re	$J_h(10^4) = \frac{h}{c_p} Pr^{2/3} (10^4)$
7	FLOW THROUGH PACKED SOLIDS	GASES	Re	$J_d(10^4) = \frac{k}{c_m} Sc^{2/3} (10^4)$
8	FLOW PAST RECT. SECTIONED OBJECT	GASES	Re	$J_d = \frac{k_g M P_{BM}}{\rho V} Sc^{0.67}$

FIG. 4. 24.

the j factor method of equating heat and mass transfer would appear to be satisfactory.

4.4.6. Application of j-Factors.

From the preceding discussion on the results of the present and other investigations, it would appear that while the ratio j_d/j_h is approximately unity, to within the 10 per cent accuracy claimed by Chilton and Colburn, its application to different systems depends on a knowledge of the relationship between either j_h or j_d and the Reynolds group for that particular system. This tends to limit its application to the more geometrically well defined systems. A continuous fibre drier is one such case and as can be seen from the experimental results fairly good agreement was obtained. In fig. 4.24 the relationships between j_d and Reynolds group are shown for several systems.

RESULTS - PART 2

Falling Rate Period of Drying.

5.1. Introduction.

The fibre tow comprises of thousands of continuous fibres bunched together to give a slab like porous belt of indefinite length. By means of the rollers and guides the tow width is kept constant to within 5 per cent total variation. This arrangement of rollers tended to limit the possible variation in tow thickness, any increase in the number of fibres per tow resulted in an increase in tow width rather than in thickness. Hence it was found impossible to vary the tow thickness sufficiently to warrant investigation of this factor.

As has been stated previously on page 23, the process of drying during the falling rate period is very complex. Of the two theories proposed for the various types of materials, the diffusion theory would appear to be the most likely as the physical appearance of the tow resembles a porous slab. The experimental work was designed to examine this assumption and determine the effect of temperature, etc. on the diffusion coefficient.

5.2. Procedure.

The procedure was as described on page 46. The drier was run at much slower speeds during these experiments to ensure that the material in the drier was dry enough to fall within the range of moisture contents of the falling rate period. In several of the experiments the drier was stopped for a time before samples were taken

MOISTURE CONTENT VS TIME

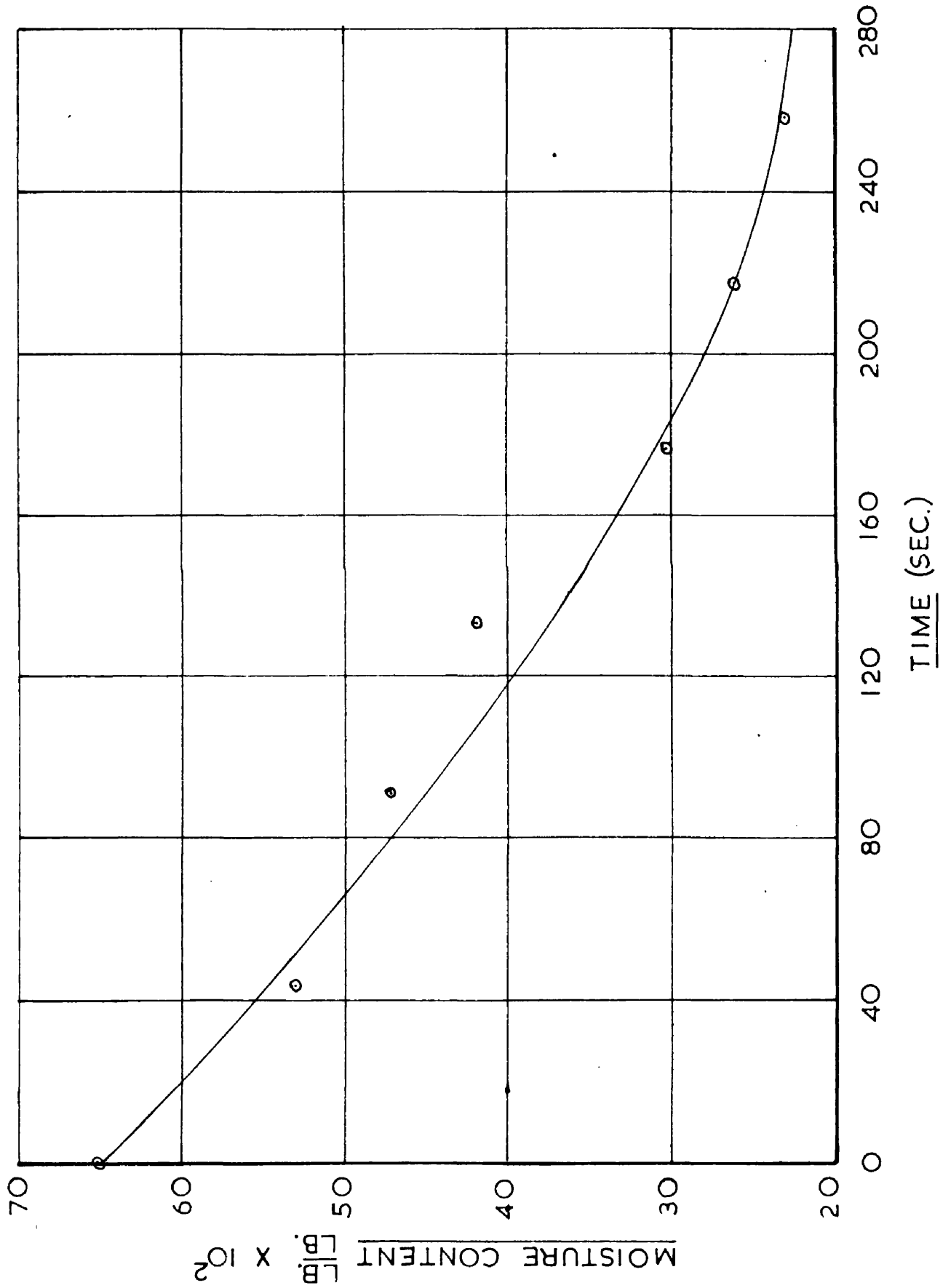


FIG. 5.1.

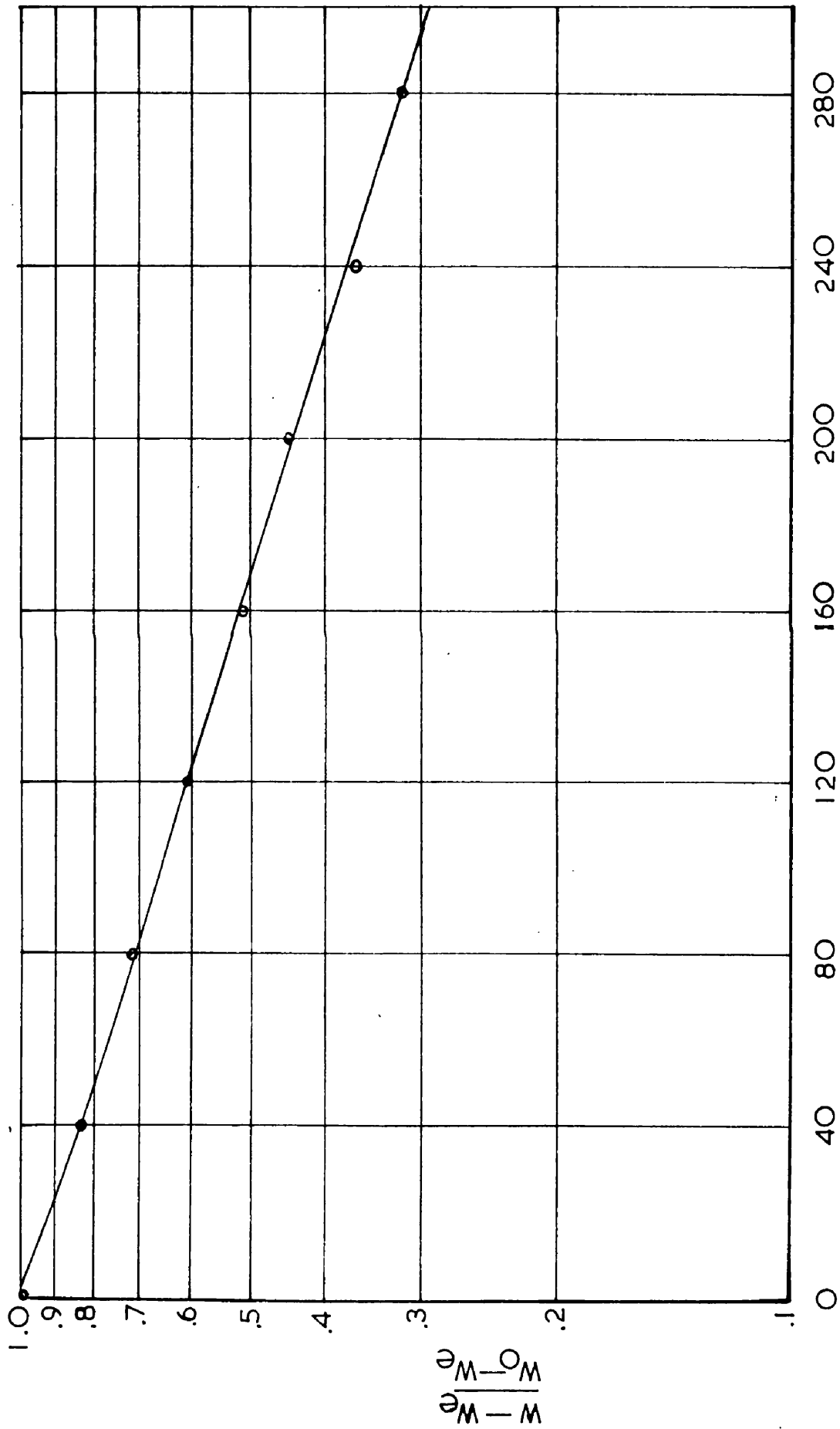
to allow the moisture content of the tow to fall within this range. These were mainly experiments at 122°F and high relative humidity. The variables investigated were air velocity, temperature, and the effect of variations in humidity at constant temperature. The method of investigating the variables was to keep two of the variables constant while varying the third, and subsequently varying each of the others in turn. The method of factorial experimentation was considered to assess the effect of the variables but it was not possible to arrange the partial pressure of the vapour as required by the method. The possibility of interactions between the variables can be revealed by using log-log plots.

5.3. Results.

To investigate the original conception of the tow as approximating to a porous slab of indefinite length, an initial run was carried out at 212°F to obtain the necessary data to compare with the equation of Sherwood mentioned on page 25. The simplified version of this equation given on page 25 was used.

From the graph moisture content against time, the critical moisture content W_0 is obtained. The term W_e is obtained from the equilibrium moisture graph, fig. A.1, taking the temperature and humidity of the air stream into consideration. The latter graph is obtained experimentally by methods such as the one indicated in appendix 1. Values of W from the smoothed curve are used to obtain the expression $\frac{W - W_e}{W_0 - W_e}$.

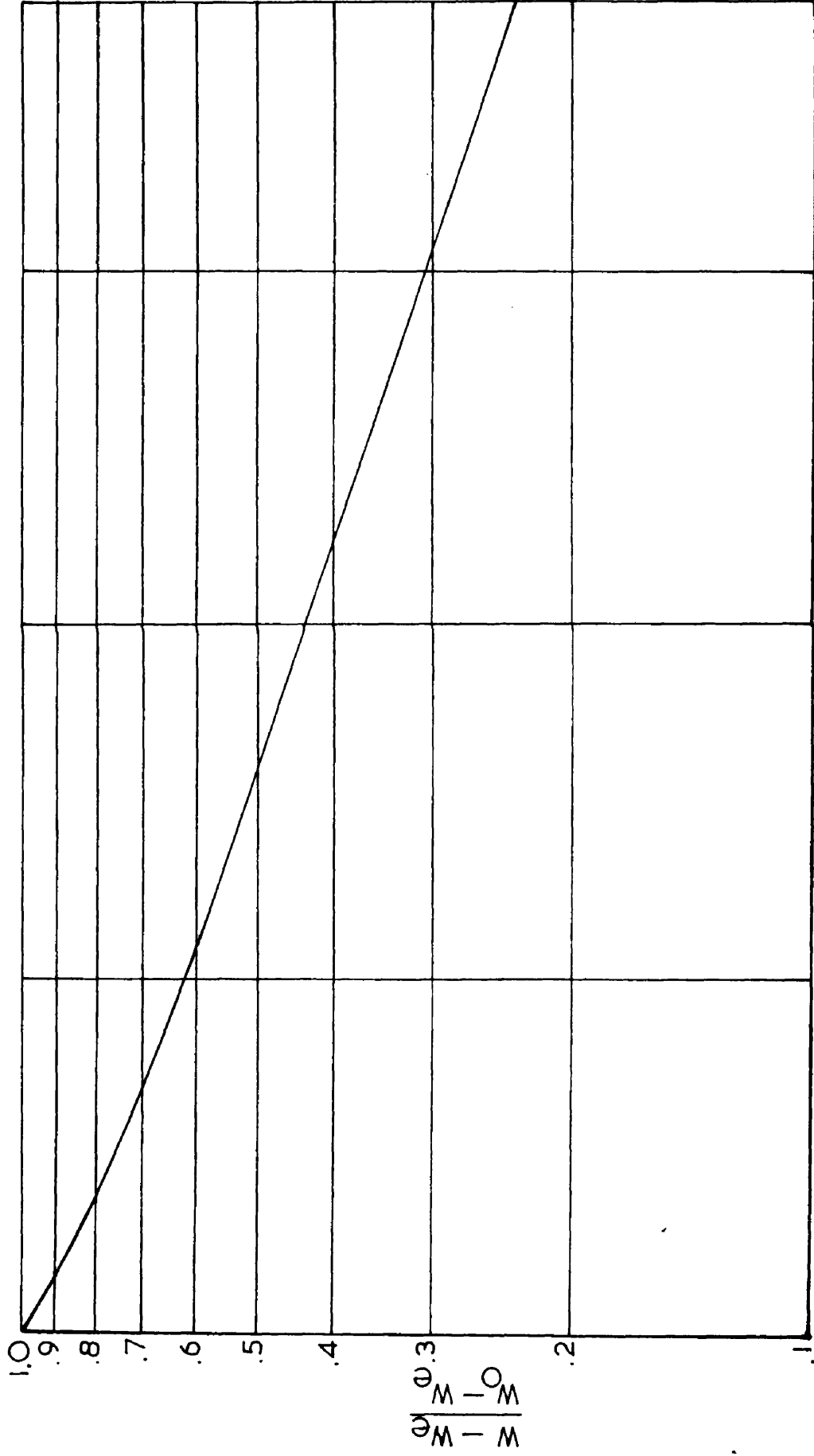
$\frac{W - W_e}{W_0 - W_e}$ VS TIME



TIME (SEC)

FIG. 5.2.

TYPICAL DIFFUSION RELATIONSHIP



TIME Θ

FIG. 5.3.

Table 5.1.

W	We	W - We	Wo	Wo - We	$\frac{W - We}{Wo - We}$	e
62.5	6.5	56.0	62.5	56.0	1.0	0
58.6	6.5	52.1	62.5	56.0	0.928	40
51.4	6.5	44.9	62.5	56.0	0.801	80
44.6	6.5	38.1	62.5	56.0	0.680	120
38.8	6.5	32.3	62.5	56.0	0.576	160
33.4	6.5	26.9	62.5	56.0	0.481	200
28.4	6.5	21.9	62.5	56.0	0.391	240
24.5	6.5	18.0	62.5	56.0	0.322	280
21.6	6.5	15.1	62.5	56.0	0.269	320

Graphing the term $\frac{W - We}{Wo - We}$ against time, e, using a semi-log. plot gives a relationship of the type shown in fig. 5.2. Comparing this plot with that shown in fig. 5.3 for the case of diffusion from a porous slab, the two plots appear to be similar in form. Hence the original assumption of diffusion control appears to be valid for the system. From equation the gradient of the semi-log plot is equal to $\frac{\pi^2 D_F}{4 a^2}$, the gradient being measured on that portion of the graph below $\frac{W - We}{Wo - We}$ equal to 0.6.

DIFFUSION COEFFICIENT VS AIR VELOCITY

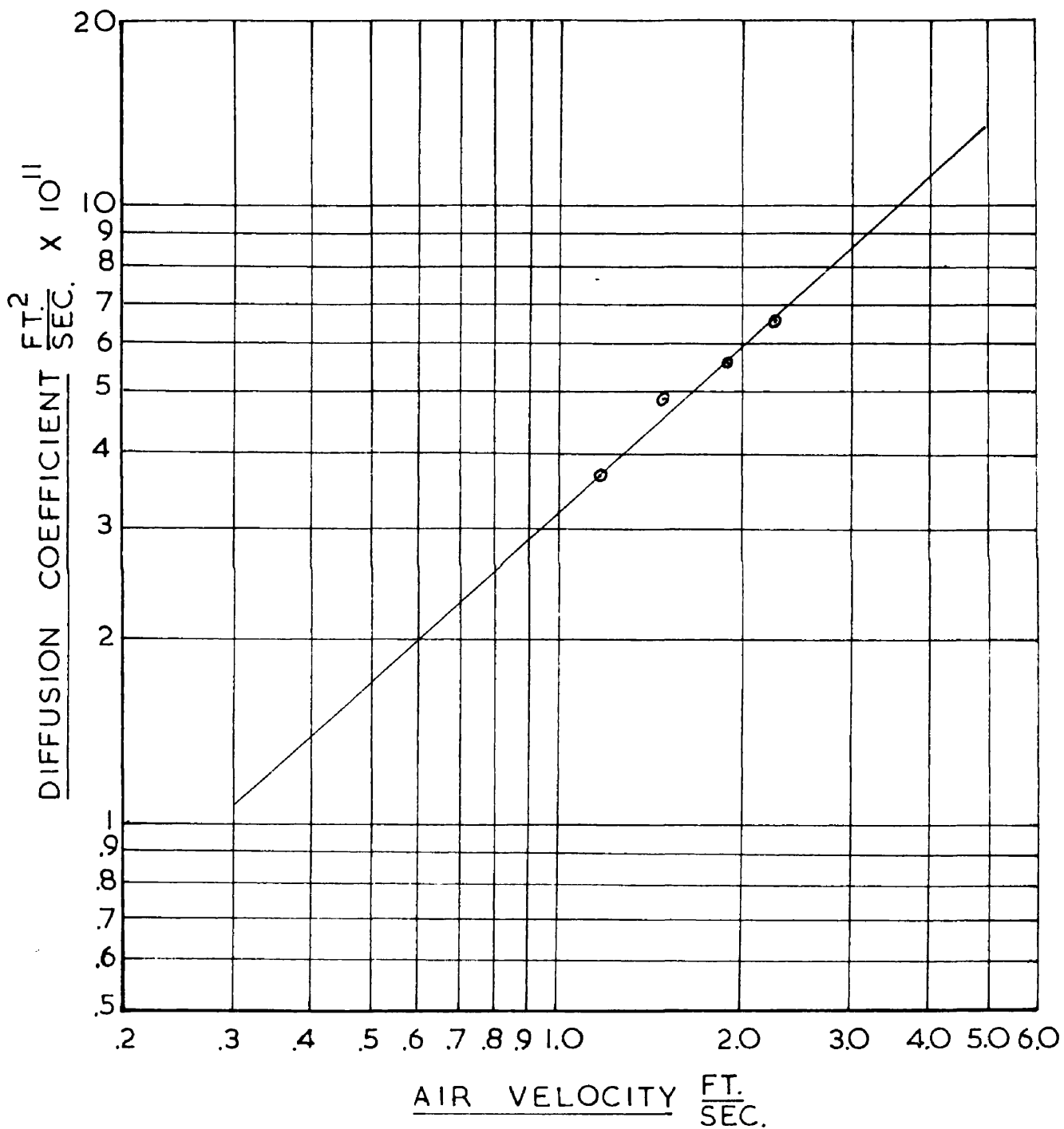


FIG. 5.4

5.3.1. Air Velocity.

At an air temperature of 212°F a series of four runs were carried out at different air velocities, the humidity of the air being kept constant and using the same width of tow throughout. The gradients of the plots, of the type in fig. 5.4, were calculated in a similar manner. From the gradients, the diffusion coefficients were calculated, the values being shown in table 5.2.

Table 5.2.

Diffusion Coefficient $D_F \text{ ft}^2/\text{sec} \times 10^{11}$	Air Velocity ft/min.
3.85	137
3.80	114
2.90	88
2.45	70

An increase in air velocity appears to cause an increase in the value of the diffusion coefficient. In this the system varies from the results of previous workers in through circulation drying who found that the diffusion coefficient was unaffected by variations in air velocity. The effect of air velocity was found to be correlated by the equation,

$$D_F \propto V^{0.83}$$

EFFECT OF TEMPERATURE

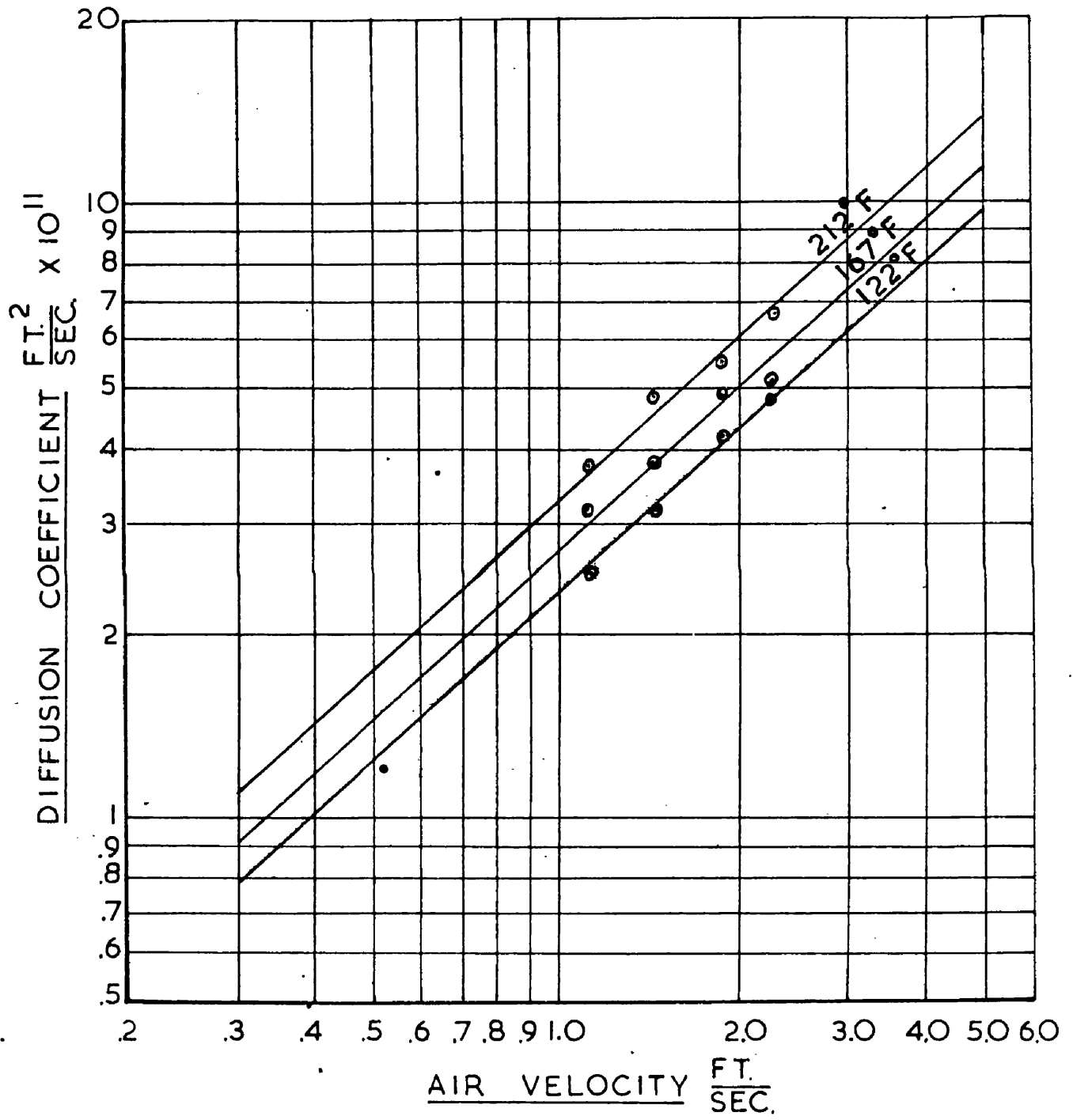


FIG. 5.5

EFFECT OF HUMIDITY

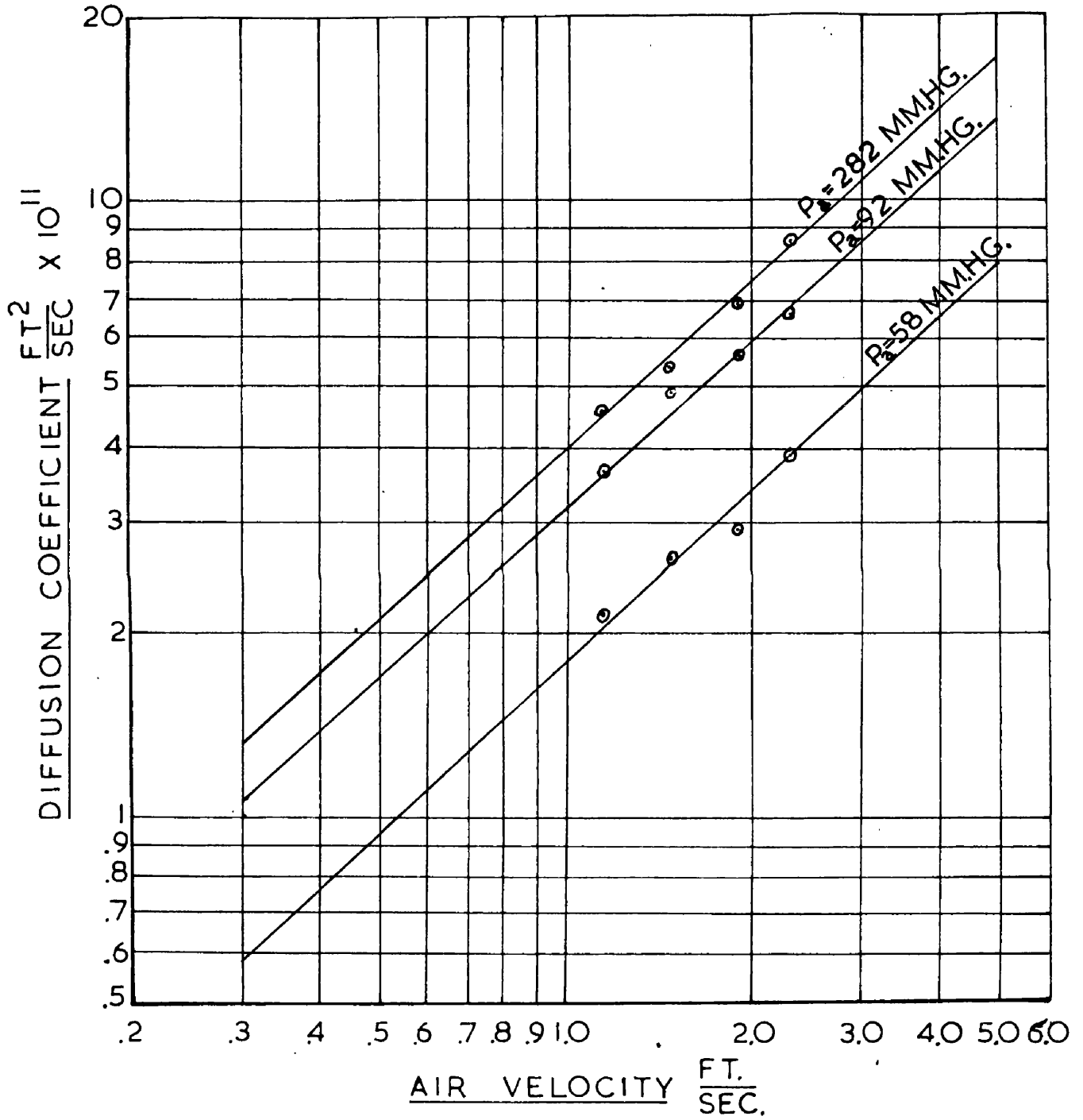


FIG. 5.6

5.3.2. Air Temperature.

In assessing the effect of variations in air temperature a series of runs were carried out at three different temperatures, varying the air velocity at each level of temperature. When the diffusion coefficients were plotted against velocity, this resulted in a series of parallel lines as shown in fig. 5.5. The fact that the lines were parallel indicates that there was no perceptible interaction between the effects of temperature and velocity.

5.3.3. Air Humidity.

A series of runs were carried out at 212°F at three different values of humidity, the velocity being varied at each level of humidity. The results are shown in fig. 5.6 as a series of parallel lines. Hence there was no interaction between the air velocity and humidity.

5.4. Discussion.

In describing the characteristics of any material during the drying process, it is necessary to be able to predict the critical moisture content under various sets of conditions. Although a considerable amount of data was obtained no method of prediction or indeed pattern could be deduced from it. In most cases the value obtained experimentally was approximately $0.625 \frac{\text{lb. H}_2\text{O}}{\text{lb. dry fibre}}$. The air conditions did not appear to influence this value to any marked extent and such fluctuations as were noted appeared to be random in nature. These fluctuations were also small enough to be considered within the experimental error of the method. Hence it was decided that, from the results available, the only satisfactory method of assessing the critical moisture content was by experiment.

Investigations into the factors controlling the rate of drying during the falling rate period of drying were conducted with a view to verifying the comparison of a fibre tow to a porous slab. The latter has been investigated for the process of diffusion by several workers, including Sherwood and Newman as stated in pages 24 and 25. The method of verifying the above was to plot the results, as shown in fig. 5.2, $\log_e \frac{W - W_e}{W_0 - W_e}$ against time and compare the characteristics of the curve with those of the theoretical results for a porous slab. As the general characteristics of the two curves were similar, the two processes were judged to be similar and hence diffusion

to be the controlling factor in the falling rate period of continuous fibre tows.

As the conditions of the air were varied the value of the diffusion coefficient was found to vary. Investigations into the effects of temperature, humidity, and air velocity were carried out. The effect of temperature and humidity on the diffusion process has been noted by several workers, Van Arsdel⁽⁵⁶⁾, Jason⁽⁸³⁾, etc. The results obtained for the effect of these variables on the diffusion coefficient agrees with previous published work and confirms the difficulty in translating these effects into mathematical form when the surface temperature is unknown. Although in the present investigation attempts were made to measure the surface temperature during the falling rate period, only very limited success was achieved for several reasons. When the fibre blocks were used within the drying compartment, only the temperature difference could be measured as the ambient temperature was greater than that of the surface to be measured. In such experiments the accuracy of the measurement depends on obtaining a steady value of air temperature at the position where the "cold junction" is situated, immediately behind or alongside the tow. Due to the turbulence this was not always obtained. There was also the error associated with the fact that it was impossible to determine when the fibre was in complete contact with the small brass disc of the plastic block, excluding the air, as the block was no

longer rigidly fixed as it was necessary to move it along the fibre length to obtain the required curve. These defects caused considerable scatter in the results obtained as shown in fig. 4.1. The effect of velocity which has been investigated previously for the falling rate period of drying by Van Arsdel, etc. was found in the present investigation to be quite considerable as shown in fig. 5.4. This effect has previously been stated to be negligible by Van Arsdel⁽⁵⁶⁾ and Jason⁽⁸³⁾. This effect can be explained in terms of the heat transfer coefficient which is a fraction of the air velocity and is independent of whether or not mass transfer is taking place. Since the rates of heat and mass transfer are related it follows that the diffusion coefficient will be affected by the air velocity.

NOMENCLATURE.

Nomenclature

<u>Symbol</u>		<u>Units</u>
α	Tow section perimeter.	ft
C_p	Specific heat at constant pressure.	$\frac{\text{Btu}}{\text{lb}^\circ\text{F}}$
D	Diffusion coefficient.	$\text{ft}^2/\text{sec.}$
d	Tow width.	ft.
$\frac{dw}{de}$	Rate of evaporation.	$\frac{\text{lb}}{\text{ft}^2\text{min.}}$
f	Fanning's friction factor.	
G	Gas flow.	$\text{ft}^3/\text{hr.}$
h	Heat transfer coefficient.	$\frac{\text{Btu}}{\text{ft}^2\text{hr}^\circ\text{F}}$
h_d	Mass Transfer coefficient.	
j_h	Heat transfer, j factor.	Dimensionless
j_d	Mass Transfer, j factor.	Dimensionless
k	Thermal conductivity.	$\frac{\text{Btu}}{\text{ft}^2\text{hr}^\circ\text{F}/\text{ft.}}$
kg	Mass Transfer coefficient.	$\frac{\text{moles}}{\text{ft}^2\text{sec.}\text{atmos.}}$
kc	Mass Transfer coefficient.	$\frac{\text{moles}}{\text{ft}^2\text{sec.}\text{mole diff.}}$
L, l	Length.	ft.
P	Total Pressure.	mm. hg.
p_a	Partial Pressure of vapour in air.	mm. hg.
p	Vapour Pressure of liquid at surface temperature.	mm. hg.

<u>Symbol</u>		<u>Units</u>
P_{bm}	Mean partial pressure difference.	mm. hg.
t_a	Air temperature.	$^{\circ}F$
t_s	Surface temperature.	$^{\circ}F$
V, U	Air velocity.	ft./min.
W	Moisture content.	$\frac{lb\ H_2O}{lb\ dry\ fibre}$
ρ	Density.	lb/ft^3
μ	Viscosity.	$\frac{lb}{ft.\ sec.}$
λ	Latent heat.	$\frac{Btu}{lb}$
σ	Surface tension.	lb.
θ	Time.	sec.
Re	Reynolds number.	Dimensionless
Sc	Schmidt number.	Dimensionless
St	Stanton number.	Dimensionless
Sh	Sherwood number	Dimensionless
Nu	Nusselt number.	Dimensionless
Pr	Prandtl number.	Dimensionless
Pe	Peclet number.	Dimensionless

REFERENCES.

REFERENCES

- NO.
1. Nusselt, W., Z. Angew. Math. Mech. 10, 105-121, (1930).
 2. Prandtl, L. Z. Physik, 11, 1072, (1910), 29, 487, (1928).
 3. Stanton, T., J. Pannell, Phil. Trans. Roy. Soc. 214, 199, (1914).
 4. Schmidt, E., Gesundh. Ing. 52, 525-529, (1929).
 5. Eckert, E.R.G., "Introduction to the transfer of Heat and Mass", McGraw-Hill, pps. 249-251.
 6. Reynolds, O., Proc. Manchester Lit. Phil. Soc. 8 (1874).
 7. Taylor, G. I., Brit. Advisory Comm. Aeronaut. Repts. and Mem. 272, 423, (1916).
 8. Von Karman, Th., Trans. Am. Soc. Mech. Engrs. 61, 705, (1935).
 9. Nikuradse, J., Forschungsheft, No. 356, (1932), No. 361, (1933).
 10. Boelter, L.M.K. et al., Trans. Am. Soc. Mech. Engrs. 63, 447, (1941).
 11. Sherwood, T. K., Trans. Am. Inst. Chem. Eng. 36, 817, (1940).
 12. Chilton, T. H., A.P. Colburn, Ind. Eng. Chem., 26, 1183, (1934).
 13. Hinton, A. G., "Technical Data on Fuels", H.M. Speirs, pp.101-103.
 14. Dittus, F.W., L.M.K.Boelter, Univ. Calif. Pub. 2, 443, (1932).
 15. Sherwood, T.K., J.M. Petrie, Ind. Eng. Chem., 24, 736, (1932).
 16. Colburn, A.P., Trans. Am. Inst. Chem. Eng. 29, 174-210, (1933).
 17. Sieder, E.N., G.E. Tate, Ind. Eng. Chem. 28, 1429-1436, (1929).
 18. McAdams, W.H., "Heat Transmission", McGraw-Hill, page 166.
 19. King, W.J., J. Knaus, "Refrigerating Data Book", A.S.R.E. p. 145, (1942).

NO.

20. McAdams, W.H., "Heat Transmission", McGraw-Hill, page 222.
21. Gilliland, E.R., T.K. Sherwood, Ind. Eng. Chem. 26, 516, (1934).
22. Barnet, W.I., K.A. Kobe, Ind. Eng. Chem. 33, 436, (1941).
23. Uchida, S., S. Maeda, J. Soc. Chem. Ind. Japan, 38, 625, (1935).
24. Kerbs, R.W., Thesis, Univ. of Illinois, (1938).
25. Greenwalt, C.H., Ind. Eng. Chem., 18, 1291, (1926).
26. Cogan, J.C., J.P. Cogan, Thesis in Chem. Eng., M.I.T. (1932).
27. Johnstone, H.F., R.L. Pigford, Trans. Am. Inst. Chem. Eng.
37, 25, (1941).
28. Jackson, M.L., N.H. Ceagelske, Ind. Eng. Chem., 42, 1188, (1950).
29. Hinchley, J.W., G.W. Himus, Trans. Inst. Chem. Eng., 2, 57, (1924).
30. Lurie, M., M. Michailoff, Ind. Eng. Chem., 28, 345, (1936).
31. Powell, R.W., E. Griffiths, Trans. Inst. Chem. Eng., 13, 175, (1935).
32. Wade, S.H., Trans. Inst. Chem. Eng. 20, 1, (1942).
33. Hine, T.B., Phys. Rev., 24, 79, (1924).
34. Pasquill, F., Proc. Roy. Soc. 182A, 75, (1943).
35. Coulson, J.M., J.F. Richardson, "Chemical Engineering",
Pergamon Press p. 257.
36. Powell, R.W., Trans. Inst. Chem. Eng. 18, 36, (1940).
37. Lohrisch, W., Mitt. Forsch, 322, 46, (1929).
38. Vint, A.W., Thesis in Chem. Eng., M.I.T., (1932).
39. Linton, W.M., T.K. Sherwood, Chem. Eng. Prog., 46, 258, (1950).
40. Comings, E.W., J.T. Clapp, and J.F. Taylor,
Ind. Eng. Chem. 40, 1076, (1948).

NO.

41. Maisel, D.S., T.K. Sherwood, Chem. Eng. Prog., 46, 131,172(1950).
42. Frossling, N., Gerlands Beitr. Geophys. 32, 170, (1938).
43. Williams, G.C., Sc.D. Thesis, 1942, M.I.T.
44. Garner, F.H., R.W. Grafton, Proc. Roy. Soc., A224, 64, (1954).
45. Garner, F.H., R.D. Sockling, A.I.Ch.E. Journal, 4, 114, (1958).
46. Gamson, B.W., et al., Trans. Am. Inst. Chem. Engrs., 39, 1, (1943).
47. Heertjees, P.M., W.P. Ringens, Chem. Eng. Sci., 5, 226, (1956).
48. Coles and Ruggeri, unpublished report - Lewis Flight Laboratories,
Ohio.
49. Milne-Thompson, I.M., "Theoretical Hydrodynamics", McMillan,
pp. 299-301.
50. Gilliland, E.R., Ind. Eng. Chem. 30, 506, (1938).
51. Powell, R.W., E. Griffiths, Trans. Inst. Chem. Eng., 13,175,(1935).
52. Sherwood, T.K. Ind. Eng. Chem., 21, 12, 976, (1929).
53. Newman, A.B., Trans. Am. Inst. Chem. Eng. 27, 203, (1931).
54. Bateman, E., J.P. Hoff, and A.S. Stamm,
Ind. Eng. Chem., 31, 1150, (1939).
55. Hougen, O.A., H.J. McCauley, and W.R. Marshall,
Trans. Am. Inst. Chem. Eng., 36, 183, (1940).
56. Van Arsdel, W.B. Chem. Eng. Prog., 43, 13T. (1947).
57. Ceaglske, N.H., O.A. Hougen, Trans. Am. Inst. Chem. Eng., 33,388,(1937).
58. Slichter, C.S., U.S. Geol. Survey, 19, Pt. 2, 301, (1897-98).
59. Haines, W.B., J. Agric. Science, 17, 264, (1927).
60. Haines, W.B., J. Agric. Science, 20, 97, (1930).

NO.

61. Oliver, T.R., D.M. Newitt, Trans.Inst.Chem.Eng. 27, 9, (1949).
Coleman, M., D.M. Newitt, Trans.Inst.Chem.Eng. 30, 27, (1952).
Corben, R.W., D.M. Newitt, Trans.Inst.Chem.Eng. 33, 52, (1955).
King, A.R., D.M. Newitt, Trans.Inst.Chem.Eng. 33, 64, (1955).
62. Preston, J.M., M.U. Nimkar, Textile Research J., 23, 64, (1953).
63. Marshall, W.R., O.A. Hougen, Trans.Am.Inst.Chem.Eng. 38, 91,(1942).
64. Wilke, C.R., O.A. Hougen, Trans.Am.Inst.Chem.Eng. 41, 445, (1945).
65. Marshall, W.R., Heating, Piping, Air Conditioning, 14, 313,(1942).
66. Brown, A.H., P.W. Kilpatrick, W.B. Van Arsdel,
Trans. Am. Soc. Mech. Eng. 65, 837, (1943).
67. Ede, A.J., K.G. Hales, D.S.I.R. Food Investigation Special
Report No. 53, 1948.
68. Gardner, R.G., T.J. Mitchell, J. Sci. Food Agric., 3, 113, (1953).
" " " " , 5, 237, (1953).
" " " " , 8, 364, (1953).
" " " " , 10, 481, (1954).
69. Potts, C.S., T.J. Mitchell, J. Sci. Food Agric., 9, 20, (1958).
" " " " , 9, 29, (1958).
" " " " , 9, 93, (1958).
" " " " , 9, 99 (1958).
70. Hughes, J., T.J. Mitchell, J. Sci. Food Agric., 10, 39, (1959).
" " " " , 10, 45, (1959).
" " " " , 10, 180, (1959).
" " " " , 10, 185, (1959).

NO.

71. Simons, H.P., J.H. Koffolt, J.R. Withrow,
Trans. Am. Inst. Chem. Eng. 39, 133, (1943).
72. Coles, W.V., J. Inst. Fuel, 25, 60, (1952).
73. Nissan, A.H., W.G. Kaye, J.R. Bell,
A. I. Ch. E. Journal, 5, 103, (1952).
74. Coplan, M.J., Textile Research J, 23, 897, (1953).
75. Lowe, E., J.R. Hawes, Food Tech., 3(7), 241-243, (1949).
76. Fischer, K. B.S. 2511: 1954.
77. Cox, D.R. "Planning of Experiments", Wiley, p. 106.
78. Davies, O.L., "Statistical Methods in Research and Production",
Oliver and Boyd, p. 194-198.
79. Williams, E.J., "Regression Analysis", Wiley, p. 132.
80. Coulson, J. N., J.P. Richardson, "Chemical Engineering", Vol. 1,
Pergamon Press, p. 239.
81. Griffiths, E., J.H. Awberry, Proc. Inst. Mech. Engrs., 125,
319-382 (1933).
82. Callighan, E.E., N.A.C.A. Repts, No. 3045, 1953.
83. Jason, A.C., Society of Chemical Industry Symposium
"Dehydration of Foodstuffs" 1958.

APPENDIX I

Equilibrium Moisture Content.

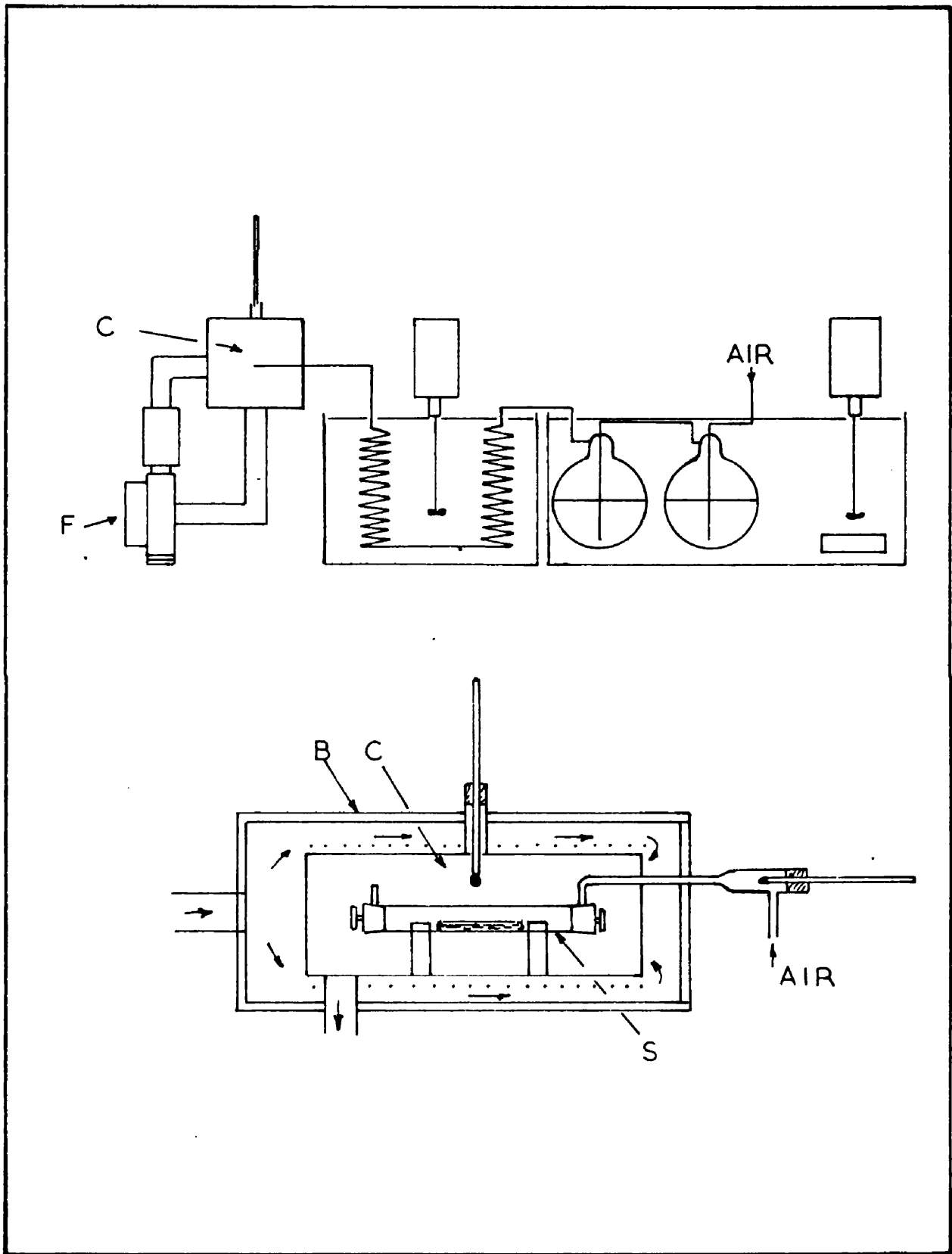


FIG. A1. EQUILIBRIUM MOISTURE CONTENT APPARATUS

Equilibrium Moisture Contents

Introduction

In investigations into the falling rate period of drying it is usual to express the moisture content of the material in terms of the free moisture content, i.e. the total moisture content of the material minus the equilibrium moisture content. Since the equilibrium moisture content varies according to the material and the ambient air conditions, it is necessary to obtain values of the equilibrium moisture content over a wide range of conditions. The factors influencing the equilibrium moisture contents of various textile materials have been extensively investigated by Weigerink. There are two methods of investigating the above, (a) a static method (b) a dynamic method.

The static method consists of placing a wet sample in a dessicator over a solution of sulphuric acid, etc., to control the humidity under conditions of constant temperature. The system is allowed to come to equilibrium, i.e. the weight of the sample becomes constant. The concentration of the acid is then determined giving the humidity of the atmosphere surrounding the sample in the dessicator. The sample is then placed in a vacuum oven for several hours until a constant weight is obtained. Hence the moisture content of the sample can be evaluated, usually expressed as a percentage of the dry weight.

The alternative method is the dynamic method which is somewhat similar to the static one. The main difference being that the air flows over the sample at constant values of temperature and humidity. This has the effect of reducing the time required for the system to come to equilibrium. The method of controlling the humidity of the air stream is different. The air is passed through a series of bubblers containing water at a fixed temperature T_1 . The air on leaving the bubblers is saturated and is then heated to a predetermined temperature T_2 . The air is then passed over the sample which is maintained at temperature T_2 . From the values T_1 and T_2 the humidity of the air stream can be evaluated. The equilibrium moisture content of the sample is evaluated as in the static method. The dynamic method was chosen for the present investigation because it is more rapid and can be used at temperatures near and above 100°C which is not satisfactory with the static method.

Apparatus.

The apparatus, as shown in fig. A.1., consists of a train of saturators in series immersed in a thermostatically controlled water bath. The air stream, after passing through the saturators is then passed through a heated pipe into a pair of heating coils which are immersed in an oil bath which is thermostatically controlled. From the coils the air stream, which is now at the

desired temperature and humidity, passes into the sample tube which is within a heated compartment. The heated compartment consists of two sections, C the inner rectangular copper box open at one end in which the sample tube rests, B the outer compartment made of asbestos sheet. The compartment B is heated by a coil of wire wound round the inside walls of the box. A small fan F is used to circulate air first through a coil heater then up into B over the heaters and then into C passed through the sample tube and is then recirculated to the fan. Part of the tube to the fan is left unlagged to allow moisture to condense out. The moisture is removed at intervals. The temperature of the circulating air is controlled by a thermostat in C.

Procedure.

The oil and water baths are raised to the desired values of temperature. The air is then passed slowly through the system, venting to atmosphere after the heating coils and the temperatures of the baths adjusted to give the desired values of temperature. The sample, which has been immersed in water overnight, is squeezed to extract excess moisture and then inserted in the tube (S). The tube is then inserted in the compartment (C) which had been previously raised to the desired temperature. The taps on the sample tube were then opened and the air stream connected to it. The apparatus was allowed to settle down for about 15 minutes and then the

ARDIL

MOISTURE CONTENT VS RELATIVE HUMIDITY

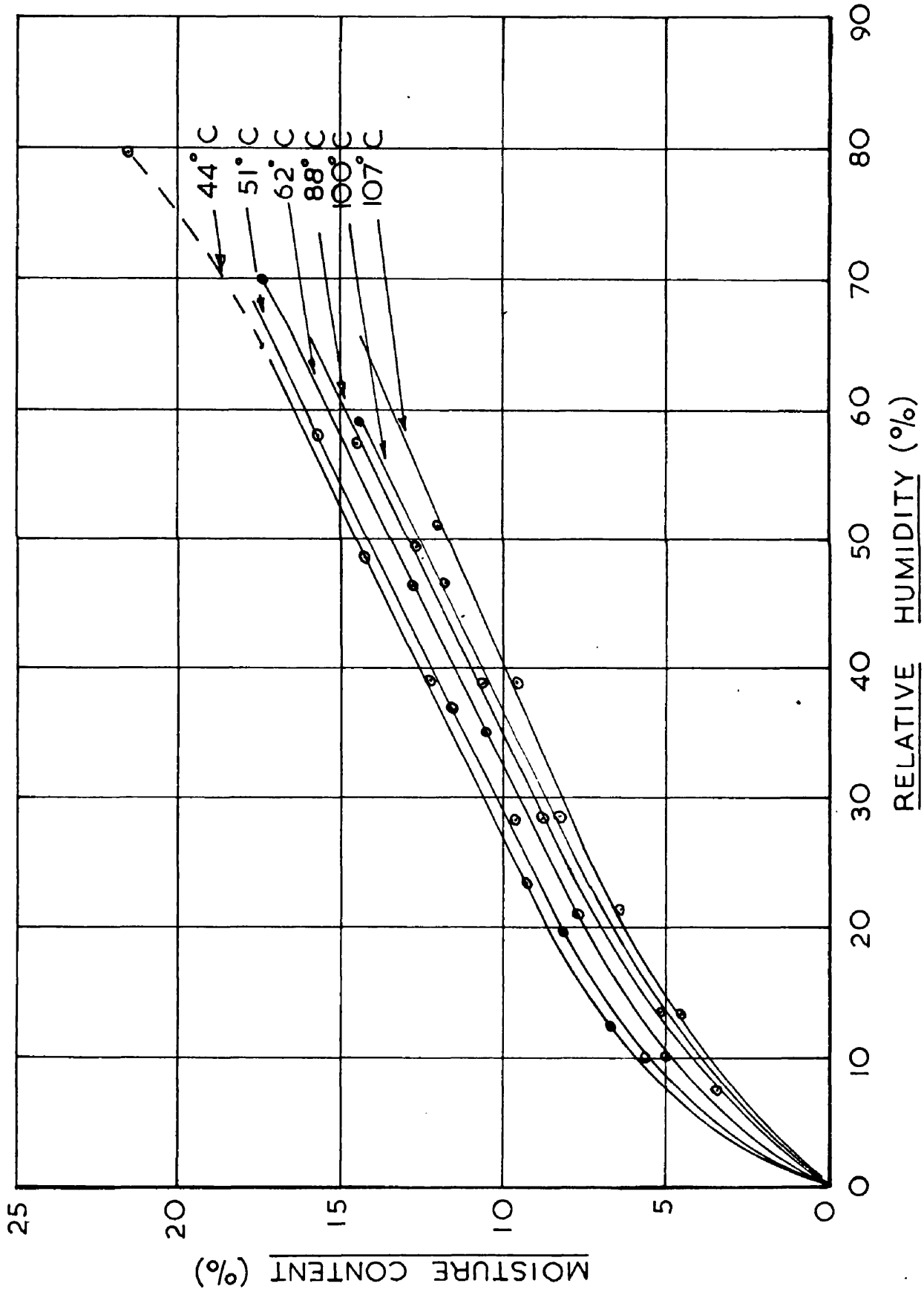


FIG. A 2.

temperatures of the water and oil baths adjusted as required. The apparatus was then allowed to run for about 8 - 10 hrs. before the initial weighing. The sample was then weighed at regular intervals until a constant value was obtained. The sample was then placed in a vacuum oven and the taps at either end removed. After about 12 hrs. the sample was weighed and weighing was continued at regular intervals until a constant weight was obtained. From the two weighings the moisture content was evaluated.

Results: Ardil.

Effect of Relative Humidity.

A series of experiments using Ardil, 22 denier, were conducted at 44°C varying the relative humidity. The results were plotted in the form, moisture content against relative humidity as in fig. A.2. This resulted in a smooth curve in which there is a linear section over a wide range of relative humidity (25-65 per cent). The gradient of the curve increases steadily with increase in relative humidity.

Effect of Temperature.

In order to investigate the effect of temperature several series similar to the one above were carried out at different temperatures. These are shown in fig. A.2. as a family of curves

ARDIL

MOISTURE CONTENT VS $1/T$

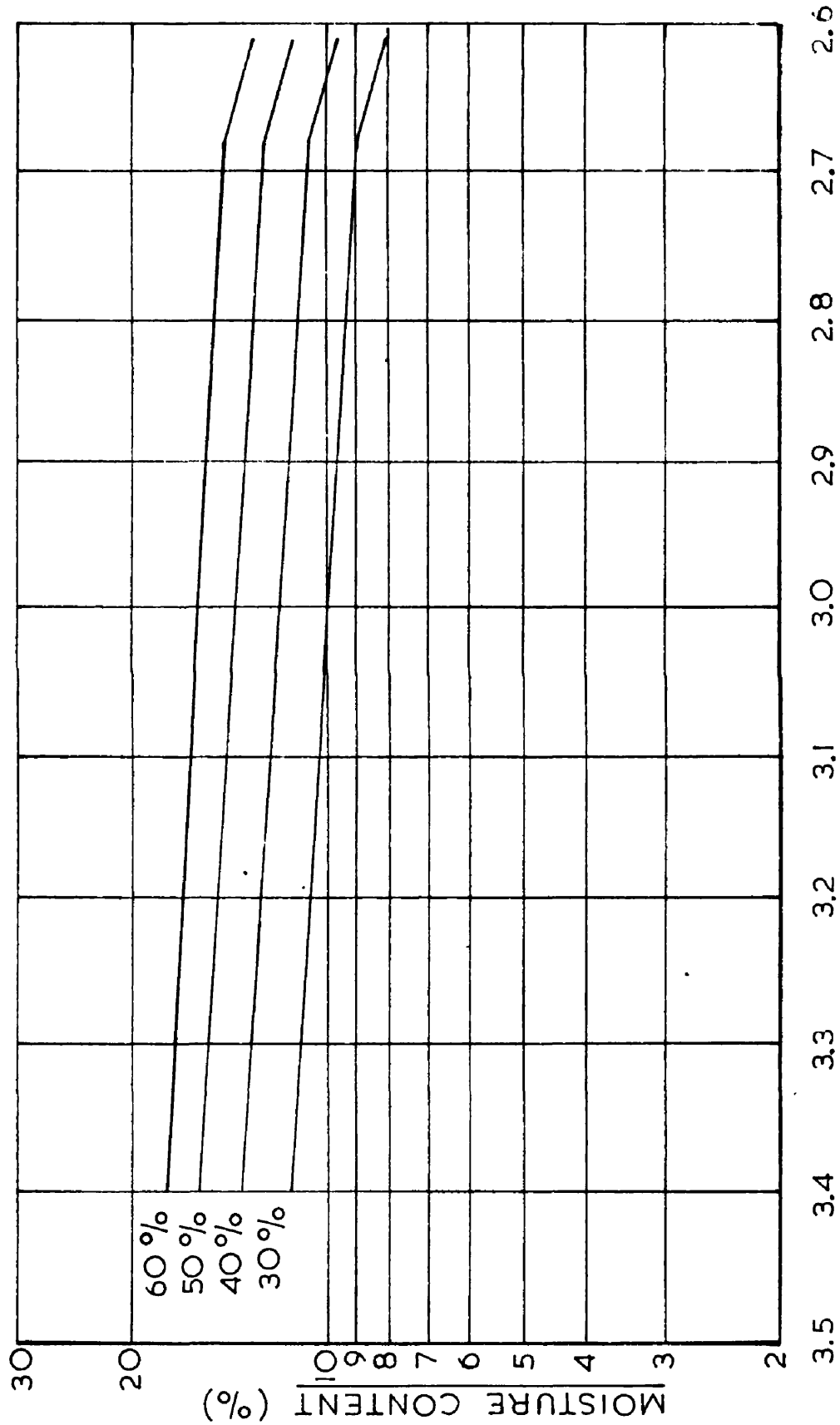


FIG. A3.

TERYLENE

MOISTURE CONTENT VS RELATIVE HUMIDITY

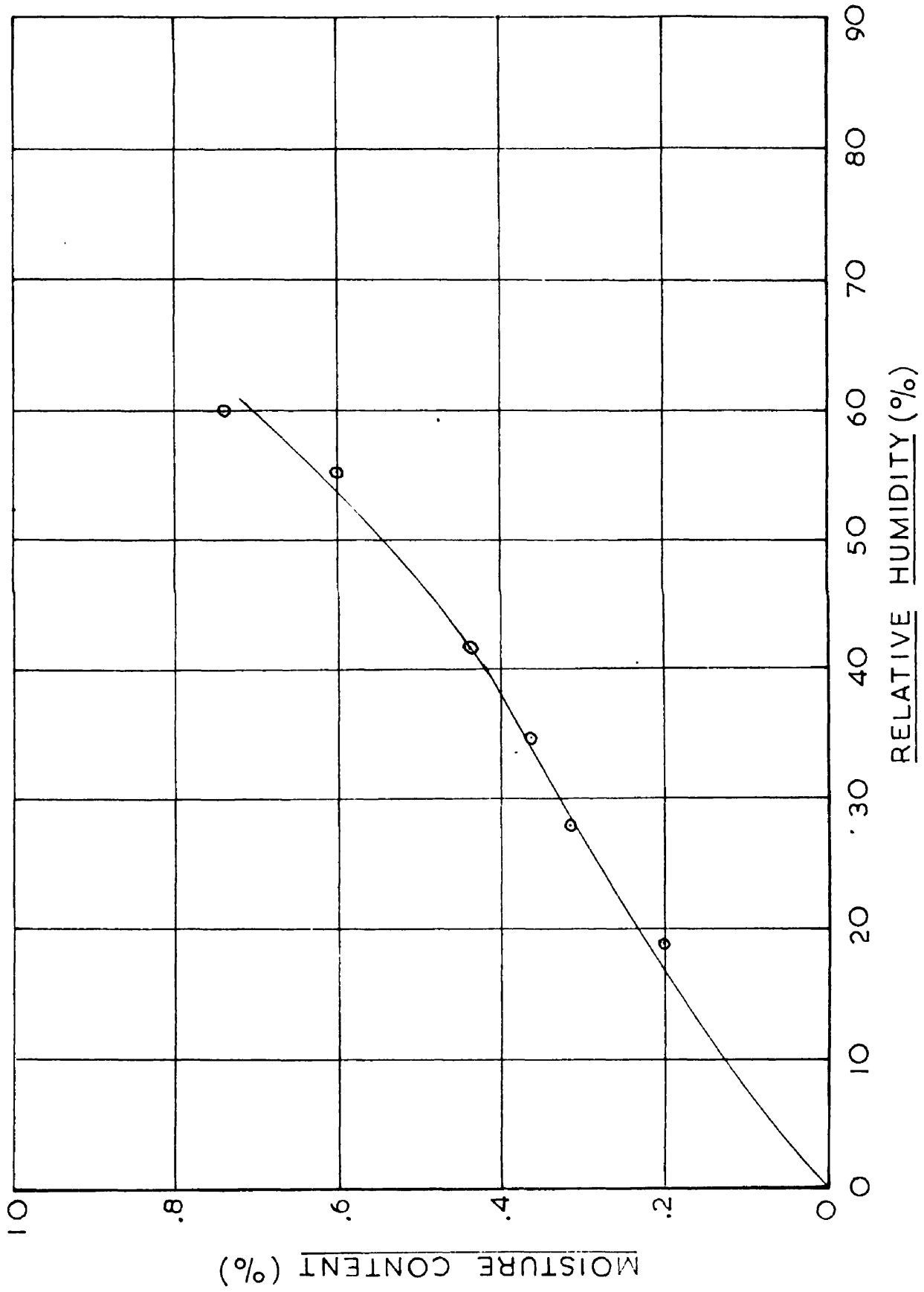


FIG. A.4.

similar in form. The data was plotted in semi-log. form as suggested by Weigerink. The results are shown in fig. A.3. where the logarithm of the moisture content is plotted against the reciprocal of the absolute temperature, giving a straight line correlation up to 212°F with a tendency for the gradient to assume a different value at higher values.

Terylene.

The data (fig. A.4.) for terylene is less extensive as in repeating a series of the type described above for Ardil, for a different value of temperature there was no perceptible difference in the curve. Thus the effect of temperature was found to be negligible in the case of terylene. The actual values of the equilibrium moisture contents are very much lower than those for Ardil.

Discussion - Method.

The method used appeared to be satisfactory from the point of view of reproducibility and ease of operation. It is only at high relative humidities that the apparatus is unsuitable because of the difficulty of preventing the condensing out of vapour in the line between the saturators and the coil heaters. At high humidities the moisture tended to condense out and block the line. Hence the experimental work was restricted to values of relative humidity below 80 per cent. Below this value of relative humidity the tendency for

the moisture to condense out was controlled by heating the tubing; connecting the saturators to the heating coils in the oil bath with a heating tape.

Results.

The results for Ardil agreed satisfactorily with those for similar types of fibre. They gave the same general characteristics in relating relative humidity to moisture content as those shown by the work of Weigerink⁽¹⁾ and the earlier work of Urquhart and Williams⁽²⁾.

The effect of temperature on the value of the equilibrium content, at constant relative humidity, was correlated by an equation of the type,

$\log_e W = \frac{A}{T} + B$ where T is temperature, °A up to 100°C. The gradient appeared to alter above this value of temperature, a tendency noted by Weigerink.

The results for Terylene relating equilibrium moisture content to relative humidity, were similar to those for Ardil except that the effect of temperature appeared to be negligible.

References

1. Weigerink, J. G., Textile Research J., 10, 357-71 (1940).
2. Urquhart, J., T. Williams, J.T.I. 15, T559-572, (1924).

APPENDIX II

Calculation.

Calculation

Rate of Evaporation	=	11.18×10^{-2}	$\frac{\text{lb.}}{\text{lb.fibre.min.}}$
Width of tow	=	2.63×10^{-2}	ft.
Weight of tow per ft.	=	3.66×10^{-1}	lb.
Weight of tow per sq.ft.	=	13.9	lb.
Rate of evaporation	=	8.05×10^{-3}	$\frac{\text{lb.H}_2\text{O}}{\text{ft}^2\text{min.}}$
Partial pressure difference ($p_s - p_a$)	=	19.24	m.m. hg.
Mass transfer coefficient k_g	=	2.94×10^{-4}	$\frac{\text{moles}}{\text{ft}^2\text{sec.atmos.}}$
Air Velocity.	=	98.7	$\frac{\text{ft.}}{\text{min.}}$
$\frac{k_g M_{av} P_{bm}}{\rho V}$	=	8.31×10^{-2}	dimensionless
Diffusion coefficient	=	3.58×10^{-4}	$\frac{\text{ft}^2}{\text{sec.}}$
Air viscosity	=	1.348×10^{-5}	$\frac{\text{lb}}{\text{ft. sec.}}$
Schmidt number	=	6.08×10^{-1}	dimensionless
jd	=	5.9×10^{-2}	dimensionless
Temperature difference ($t_a - t_s$)	=	78	$^{\circ}\text{F}$
Latent heat	=	998	$\frac{\text{Btu}}{\text{lb.}}$
Heat transfer coefficient	=	6.08	$\frac{\text{Btu}}{\text{ft}^2\text{hr. } ^{\circ}\text{F.}}$

Thermal conductivity	=	1.59×10^{-2}	$\frac{\text{Btu}}{\text{ft}^2 \text{hr. } ^\circ\text{F/ft.}}$
Nusselt number	=	9.35	dimensionless
Density	=	6.21×10^{-2}	$\frac{\text{lb.}}{\text{ft}^3}$
Reynolds number	=	187	dimensionless
jh	=	5.62×10^{-2}	dimensionless
Ratio $\frac{j_d}{j_h}$	=	1.05	

APPENDIX III

Results' Tables.

TABLE I

Air-Water

Run No.	$\frac{dw \text{ lb}}{de \text{ ft}^2 \text{ min.}} \times 10^3$	V $\frac{\text{ft.}}{\text{min.}}$	d ft. $\times 10^2$	$t_a \text{ } ^\circ\text{F}$
1.	10.36	114	2.63	167
2.	10.62	114	2.63	167
3.	10.04	114	2.63	167
4.	10.35	114	2.63	167
5.	3.81	114	2.63	95
6.	3.64	114	2.63	95
7.	3.07	114	2.63	95
8.	3.71	114	2.63	95

TABLE II

Run No.	$\frac{dw \text{ lb}}{de \text{ ft}^2 \text{ min.}} \times 10^3$	V $\frac{\text{ft.}}{\text{min.}}$	d ft. $\times 10^2$	$t_a \text{ } ^\circ\text{F}$	Tow Material
1.	16.8	114	2.63	194	Ardil
2.	10.4	114	2.63	167	Ardil
3.	6.44	114	2.63	122	Ardil
4.	3.85	114	2.63	95	Ardil
5.	16.68	114	2.63	194	Terylene
6.	10.78	114	2.63	167	Terylene
7.	6.67	114	2.63	122	Terylene
8.	3.59	114	2.63	95	Terylene

TABLE III

Air-Water

Run No.	$\frac{dw}{de} \frac{lb}{ft^2 min.} \times 10^3$	$V \frac{ft.}{min.}$	$d \frac{ft.}{\times 10^2}$	$t_a \text{ } ^\circ F$	$h \frac{Btu}{ft^2 hr ^\circ F}$
1.	13.9	137.0	2.09	167	9.23
2.	10.05	114.0	2.09	167	8.95
3.	9.80	88.3	2.09	167	7.41
4.	7.66	74.7	2.09	167	6.80
5.	6.22	54.0	2.09	167	5.30
6.	11.02	137.0	2.63	167	8.30
7.	10.38	114.0	2.63	167	7.83
8.	9.29	88.3	2.63	167	7.0
9.	7.34	73.6	2.63	167	5.54
10.	5.80	54.3	2.63	167	4.37
11.	12.2	137.0	3.93	167	8.40
12.	9.53	114.0	3.93	167	6.78
13.	8.15	88.3	3.93	167	5.80
14.	6.36	74.0	3.93	167	5.10
15.	5.34	54.3	3.93	167	4.10

TABLE IV

Air-Water

Run No.	$\frac{dw}{de} \frac{lb}{ft^2 min.} \times 10^3$	$V \frac{ft.}{min.}$	$p_s - p_a$ mm. hg.	$d \text{ ft.} \times 10^2$	$t_a \text{ } ^\circ F$
1.	3.17	88.0	8.3	2.63	95
2.	2.45	74.4	8.3	2.63	95
3.	2.62	57.1	8.3	2.63	95
4.	1.66	39.4	8.3	2.63	95
5.	4.03	138.0	8.3	2.63	95
6.	3.82	114.0	8.3	2.63	95
7.	3.46	88.3	8.3	2.63	95
8.	5.01	93.0	14.6	2.63	122
9.	4.46	68.4	14.6	2.63	122
10.	2.64	36.6	14.6	2.63	122
11.	4.11	75.7	14.6	2.63	122
12.	6.11	89.0	14.6	2.63	122
13.	6.42	115.0	14.6	2.63	122
14.	7.33	137.0	14.6	2.63	122

Air-Water

Run No.	$\frac{dw \text{ lb}}{de \text{ ft}^2 \text{ min.} \times 10^3}$	V $\frac{\text{ft.}}{\text{min.}}$	$p_s - p_a$ mm. hg.	d ft. $\times 10^2$	t_a °F
15.	9.29	88.3	19.24	2.63	167
16.	10.38	114.0	19.24	2.63	167
17.	11.02	137.0	19.24	2.63	167
18.	8.05	98.7	19.24	2.63	167
19.	7.34	73.6	19.24	2.63	167
20.	6.58	64.0	19.24	2.63	167
21.	5.80	54.3	19.24	2.63	167
22.	4.93	37.0	19.24	2.63	167
23.	4.75	48.0	19.24	2.63	167
24.	18.43	137.0	29.4	2.63	194
25.	16.85	114.0	29.4	2.63	194
26.	13.75	88.7	29.4	2.63	194
27.	12.10	72.0	29.4	2.63	194
28.	8.14	64.0	29.4	2.63	194
29.	7.19	37.0	29.4	2.63	194

Air-Water system.

Run No.	$h \frac{\text{Btu}}{\text{ft}^2 \text{hr}^\circ\text{F}}$	$k_g \frac{\text{moles}}{\text{ft sec. atmos.} \times 10^4}$	Re	Nu	Pr	$St_h \times 10^2$
1.	7.62	2.69	214	12.95	0.712	8.41
2.	5.88	2.10	182	10.0	0.712	7.76
3.	6.22	2.23	139	10.0	0.712	10.75
4.	3.93	1.04	96	6.68	0.712	9.83
5.	9.56	3.43	336	16.40	0.712	6.86
6.	9.06	3.24	277	15.40	0.712	7.82
7.	8.20	2.93	215	13.92	0.712	9.10
8.	6.94	2.42	206	11.30	0.709	7.84
9.	6.18	2.16	151	10.08	0.709	9.41
10.	3.65	1.28	81	5.95	0.709	10.25
11.	5.69	1.98	169	9.28	0.709	7.74
12.	8.45	2.95	217	13.80	0.709	8.97
13.	8.89	3.10	279	14.50	0.709	7.32
14.	10.55	3.53	333	16.55	0.709	7.00

Air-Water.

Run No.	$h \frac{\text{Btu}}{\text{hr.ft}^2\text{°F}}$	$k_g \frac{\text{moles}}{\text{ft}^2\text{sec.atmos.}} \times 10^4$	Re	Nu	Pr	$St_h \times 10^2$
15.	7.0	3.39	215	10.76	0.703	7.12
16.	7.83	3.95	277	12.05	0.703	6.18
17.	8.30	4.03	334	12.80	0.703	5.44
18.	6.08	2.94	187	9.35	0.703	7.13
19.	5.54	2.69	140	8.51	0.703	8.60
20.	4.96	2.41	121	7.62	0.703	8.96
21.	4.37	2.12	103	6.71	0.703	9.33
22.	3.72	1.80	69	5.72	0.703	11.68
23.	3.58	1.74	89	5.50	0.703	8.74
24.	10.30	4.43	334	15.2	0.694	6.64
25.	8.93	3.87	278	13.2	0.694	6.84
26.	7.65	3.30	216	11.3	0.694	7.53
27.	6.73	2.90	137	9.9	0.694	9.38
28.	4.53	1.95	122	6.68	0.694	7.87
29.	4.00	1.73	70	5.91	0.694	12.15

Air-Water.

Run No.	jh x 10 ²	$\frac{k_g M_{av} P_{bm}}{\rho V}$ x 10 ²	Sc	jd x 10 ²
1.	6.64	7.79	0.602	5.45
2.	6.05	7.31	0.602	5.20
3.	8.84	9.92	0.602	7.07
4.	7.75	9.10	0.602	6.48
5.	5.41	6.43	0.602	4.51
6.	6.17	7.24	0.602	5.15
7.	7.17	8.60	0.602	6.12
8.	6.16	7.36	0.606	5.26
9.	7.40	8.44	0.606	6.04
10.	8.05	9.31	0.606	6.66
11.	6.08	7.00	0.606	5.00
12.	7.05	8.84	0.606	6.22
13.	5.76	7.15	0.606	5.11
14.	5.51	6.84	0.606	4.83

Air-Water.

Run No.	jh x 10 ²	$\frac{k_g M_{av} P_{bm}}{\rho V}$ x 10 ²	Sc	jd x 10 ²
15.	5.61	10.70	0.608	7.60
16.	4.87	9.26	0.608	6.58
17.	4.28	8.18	0.608	5.81
18.	5.62	8.31	0.608	5.90
19.	6.78	10.00	0.608	7.10
20.	7.07	10.30	0.608	7.31
21.	7.35	11.05	0.608	7.85
22.	9.20	13.28	0.608	9.44
23.	6.88	9.90	0.608	7.03
24.	5.24	9.18	0.616	6.63
25.	5.37	9.57	0.616	6.90
26.	5.92	10.58	0.616	7.62
27.	7.38	11.45	0.616	8.26
28.	6.20	8.69	0.616	6.27
29.	9.55	13.21	0.616	9.58

TABLE V

Methanol-Air.

Run No.	$\frac{dw \text{ lb}}{de \text{ ft}^2 \text{ min.}} \times 10^2$	$V \frac{\text{ft.}}{\text{min.}}$	$p_s - p_a$ mm.hg.	$d \text{ ft.} \times 10^2$	$t_a \text{ } ^\circ\text{F}$
1.	3.31	137.0	44	2.63	167
2.	2.78	114.0	44	2.63	167
3.	2.45	88.3	44	2.63	167
4.	2.09	72.0	44	2.63	167
5.	4.75	137.0	67	2.63	194
6.	4.11	114.0	67	2.63	194
7.	3.46	88.3	67	2.63	194
8.	2.95	72.0	67	2.63	194
9.	2.45	137.0	32	2.63	122
10.	2.16	114.0	32	2.63	122
11.	1.87	88.3	32	2.63	122
12.	1.48	72.0	32	2.63	122
13.	1.66	137.0	23	2.63	95
14.	1.35	114.0	23	2.63	95
15.	1.27	88.3	23	2.63	95
16.	1.02	72.0	23	2.63	95

Methanol-Air.

Run No.	$h \frac{\text{Btu}}{\text{ft}^2 \text{hr}^\circ \text{F}}$	$k_g \frac{\text{moles}}{\text{ft}^2 \text{sec. atmos.}} \times 10^4$	Re	Nu	Pr	$St_h \times 10^2$
1.	9.9	2.98	334	15.40	0.694	6.63
2.	8.52	2.60	277	13.25	0.694	6.90
3.	7.24	2.21	215	11.25	0.694	7.55
4.	6.17	1.88	176	9.60	0.694	7.86
5.	10.58	2.80	334	16.10	0.703	6.85
6.	9.13	2.42	277	13.90	0.703	7.12
7.	7.69	2.04	215	11.72	0.703	7.77
8.	6.57	1.74	176	10.05	0.703	8.10
9.	10.60	3.02	334	16.30	0.709	6.90
10.	9.45	2.66	277	14.50	0.709	7.39
11.	8.20	2.32	215	12.60	0.709	8.29
12.	6.47	1.82	176	9.95	0.709	7.96
13.	10.40	2.86	334	16.00	0.710	6.75
14.	8.45	2.32	277	13.00	0.710	6.60
15.	7.90	2.18	215	12.15	0.710	7.94
16.	6.36	1.75	176	9.80	0.710	7.84

Methanol-Air.

Run No.	jh x 10 ²	$\frac{k_g M_{av} P_{bm}}{\rho V} \times 10^2$	Sc	jd x 10 ²
1.	5.15	5.78	1.01	5.78
2.	5.36	6.09	1.01	6.09
3.	5.86	6.67	1.01	6.67
4.	6.10	6.96	1.01	6.96
5.	5.36	5.54	0.98	5.45
6.	5.58	5.76	0.98	5.66
7.	6.03	6.28	0.98	6.16
8.	6.34	6.58	0.98	6.47
9.	5.40	6.01	0.97	5.90
10.	5.78	6.38	0.97	6.27
11.	6.48	7.20	0.97	7.07
12.	6.24	6.88	0.97	6.76
13.	5.28	5.83	0.965	5.70
14.	5.16	5.71	0.965	5.58
15.	6.21	6.92	0.965	6.77
16.	6.16	6.80	0.965	6.65

TABLE VI

Ethanol-Air.

Run No.	$\frac{dw}{d\theta} \frac{lb}{ft^2 min.} \times 10^2$	V $\frac{ft.}{min.}$	$P_s - P_a$ mm.hg.	d ft. $\times 10^2$	t_a °F
1.	4.11	137	44	2.63	194
2.	2.78	88	44	2.63	194
3.	2.38	70	44	2.63	194
4.	2.16	57	44	2.63	194
5.	3.03	137	37	2.63	167
6.	2.45	88	37	2.63	167
7.	2.23	70	37	2.63	167
8.	1.73	57	37	2.63	167
9.	2.59	137	28	2.63	122
10.	1.95	88	28	2.63	122
11.	1.73	70	28	2.63	122
12.	1.51	57	28	2.63	122
13.	2.09	137	22	2.63	95
14.	1.59	88	22	2.63	95
15.	1.30	70	22	2.63	95
16.	1.15	57	22	2.63	95

Ethanol-Air.

Run No.	$h \frac{\text{Btu}}{\text{ft}^2 \text{hr}^\circ\text{F}}$	$\text{kg} \frac{\text{moles}}{\text{ft}^2 \text{sec. atmos.}} \times 10^4$	Re	Nu	Pr	St. $\times 10^2$
1.	10.2	2.59	336	15.7	0.694	6.70
2.	7.16	1.81	214	11.0	0.694	7.39
3.	5.91	1.49	172	9.1	0.694	7.65
4.	5.36	1.36	132	8.25	0.694	8.98
5.	10.70	2.24	336	6.96	0.703	6.96
6.	8.65	1.83	214	8.80	0.703	8.80
7.	7.90	1.67	172	10.05	0.703	10.05
8.	6.12	1.30	132	10.10	0.703	10.10
9.	11.80	2.56	336	7.97	0.708	7.97
10.	8.80	1.92	214	9.00	0.708	9.00
11.	7.80	1.73	172	9.91	0.708	9.91
12.	6.85	1.50	132	10.10	0.708	10.10
13.	12.10	2.63	336	7.80	0.710	7.80
14.	9.20	1.99	214	9.26	0.710	9.26
15.	7.50	1.63	172	9.24	0.710	9.40
16.	6.65	1.45	132	10.90	0.710	10.90

Ethanol-Air.

Run No.	jh x 10 ²	$\frac{k_g M_{av} p_{bm}}{\rho V}$ x 10 ²	Sc	jd x 10 ²
1.	5.21	4.91	1.34	5.98
2.	5.75	5.37	1.34	6.48
3.	5.95	5.54	1.34	6.74
4.	6.98	6.08	1.34	7.40
5.	5.50	4.42	1.32	5.25
6.	6.95	5.67	1.32	6.83
7.	7.95	6.46	1.32	7.80
8.	7.98	6.08	1.32	7.33
9.	6.30	5.29	1.31	6.24
10.	7.10	5.81	1.31	6.96
11.	7.86	6.57	1.31	7.88
12.	7.98	6.88	1.31	8.35
13.	6.18	5.35	1.30	6.40
14.	7.35	6.34	1.30	7.57
15.	7.45	6.50	1.30	7.76
16.	8.56	6.97	1.30	8.35

TABLE VII

N-Propanol - Air.

Run No.	$\frac{dw}{de} \frac{\text{lb}}{\text{ft}^2 \text{min.}} \times 10^2$	V $\frac{\text{ft.}}{\text{min.}}$	$P_s - P_a$ mm.hg.	d ft. $\times 10^2$	t_a °F
1.	4.25	137	42.0	2.63	194
2.	3.82	114	42.0	2.63	194
3.	3.24	88	42.0	2.63	194
4.	2.68	70	42.0	2.63	194
5.	3.82	137	33.0	2.63	167
6.	3.31	114	33.0	2.63	167
7.	2.59	88	33.0	2.63	167
8.	2.31	70	33.0	2.63	167
9.	2.92	137	25.0	2.63	122
10.	2.52	114	25.0	2.63	122
11.	2.09	88	25.0	2.63	122
12.	1.80	70	25.0	2.63	122
13.	2.02	137	16.5	2.63	95
14.	1.87	114	16.5	2.63	95
15.	1.51	88	16.5	2.63	95
16.	1.26	70	16.5	2.63	95

N-propanol - Air.

Run No.	$h \frac{\text{Btu}}{\text{ft}^2 \text{hr}^\circ\text{F}}$	$\text{kg} \frac{\text{moles}}{\text{ft}^2 \text{sec. atmos.}} \times 10^4$	Re	Nu	Pr	$\text{St}_h \times 10^2$
1.	10.40	2.14	336	15.90	0.694	6.83
2.	9.41	1.91	277	14.30	0.694	7.44
3.	7.98	1.62	214	12.12	0.694	8.19
4.	6.56	1.34	172	9.96	0.694	8.37
5.	12.20	2.47	336	18.50	0.703	7.83
6.	10.60	2.15	277	16.10	0.703	8.26
7.	8.28	1.68	214	12.60	0.703	8.40
8.	7.35	1.49	172	11.18	0.703	9.76
9.	12.00	2.40	337	18.20	0.709	7.65
10.	10.38	2.12	277	15.75	0.709	8.03
11.	8.58	1.73	214	13.05	0.709	8.59
12.	7.40	1.39	172	11.25	0.709	9.21
13.	11.60	2.60	336	17.60	0.710	7.36
14.	10.80	2.34	277	16.40	0.710	8.34
15.	8.71	1.93	214	13.25	0.710	8.71
16.	7.27	1.61	172	11.05	0.710	9.06

N-propanol - Air.

Run No	jh x 10 ²	$\frac{k_g M_{av} P_{bm}}{\rho V}$ x 10 ²	Sc	jd x 10 ²
1.	5.31	4.35	1.59	5.94
2.	5.79	4.63	1.59	6.32
3.	6.37	5.14	1.59	7.02
4.	6.51	5.30	1.59	7.24
5.	6.09	4.86	1.56	6.55
6.	6.44	5.03	1.56	6.77
7.	6.54	5.12	1.56	6.88
8.	7.60	5.72	1.56	7.70
9.	5.95	4.77	1.55	6.42
10.	6.40	5.01	1.55	6.75
11.	6.67	5.34	1.55	7.19
12.	7.18	5.40	1.55	7.27
13.	5.74	4.92	1.54	6.56
14.	6.60	5.45	1.54	7.26
15.	6.79	5.75	1.54	7.66
16.	7.07	5.96	1.54	7.95

TABLE VIII

N-butanol - Air.

Run No.	$\frac{dw}{de} \frac{lb}{ft^2 min.} \times 10^2$	$V \frac{ft.}{min.}$	$p_s - p_a$ mm.hg.	$d \text{ ft.} \times 10^2$	$t_a \text{ } ^\circ F$
1.	4.83	137.0	40	2.63	194
2.	4.17	114.0	40	2.63	194
3.	3.10	88.3	40	2.63	194
4.	2.45	55.0	40	2.63	194
5.	3.46	137.0	28.5	2.63	167
6.	3.02	114.0	28.5	2.63	167
7.	2.45	88.3	28.5	2.63	167
8.	1.84	55.0	28.5	2.63	167
9.	1.08	137.0	9.0	2.63	95
10.	0.97	114.0	9.0	2.63	95
11.	0.79	88.3	9.0	2.63	95
12.	0.54	55.0	9.0	2.63	95
13.	1.73	137.0	14.5	2.63	122
14.	1.48	114.0	14.5	2.63	122
15.	1.15	88.3	14.5	2.63	122
16.	0.86	55.0	14.5	2.63	122

N-butanol - Air.

Run No.	$h \frac{\text{Btu}}{\text{ft}^2 \text{hr}^\circ \text{F}}$	$\text{kg} \frac{\text{moles}}{\text{ft}^2 \text{sec. atmos.}} \times 10^4$	Re	Nu	Pr	$\text{St}_h \times 10^2$
1.	11.40	2.045	336	17.3	0.694	7.41
2.	9.70	1.78	277	14.9	0.694	7.73
3.	7.30	1.32	214	11.10	0.694	7.45
4.	6.10	1.105	132	9.25	0.694	10.50
5.	10.90	2.075	336	16.7	0.703	7.05
6.	9.56	1.815	277	14.6	0.703	7.41
7.	8.42	1.595	214	12.9	0.703	8.54
8.	5.82	1.105	132	8.9	0.703	9.58
9.	10.70	2.05	336	16.4	0.712	6.86
10.	9.65	1.84	277	14.8	0.712	7.51
11.	7.86	1.50	214	12.1	0.712	7.96
12.	5.36	1.14	132	8.2	0.712	8.76
13.	10.40	2.04	336	15.9	0.709	6.86
14.	8.90	1.75	277	13.6	0.709	6.94
15.	6.95	1.36	214	10.65	0.709	7.02
16.	5.65	1.11	132	8.65	0.709	9.30

N-butanol - Air.

Run No.	jh x 10 ²	$\frac{k_g M_{av} P_{bm}}{\rho V}$ x 10 ²	Sc	jd x 10 ²
1.	5.77	4.19	1.77	6.11
2.	6.02	4.36	1.77	6.35
3.	5.80	5.08	1.77	7.41
4.	8.17	5.60	1.77	8.17
5.	5.55	4.07	1.74	5.95
6.	5.84	4.28	1.74	6.18
7.	6.73	4.90	1.74	7.07
8.	7.55	5.28	1.74	7.54
9.	5.45	3.88	1.72	5.85
10.	5.96	4.24	1.72	6.07
11.	6.32	4.35	1.72	6.39
12.	6.95	5.36	1.72	7.70
13.	5.43	4.05	1.73	5.97
14.	5.50	4.20	1.73	6.03
15.	5.56	4.22	1.73	6.07
16.	7.36	5.48	1.73	7.88

TABLE IX

Trichloroethylene-Air.

Run No.	$\frac{dw}{de} \frac{lb}{ft^2 \min.} \times 10^2$	$V \frac{ft.}{\min.}$	$p_s - p_a$ mm.hg.	d ft. $\times 10^2$	t_a °F
1.	4.18	88.3	28.5	2.63	95
2.	4.90	114.0	28.5	2.63	95
3.	5.18	137.0	28.5	2.63	95
4.	2.95	72.0	28.5	2.63	95
5.	3.06	55.0	28.5	2.63	95
6.	7.13	114.0	47.0	2.63	122
7.	8.36	137.0	47.0	2.63	122
8.	5.98	88.3	47.0	2.63	122
9.	4.75	72.0	47.0	2.63	122
10.	4.61	55.0	47.0	2.63	122
11.	8.00	72.0	69.0	2.63	167
12.	10.30	88.3	69.0	2.63	167
13.	11.80	114.0	69.0	2.63	167
14.	13.70	137.0	69.0	2.63	167
15.	7.35	55.0	69.0	2.63	167

Trichloroethylene-Air.

Run No.	$\frac{dw}{de} \frac{lb}{ft^2 min.} \times 10^2$	$V \frac{ft.}{min.}$	$p_s - p_a$ mm. hg.	$d \text{ ft.} \times 10^2$	$t_a \text{ } ^\circ F$
16.	16.80	114.0	96.0	2.63	194
17.	19.50	137.0	96.0	2.63	194
18.	15.10	88.3	96.0	2.63	194
19.	12.30	72.0	96.0	2.63	194
20.	9.50	55.0	96.0	2.63	194

Trichloroethylene-Air.

Run No.	$h \frac{\text{Btu}}{\text{ft}^2 \text{hr}^\circ \text{F}}$	$k_g \frac{\text{moles}}{\text{ft}^2 \text{sec. atmos.}} \times 10^4$	Re	Nu	Pr	St $\times 10^2$
1.	8.55	1.43	215	13.15	0.710	8.22
2.	10.40	1.645	277	16.0	0.710	8.13
3.	10.80	1.77	334	16.60	0.710	7.00
4.	6.15	1.01	176	9.45	0.710	7.57
5.	6.38	1.045	134	9.80	0.710	10.30
6.	8.74	1.46	277	13.40	0.709	6.84
7.	10.25	1.715	334	15.75	0.709	6.56
8.	7.32	1.225	215	11.20	0.709	7.34
9.	5.83	0.975	176	8.95	0.709	7.18
10.	5.65	0.95	134	8.68	0.709	9.14
11.	6.08	1.265	176	9.45	0.703	7.64
12.	7.85	1.445	215	12.20	0.703	8.07
13.	9.00	1.655	277	14.40	0.703	7.20
14.	10.42	1.92	334	16.20	0.703	6.90
15.	5.60	1.035	134	8.70	0.703	9.20

Trichloroethylene-Air.

Run No.	$h \frac{\text{Btu}}{\text{ft}^2 \text{hr}^\circ\text{F}}$	$k_g \frac{\text{moles}}{\text{ft}^2 \text{sec. atmos.}} \times 10^4$	Re	Nu	Pr	St $\times 10^2$
16.	9.85	1.690	277	15.15	0.694	7.80
17.	11.40	1.980	334	17.5	0.694	7.45
18.	8.87	1.53	215	13.62	0.694	9.02
19.	7.22	1.23	176	11.10	0.694	9.08
20.	5.57	0.96	134	8.55	0.694	9.20

Trichloroethylene-Air.

Run No.	jh x 10 ²	$\frac{k_g M_{av} P_{bm}}{\rho V}$ x 10 ²	Sc	jd x 10 ²
1.	6.49	4.42	2.10	7.29
2.	6.42	3.93	2.10	6.48
3.	5.53	3.50	2.10	5.78
4.	5.98	3.82	2.10	6.30
5.	8.13	5.18	2.10	8.52
6.	5.40	3.34	2.11	5.48
7.	5.18	3.25	2.11	5.34
8.	5.80	3.64	2.11	5.97
9.	5.67	3.48	2.11	5.71
10.	7.21	4.48	2.11	7.35
11.	6.03	4.78	2.12	7.74
12.	6.37	4.38	2.12	7.25
13.	5.68	3.87	2.12	6.30
14.	5.45	3.74	2.12	6.18
15.	7.26	4.98	2.12	8.26

Trichloroethylene-Air.

Run No.	jh $\times 10^2$	$\frac{kg M_{av} P_{bm}}{\rho V}$ $\times 10^2$	Sc	jd $\times 10^2$
16.	6.16	4.12	2.14	6.89
17.	5.88	4.03	2.14	6.70
18.	7.12	4.85	2.14	8.08
19.	7.16	4.76	2.14	7.94
20.	7.26	4.93	2.14	8.22

TABLE X

Diffusion Coefficients

Run No.	$D_F \frac{\text{ft}^2}{\text{sec.}} \times 10^{11}$	$V \frac{\text{ft.}}{\text{sec.}}$	$t_a \text{ } ^\circ\text{F}$	$t_w \text{ } ^\circ\text{F}$	d ft. $\times 10^2$	a ft. $\times 10^4$
1.	5.58	1.89	212	120	2.63	1.8
2.	6.55	2.28	212	120	2.63	1.8
3.	4.91	1.46	212	120	2.63	1.8
4.	3.67	1.14	212	120	2.63	1.8
5.	5.32	1.46	212	106	2.63	1.8
6.	8.60	2.28	212	106	2.63	1.8
7.	6.88	1.89	212	106	2.63	1.8
8.	4.58	1.14	212	106	2.63	1.8
9.	3.14	2.28	212	166	2.63	1.8
10.	2.96	1.89	212	166	2.63	1.8
11.	2.62	1.46	212	166	2.63	1.8
12.	2.16	1.14	212	166	2.63	1.8
13.	5.06	2.28	167	115	2.63	1.8
14.	5.00	1.89	167	115	2.63	1.8
15.	3.80	1.46	167	115	2.63	1.8
16.	3.21	1.14	167	115	2.63	1.8
17.	5.40	1.46	167	97	2.63	1.8
18.	6.42	1.89	167	97	2.63	1.8
19.	7.95	2.28	167	97	2.63	1.8
20.	4.65	1.14	167	97	2.63	1.8

Diffusion Coefficients

Run No.	$D_F \frac{\text{ft}^2}{\text{sec.}}$ $\times 10^{11}$	$V \frac{\text{ft.}}{\text{sec.}}$	t_a °F	t_w °F	d ft. $\times 10^2$	a ft. $\times 10^4$
21.	2.78	2.28	167	129	2.63	1.8
22.	2.78	1.89	167	129	2.63	1.8
23.	2.29	1.46	167	129	2.63	1.8
24.	1.77	1.14	167	129	2.63	1.8
25.	4.80	2.23	122	78	2.63	1.8
26.	4.22	1.89	122	78	2.63	1.8
27.	3.15	1.46	122	78	2.63	1.8
28.	2.50	1.14	122	78	2.63	1.8
29.	3.50	2.28	122	93	2.63	1.8
30.	2.80	1.89	122	93	2.63	1.8
31.	2.35	1.46	122	93	2.63	1.8
32.	1.70	1.14	122	93	2.63	1.8
33.	2.20	2.28	122	107	2.63	1.8
34.	1.73	1.89	122	107	2.63	1.8
35.	1.41	1.46	122	107	2.63	1.8
36.	1.04	1.14	122	107	2.63	1.8

Summary

The previous experimental and theoretical work on the relationships between the rates of heat and mass transfer was reviewed. Experimental work was conducted in order to accumulate sufficient data on the system of a gas flowing over an object of rectangular cross-section so that the rates of heat transfer, mass transfer, might be related to the flow characteristics of the system, expressed in terms of the Reynolds group.

The experimental work was carried out in a pilot plant continuous fibre drier. The fibre, moving through the drier, becomes compressed into the form of a continuous slab of rectangular section. In the drier, the air flows at right angles to one of the two larger surfaces of the fibre tow, giving the system desired. Water was evaporated from the fibre tow and the rates of heat and mass transfer measured during the constant rate period of drying over a wide range of air conditions. The following equations were used to correlate the results,

$$\frac{h_d l}{D} = f(\text{Re}, \text{Sc})$$

$$\text{Nu} = f(\text{Re}, \text{Pr})$$

In order to investigate the effect of the Schmidt group, liquids of varying physical properties, were evaporated from the fibre tow, the experiments being similar to those carried out with water. The results

were correlated by the following equations,

$$\text{Mass Transfer} \quad \frac{h_d l}{D} = 0.24 \text{Re}^{0.76} \text{Sc}^{0.33}$$

$$\text{Heat Transfer} \quad \text{Nu} = 0.32 \text{Re}^{0.70} \text{Pr}^{0.33}$$

The rates of heat and mass transfer were compared using j factors and j_d/j_h was found to be 1.05.

The drying characteristics of a continuous fibre drier were also investigated and the rate of drying during the constant rate period was found to be given by,

$$\frac{dw}{de} = 5.58 \times 10^{-6} (p_s - p_a) V^{0.74}$$

No method was found of predicting the critical moisture content under varying air conditions. The factors influencing the rate of drying during the falling rate period were also investigated and diffusion was found to be the controlling factor in the drying of fibre tows. Investigations into the falling rate period were carried out by comparing the drying curve to that for diffusion from a porous slab. The time taken for the fibre to dry from the critical moisture content W_o to some other value of moisture content (W) is given by the equation

$$\ln \frac{W - W_e}{W_o - W_e} = \frac{\pi^2 D_F}{4 a^2} e$$

The diffusion coefficient, D_F , was found to be influenced by

temperature, humidity, and air velocity. The effect of velocity was found to be related to the diffusion coefficient by the relationship,

$$D_F \propto V^{0.83}$$

However the effects of temperature and humidity could not be expressed in mathematical terms.

In order to obtain the relationship for the falling rate period, the equilibrium moisture contents over a wide range of ambient air conditions were measured.